Title

QUANTITATION OF CERTAIN ALTERATIONS IN INTERMEDIARY METABOLISM IN VIVO ASSOCIATED WITH CHANGES IN BODY CONTENT OF VITAMINS EL, B6, B12, AND FOLIC ACID USING 14C02 BREATH ANALYSIS

Author

Ngo, Tran Manh.

Publication Date

1969-04-01

UCRL-18832

cy 2

QUANTITATION OF CERTAIN ALTERATIONS IN INTERMEDIARY METABOLISM IN VIVO ASSOCIATED WITH CHANGES IN BODY CONTENT OF VITAMINS B1, B6, B12, AND FOLIC ACID USING $^{14}CO_2$ BREATH ANALYSIS

Tran Manh Ngo
(Ph. D. Thesis)

April 1969

LAWRENCE RADIATION LABORATORY
UNIVERSITY of CALIFORNIA BERKELEY

UCRL-18832

Cy 2

DISCLAIMER

QUANTITATION OF CERTAIN ALTERATIONS IN INTERMEDIARY METABOLISM *IN VIVO* ASSOCIATED WITH CHANGES IN BODY CONTENT OF VITAMINS B1, B6, B12, AND FOLIC ACID USING $^{14}CO_2$ BREATH ANALYSIS

Contents

QUANTITATION OF CERTAIN ALTERATIONS IN INTERMEDIARY METABOLISM *IN VIVO* ASSOCIATED WITH CHANGES IN BODY CONTENT OF VITAMINS B1, B6, B12, AND FOLIC ACID USING $^{14}CO_2$ BREATH ANALYSIS

Abstract

Tran Manh Ngo*

Information on biochemical actions of soluble B vitamins upon metabolic pathways is derived primarily from studies on either single-cell organisms or cell-free systems. Little information is available for higher animals concerning quantitative aspects of biochemical actions of excess or deficient soluble B vitamins on metabolic pathways.

$^{14}CO_2$ breath analysis presented here appears to be a powerful technique for the study of the biochemical processes *in vivo*. Measurement of tne rate of $^{14}CO_2$ excretion in the breath permits some estimation of cell-membrane transport of the ^{14}C-labeled materials (^{14}C-R) and metabolic processes involved in the handling of ^{14}C-R. In addition, this technique allows for evaluation of the effects of physiological and pharmacological doses of a variety of materials such as the B vitamins. An example of the study of cell-membrane transport of amino acids was the determination of the competitive effect of L-methionine on L-histidine or L-serine transport across

the cell membrane. In the work presented here, decreased $^{14}CO_2$ production but a normally shaped curve was noted in the breath of L-methionine-treated rats subsequent to the intravenous administration of L-histidine (imidazole-2-^{14}C) and L-serine-3-^{14}C.

Administration of pharmacological doses of pyridoxine resulted in decreased $^{14}CO_2$ excretion in the breath and a delayed T_{max} in normal rats given pyridoxine prior to the intravenous injection of L-tryptophane-I-^{14}C. This result was felt to arise from hypertrophy of the intracellular L-tryptophane pool subsequent to its enhanced cell-membrane transport by pyridoxine.

An example of the study of alterations in intermediary metabolism of certain ^{14}C-labeled materials by changes in body content of soluble B vitamins was the analysis of thiamine deficiency in rats. There was a significant delay in $^{14}CO_2$ excretion in the breath of thiamine-deficient rats subsequent to the intravenous administration of pyruvate-I-^{14}C and acetate-I-^{14}C, which was normalized within 45 minutes after the administration of thiamine. Similar results were obtained in irradiated rats after the administration of labeled monocarbon pool precursors, which suggested radiation inactivation of tetrahydrofolic acid or the processes responsible for its production. We may suggest that $^{14}CO_2$ breath analysis might be a sensitive method for essay of <u>in vivo</u>

biochemical activity of large doses of soluble B vitamins in higher animals. One example of this type of study was the demonstration of increased $^{14}CO_2$ production after the injection of L-histidine (imidazole-2-^{14}C) in normal rats treated with pharmacological doses of cyanocobalamin and decreased $^{14}CO_2$ excretion in normal rats given pharmacological doses of folic acid.

I. INTRODUCTION

The basis for present information concerning biochemical actions of soluble B vitamins upon metabolic pathways is derived primarily from studies on either single-cell organisms (e.g., bacteria) or cell-free systems (1-4). Little information concerning quantitative aspects of biochemical actions of excess or deficient soluble B vitamins on intermediary pathways is available in intact animals. Furthermore, despite a lack of specific evidence, it is generally held that the presence of soluble B vitamin concentrations in body tissues in excess of that required physiologically has no effect on the biochemical pathways related to the vitamins' known biochemical functions (1,5,6).

The work presented here utilizes the $^{14}CO_2$ breath analyzer to provide quantitative information concerning how in vivo biochemical kinetics are influenced by certain B vitamins when they are administered therapeutically in treatment of specific deficiency states, or pharmacologically to normal animals.

The $^{14}CO_2$ breath analyzer was introduced by Tolbert and collaborators (7). This apparatus permits continuous quantitation of the rate of $^{14}CO_2$ appearance in the breath of animals and human subjects (8-14) given materials labeled with ^{14}C. Such quantitation has been used previously in animals studied for evaluation of the effects of

of parathion and carbon tetrachloride on glucose metabolism (15), the effects of glucagon and hydrocortisone on L-histidine kinetics (16,17), the effects of coenzyme A and pantothenic acid deficiency on the metabolism of labeled fatty acid acetate and heptanoate (18,19), and the relative rates of oxidation to CO_2 of the carbon atoms at the 3,4 and 8 positions of 3,4 dimethoxyphenethylamine (20). With regard to studies in human subjects, previous investigators have used this technique to demonstrate effects of insulin and tolbutamide on glucose kinetics in normal and diabetic subjects (21,22), differentiation between vitamin B12-deficient and folic acid-deficient megaloblastic anemias with L-histidine (imidazole-2-^{14}C) and Na propionate-^{14}C (23,24), phenylalanine metabolism in phenylketonuria (PKR) and related hyperphenylalaninemic states, glyoxalate oxidation in primary hyperoxaluria, tyrosine metabolism in hyperthyroidism (25,26), and methionine-methyl oxidation in acute schizophrenia (27).

The rate of $^{14}CO_2$ appearance in the breath is a function of several factors. These factors are (a) delivery of the administered ^{14}C labeled materials (^{14}C-R) to the cellular site of metabolism, (b) transport of the materials across the cell membrane, (c) actual biochemical processes involved in metabolism of ^{14}C-R, (d) processes involved in excretion of the ^{14}C oxidized to $^{14}CO_2$ in the breath. In actual animal experiments the influence of (a)

and (b) on the rate of $^{14}CO_2$ excretion in the breath can be nullified by comparing breath curves in the same animals before or after a given treatment or in animals of comparable size treated identically save for perturbations in the processes involved in cell membrane transport and metabolism of ^{14}C-R (28).

Each of the experimental presentations in Sections III through VI is preceded by introductory remarks relating pertinent available information to the design of experiments involved in the study of the particular B vitamin.

II. MATERIALS AND METHODS

Description and calibration of the apparatus

The $^{14}CO_2$ breath analyzer is shown diagrammatically in Fig. 1 and in its actual form in Fig. 2. Compressed air (tank seen on the far right in Fig. 2) is passed through the animal cage containing the rat at a constant flow rate determined by a precision flow regulator (Millaflow Division, Richmond, Calif.) Air mixed with expired gases from the rat exits from the animal cage and passes through a water absorber ($CaSO_4$, Hammond Drierite Company, Xenia, Ohio). Subsequent to removal of water, the gases are serially passed through a 0.377-liter ionization chamber containing a vibrating-reed electrometer (Model 30, Applied Physics Corporation, Pasadena, California), an infrared carbon dioxide analyzer (type KK 5802, N.V. Godart,

De Bilt, Holland), and a paramagnetic oxygen analyzer (Model F_3, Beckman Instruments Inc., Fullterton, California). Continuous graphical plotting of the $^{14}CO_2$, CO_2, and O_2 data was achieved by using a multichannel chart recorder (Speedomax, Leeds and Northrup Co., Philadelphia).

For stable performance the components required the following "warm up" times: 10 minutes for the voltage regulator, 1 hour for the vibrating-reed electrometer, 2 hours for the infrared carbon dioxide analyzer, and 24 hours for the paramagnetic oxygen analyzer. The background current from the electrometer was determined in the absence of an ionization chamber and was found to be identical to that obtained when a regulator flow rate of a tank air (0.4 to 3 liters per minute) was passed through the ionization chamber containing the electrometer.

The ionization chamber was calibrated by introducing standard $^{14}CO_2$ gases into the ionization chamber and measuring current flow after equilibrium was reached. Standard $^{14}CO_2$ gases were calibrated as follows (29,30). Ten liters of $^{14}CO_2$ gas were passed through 13 ml of absorber solution (1:2 (v/v) solution of ethanolamine in ethylene glycol monoethyl ether) at a flow rate of 0.4 liter per minute. Three ml of this absorber solution was added to 15 ml scintillation liquid of 1:2 (v/v) ethyl-eneglycol monoethyl ether in toluene, containing 5.50 g per liter of 2,5-diphenyloxazole (PPO, Scintillation Grade,

Packard Instrument Company, Downers Grove, Illinois). The ^{14}C activity in the solution was determined by using a Nuclear Chicago model 725 liquid scintillation counter. Absolute content of ^{14}C in the sample was determined from measurement of the liquid scintillation counter efficiency utilizing standard toluene-^{14}C solution ($C_6H_5CH_3$-^{14}C in toluene, specific activity: 1.59 μCi/4.96 ml, Nuclear Chicago). Counting efficiencies were in the range of 0.624 to 0.628, and background varied from 25.9 to 29.1 cpm. The calibration factors of the ionization chamber were the range of 1.480×10^{-4} to 1.521×10^{-4} μC/mV/min.

For calibration of the carbon dioxide and oxygen analyzer, a tank of gas containing 80% nitrogen, 3% carbon dioxide, and 17% oxygen was used (Pacific Oxygen Company, 2311 Magnolia Street, Oakland, California).

The apparatus was periodically tested for gas leaks to insure constancy of its performance.

Procedure for study of endogenous $^{14}CO_2$ production

Inbred male Buffalo rats (Simonsen Laboratory, Gilroy, California) were used in all experiments. In each series of studies, the rats of similar weight and age were divided into control and experimental groups. Immediately after intravenous administration of ^{14}C-labeled materials, each control or experimental rat was

placed in the animal-holding chamber of the breath analyzer. After the end of the measurement period the experimental animal was removed from the animal-holding chamber and returned to his holding cage. The holding cage was placed in a room equipped with an exhaust vent for at least 1 day to prevent $^{14}CO_2$ contamination of the laboratory.

At the completion of each study, air flow was maintained through the system until the vibrating-reed electrometer returned to the initial background levels, in order to reduce residual contamination of the apparatus.

III. $^{14}CO_2$ PRODUCTION IN THIAMINE-DEFICIENT RATS GIVEN #1-^{14}C PYRUVATE AND ACETATE

A. Review of the problem

In thiamine-deficient rats, lactic acid and pyruvic acid concentration in blood is increased (31-37), and oxygen uptake in many tissues decreased, (38). In man thiamine deficiency can also be detected by measurement of the concentration of pyruvic acid or α-ketoglutaric acid in blood (39) or by determination of the "carbohydrate index", which is based on concentration of pyruvic acid, lactic acid, and glucose in blood after standard exercise and administration of glucose (40). In addition, measurement of thiamine and its metabolites has been made in breath, blood, urine, feces, and tissues (41-48).

Fig. I is shown from left to right while Fig. 2 is shown from right to left.

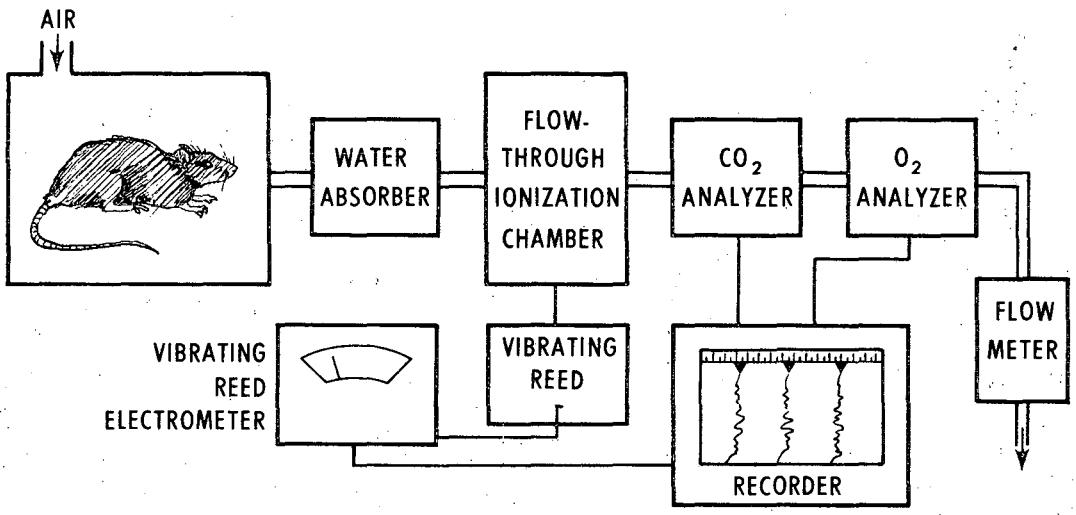

XBL 674-1331

Fig. 1

CBB 688-4843

Fig. 2

Before pyruvate can enter the tricarboxylic acid cycle, it must be decarboxylated to acetyl-CoA in the presence of thiamine pyrophosphate. Similarly, the oxidation of acetate to CO_2 involves the production of α-ketoglutarate, which requires thiamine pyrophosphate as a coenzyme in the production of succinyl CoA plus CO_2. For practical purposes both the above reactions are irreversible.

The apparent dependency of the oxidation of the #1 carbon of both pyruvate and acetate to CO_2 upon the presence of thiamine pyrophosphate suggested that appearance of $^{14}CO_2$ in the breath following administration of pyruvate-1-^{14}C and acetate-1-^{14}C might be a measure of thiamine deficiency. Such measurements might be useful in early detection of beri beri. In this study $^{14}CO_2$ appearance in the breath subsequent to administration of #1-^{14}C-pyruvate, acetate, and bicarbonate, and plasma clearance of (thiazole-2-^{14}C) thiamine, were measured in normal and thiamine-deficient rats.

B. Preparation of experimental animals

Twenty-seven male Buffalo rats (Simonsen Laboratory, Gilroy, California) weighing 110 to 135 g and 5 male Buffalo rats weighing 350 to 390 g were used in these experiments. The rats in the first group were 42 days old and the animals in the second group were about 3 months old at the start of the experiments. Each of these groups was

further subdivided into control and thiamine-deficient subgroups. The diet of the control rats had the following composition expressed as percentages: vitamin-free casein, 20.0; sucrose, 67.5; cotton-seed oil, 5.0; UCB-IRb salts, (49) 5.5; choline bitartrate, 1. 22; vitamins A, D, E premix; 1.0; and vitamins B premix, 2.0. The deficient diet contained the same formula as above except that it had no thiamine. The experiments were conducted from 14 to 20 days after initiation of these diets, when the thiamine-deficient rats showed weight loss and generalized asthenia.

1. $^{14}CO_2$ production studies

The experimental animals were divided into two groups. The control group consisted of six rats and the thiamine-deficient group consisted of seven rats. The appearance of $^{14}CO_2$ in the breath subsequent to the intravenous administration of pyruvate-1-^{14}C was determined in each of these animals. After the first series of experiments, four rats of the thiamine-deficient group received 20 mg of thiamine hydrochloride per day (Abott Laboratories, North Chicago, Ill.) intramuscularly 1 to 2 days prior to performance of a repeat study. In each study the rat received 2.5 μCi of sodium pyruvate-1-^{14}C (specific activity: 3.52 mCi/mM, New England Nuclear Corp., 575 Albany Street, Boston, Massachusetts 02118) intravenously after light ether anesthesia.

In a second series of studies $^{14}CO_2$ appearance in the breath was measured subsequent to IV administration of sodium acetate-1-^{14}C. The experimental animals consisted of three control and three thiamine-deficient rats. In each study, the rat received 2.5 μCi of sodium acetate-1-^{14}C (specific activity: 40.0 mCi/mM, Nuclear Chicago, 333 East Howard Street, Des Plaines, Illinois 60018). The experiments were repeated in thiamine-deficient rats 40 to 45 minutes after intravenous administration of 15 mg of thiamine hydrochloride and again a day later after a second IV dose of 15 mg of thiamine hydrochloride.

In a third group of animals the effect of thiamine deficiency on the HCO_3^- pool was studied. The group consisted of four controls and four thiamine-deficient rats. In each study the rat was given 1 μCi of $NaH^{14}CO_3$ intravenously (specific activity: 21.5 mCi/mM, New England Nuclear Corporation) and $^{14}CO_2$ was measured in expired air.

Immediately after intravenous administration of ^{14}C-labeled materials, each control and thiamine-deficient rat was placed in an animal holding chamber and the expired air was passed through an ionization chamber at a constant rate of 3 liters/minute in an experimental apparatus similar to that described previously (8-27, 50-52). At this gas flow rate the mean turnover time of gas in the measuring apparatus (mean washout time) was less than 1 minute. The rate of excretion and the amount of $^{14}CO_2$ excreted in the

breath of rats were recorded continuously.

2. Plasma thiamine clearance studies

Five male Buffalo rats were assembled into two groups of two controls and three thiamine-deficient rats. The rats were studied individually. Each animal received 20 μCi of (thiazole-2-^{14}C) thiamine hydrochloride (specific activity: 25.2 mCi/mM, Nuclear Chicago) intravenously under light ether anesthesia. The blood samples were obtained in heparinized capillary tubes from tail vein venepuncture at approximately 1.5, 4, 6.5, 10.5, 21, 30, 70, and 117 minutes after IV injection of (thiazole-2-^{14}C) thiamine hydrochloride. The plasma samples were then isolated by a semi-micro method. Each sample consisted of 20 microliters of plasma dissolved in 0.5 ml of Nuclear Chicago solubilizer (0.6 n solution in toluene) which was added to 15 ml of scintillation solution made of naphthalene, 2,5-diphenyloxazole (PPO, scintillation grade, Packard Instrument Company, Downers Grove, Illinois), 1,4 bis- [2-(5-phenyloxazolyl)] -benzene (POPOP, scintillation grade, same address as above), 1,4 dioxane (J.T. Baker Chemical Company, Phillipsburg, N.J.), toluene, and absolute ethyl alcohol. The ^{14}C activity in the solution was determined by utilizing a Nuclear Chicago model 725 liquid scintillation counter. Absolute content of ^{14}C in the sample was calculated from measurement of the liquid scintillation counter efficiency, utilizing an internal ^{14}C standard ($C_6H_5CH_3$-^{14}C in toluene, specific activity: 3.1 μCi/ml,

Nuclear Chicago). Counting efficiency was generally 0.8, and background varied from 27.8 to 29.2 counts/min.

C. Results

1. $^{14}CO_2$ production studies

a. #1-^{14}C-Pyruvate

Figure 3 presents representative curves showing the rate of appearance of $^{14}CO_2$ in the breath of a control rat and a thiamine-deficient rat prior to, and 1 and 2 days after, daily intramuscular injection of 20 mg thiamine hydrochloride. The ordinate represents $^{14}CO_2$ excretion rate expressed as mμCi/min and the abscissa as time in minutes following IV injection of pyruvate-1-^{14}C.

The control rat achieved a greater initial rate of $^{14}CO_2$ excretion, which subsequently decreased more rapidly than in the thiamine-deficient rat. One day after intramuscular injection of 20 mg thiamine hydrochloride the previously thiamine-deficient rat had a breath $^{14}CO_2$ curve intermediate between that seen in the thiamine-deficient state and that noted in the control. After two daily injections of 20 mg thiamine hydrochloride (i.e., integral dose of 40 mg) to the previously thiamine-deficient rat, the appearance of $^{14}CO_2$ in the breath is similar to that seen in the control animal..

Figure 4 presents composite data for the rate of $^{14}CO_2$ production following IV administration of pyruvate-1-^{14}C

Rate of appearance of $^{14}CO_2$ in the breath of representative control, thiamine-deficient, and treated thiamine-deficient rats given pyruvate-1-^{14}C.

Figure 3 presents representative curves showing the rate of appearance of $^{14}CO_2$ in the breath of a control rat and a thiamine-deficient rat prior to, and 1 and 2 days after, daily intramuscular injection of 20 mg thiamine hydrochloride. The ordinate represents $^{14}CO_2$ excretion rate expressed as mμCi/min and the abscissa as time in minutes following IV injection of pyruvate-1-^{14}C.

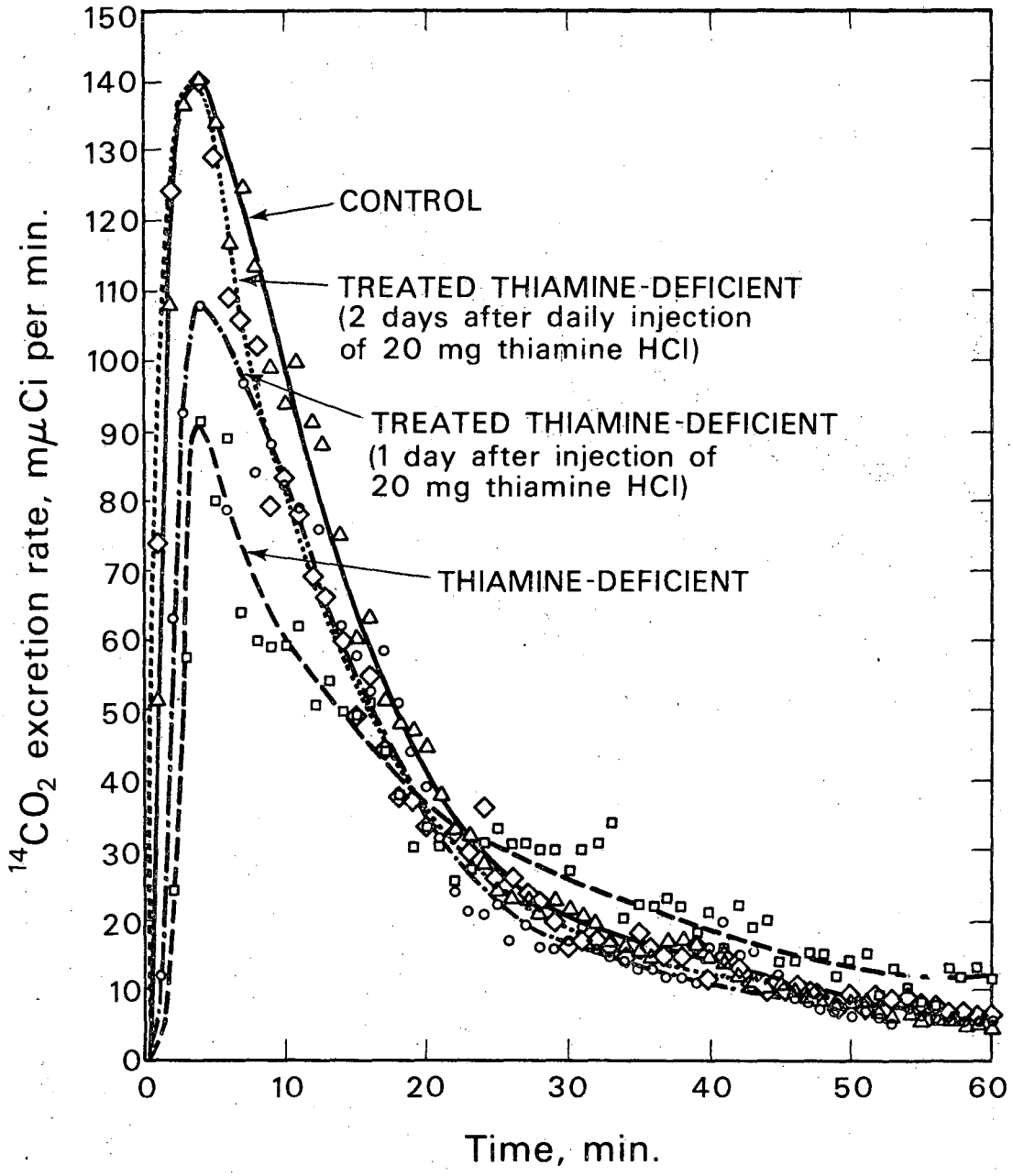

DBL 689-5424

Fig. 3

Changes in the rate of excretion of $^{14}CO_2$ in the breath of groups of control, thiamine-deficient, and treated thiamine-deficient rats at times greater than 5 minutes after IV administration of pyruvate-1-^{14}C.

Figure 4 presents composite data of the rate of $^{14}CO_2$ following IV administration of pyruvate-1-^{14}C in six control rats, seven thiamine-deficient rats, and four thiamine-deficient rats on the first and second day after daily intramuscular injections of 20 mg of thiamine hydrochloride. The ordinate represents $^{14}CO_2$ excretion rate expressed as x 1.521 muCi/min and the abscissa as time in minutes following IV injection of pyruvate-1-^{14}C. Vertical bars through each point define precision of position of the mean of excretion rates of $^{14}CO_2$ for each group of rats with 95% limits based on $t_{.95}\ S_{y.x}$. The broken lines above and below each curve are regression lines of $\pm$ 1 standard error of the estimate ($S_{x.y}$).

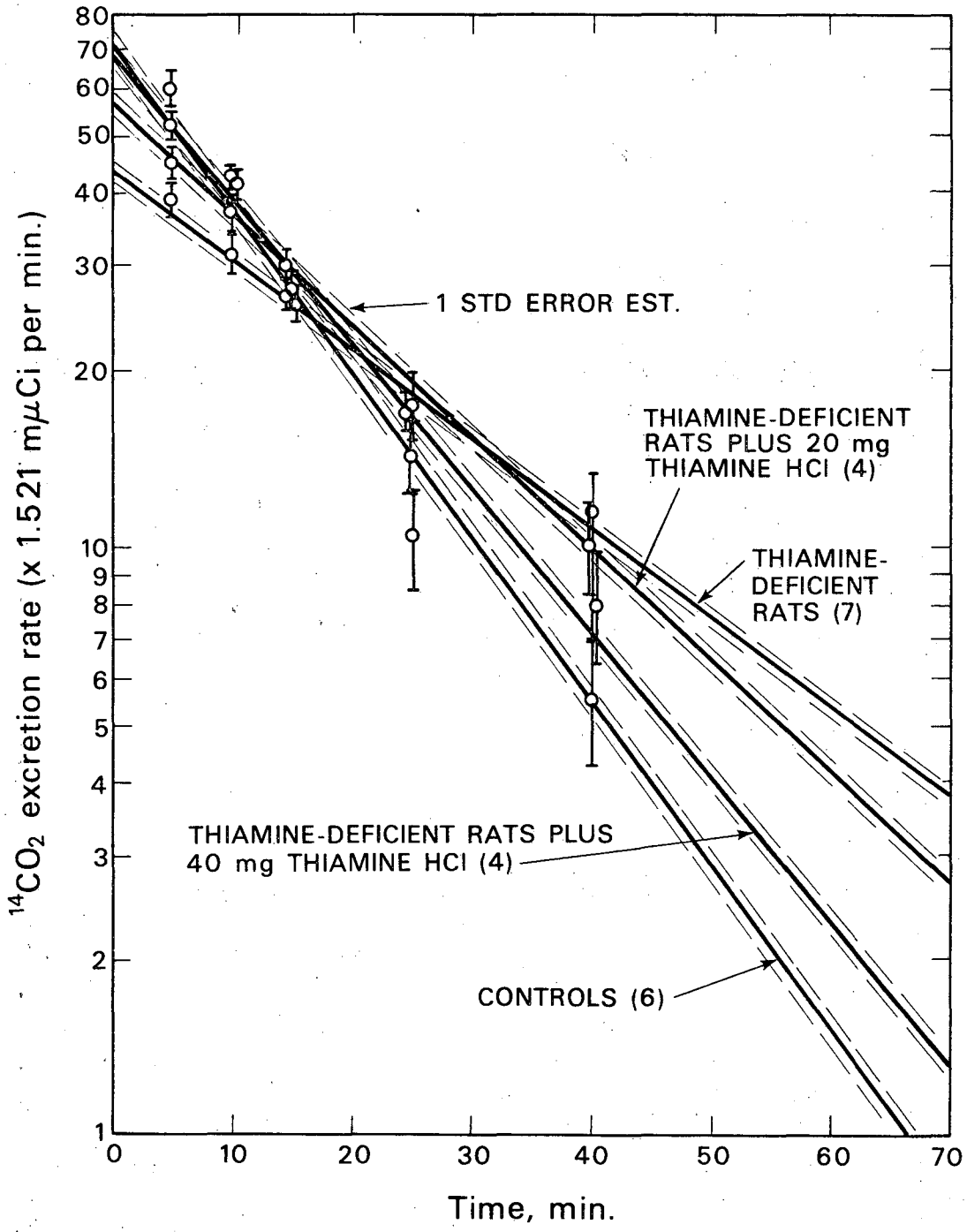
80
70
60
50
40
30
20
10
9
8
7
6
5
4
3
2
1
0
10
20
30
40
50
60
70
$^{14}CO_2$ excretion rate (x 1.521 mμCi per min.)
Time, min.
1 STD ERROR EST.
THIAMINE-DEFICIENT RATS PLUS 20 mg THIAMINE HCl (4)
THIAMINE-DEFICIENT RATS (7)
THIAMINE-DEFICIENT RATS PLUS 40 mg THIAMINE HCl (4)
CONTROLS (6)
DBL 689-5444

Fig. 4

in six control rats, seven thiamine-deficient rats, and four other thiamine-deficient rats on the first and second day after daily intramuscular injection of 20 mg of thiamine hydrochloride. Each point at 5, 10, 15, 25 and 40 minutes represents the mean of excretion rates of $^{14}CO_2$ for each group of rats. Vertical bars through each point define precision of position of the mean with 95% limits based on $t_{.95}\ S_{y.x}$ ($S_{y.x}$ = 1 standard error of the estimate). The zero-time intercept (A), the slope of the regression function (B), and the standard error of the slope [$S_{b(x).(y)}$] were determined by least-squares best fit of the data to the function

$$Y = A + (B \pm S_{b(x).(y)})\ X.$$

The broken lines immediately above and below each curve are regression lines of ± 1 standard error of the estimate ($S_{x.y}$).

In determining the significance of differences between the curves obtained in the control and thiamine-deficient groups, a P value of 0.01 was obtained. In this analytic approach only the downslopes of the $^{14}CO_2$ breath curves were analyzed ($\geq$ 5 min after IV injection of pyruvate). Since the initial rate of $^{14}CO_2$ production from pyruvate-1-^{14}C is sufficiently rapid to be of the order of magnitude of the turnover rate of the $^{14}CO_2$ measurement apparatus, little reliable information can be

extracted from the initial portion of the breath $^{14}CO_2$ curve. The slope (expressed as $T_{1/2}$) and integral amount of ^{14}C administered excreted in the breath (expressed as %) during the initial 60 minutes of the study for each group of rats are presented in Table I. It is clear that both the $T_{1/2}$ and the integral amount of ^{14}C excreted in the breath in 60 minutes are significantly different in control and thiamine-deficient rats. The $T_{1/2}$ in deficient rats is about double that in control rats. All parameters in deficient rats closely approached the normal range 2 days after initiation of daily administration of 20 mg of thiamine hydrochloride.

b. #1-^{14}C Acetate

The curves describing appearance of $^{14}CO_2$ in the breath of control and thiamine-deficient rats given acetate-1-^{14}C are similar to those obtained after administration of pyruvate-1-^{14}C. Figure 5 presents representative curves describing the excretion of $^{14}CO_2$ in the breath following IV administration of acetate-1-^{14}C in a control, a thiamine-deficient rat, and the same thiamine-deficient rat 45 minutes after IV administration of 15 mg thiamine hydrochloride. A significant difference is noted between the $^{14}CO_2$ curves for control and for thiamine-deficient rats. Within 45 minutes after IV administration of thiamine the previously thiamine-deficient rat had a normal $^{14}CO_2$ breath curve. Figure 6,

Rate of appearance of $^{14}CO_2$ in the breath of representative control, thiamine-deficient, and treated thiamine-deficient rats given acetate-1-^{14}C.

Figure 5 presents representative curves showing the rate of appearance of $^{14}CO_2$ in the breath of a control rat and a thiamine-deficient rat prior to, and 45 minutes after, IV injection of 15 mg thiamine hydrochloride. The ordinate represents $^{14}CO_2$ excretion rate expressed as mμCi/min, and the abscissa as time in minutes following IV injection of acetate-1-^{14}C.

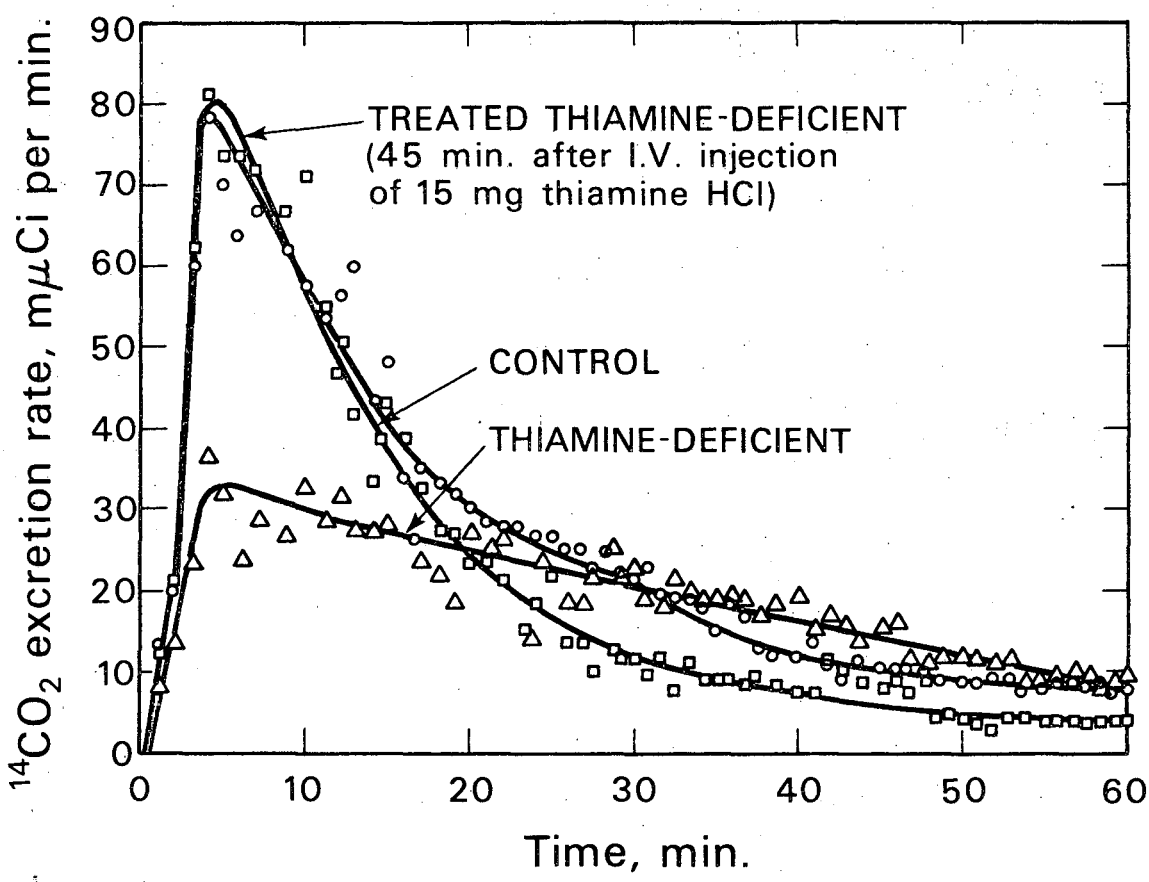

DBL 689-5423

Fig. 5

similar to Fig. 2, presents composite data describing the rate of $^{14}CO_2$ production following IV administration of acetate-1-^{14}C to three control rats, three thiamine-deficient rats, and three thiamine-deficient rats given 15 mg thiamine hydrochloride IV 45 minutes prior to initiation of the study. The method for plotting the data and for analysis of the least-squares best fit single exponential regression curve with its confidence limits is identical to that described for Fig. 2. The curve defined by the data obtained in control rats is significantly different ($p < 0.01$) from that obtained in thiamine-deficient rats. However, the pattern of appearance of $^{14}CO_2$ in the breath of thiamine-deficient rats given #1-^{14}C-acetate 45 minutes after IV administration of 15 mg thiamine hydrochloride was essentially identical to that noted in control animals. A repeat study on such thiamine-deficient animals 45 minutes after a second IV injection, 24 hours after the first such treatment, again yielded a normal pattern of $^{14}CO_2$ excretion. These data are presented in tabular form in Table II, where the slope of the breath $^{14}CO_2$ curve expressed as $T_{1/2}$ and the integral % ^{14}C excreted in 60 minutes are listed for each group of animals.

c. $H^{14}CO_3^-$

Since $^{14}CO_2$ produced at intracellular sites must traverse the body CO_2-H_2CO_3 pools prior to its excretion in

Table I

Slope ($T_{1/2}$) and integral ^{14}C excretion determined from $^{14}CO_2$ appearance in breath following IV administration of pyruvate-1-^{14}C in control and experimental rats (the number of animals in each group is noted in parentheses).

Category	Half-time $T_{1/2}$ (minutes) ± S.E.	^{14}C excretion in 60 minutes (%) ± S.E.
Normal rats (6)	10.728 ± 0.222	64.8095 ± 2.2642
Thiamine-deficient rats (7)	19.687 ± 0.241	42.9687 ± 4.1139
Thiamine-deficient rats 24 hours after intramuscular administration of 20 mg thiamine hydrochloride (4)	15.928 ± 0.379	49.2882 ± 2.8866
Thiamine-deficient rats 48 hours after intramuscular administration of 40 mg thiamine hydrochloride (4)	12.317 ± 0.910	57.1520 ± 3.4390

Changes in the rate of excretion of $^{14}CO_2$ in the breath of groups of control, thiamine-deficient, and treated thiamine-deficient rats at times greater than 5 minutes after IV administration of acetate-1-^{14}C.

Figure 6 presents composite data of the rate of $^{14}CO_2$ production following IV administration of acetate-1-^{14}C in three control rats, three thiamine-deficient rats, and three thiamine-deficient rats given 15 mg thiamine hydrochloride IV 45 minutes prior to initiation of the study. The ordinate represents $^{14}CO_2$ excretion rate expressed as x 1.521 mμCi/min and the abscissa as time in minutes following IV injection of #1-^{14}C-acetate. Vertical bars through each point define the precision of position of the mean of excretion rates of $^{14}CO_2$ for each group of rats with 95% limits based on $t_{.95}\ S_{y.x}$. The broken lines above and below each curve are regression lines of ± 1 standard error of the estimate ($S_{x.y}$).

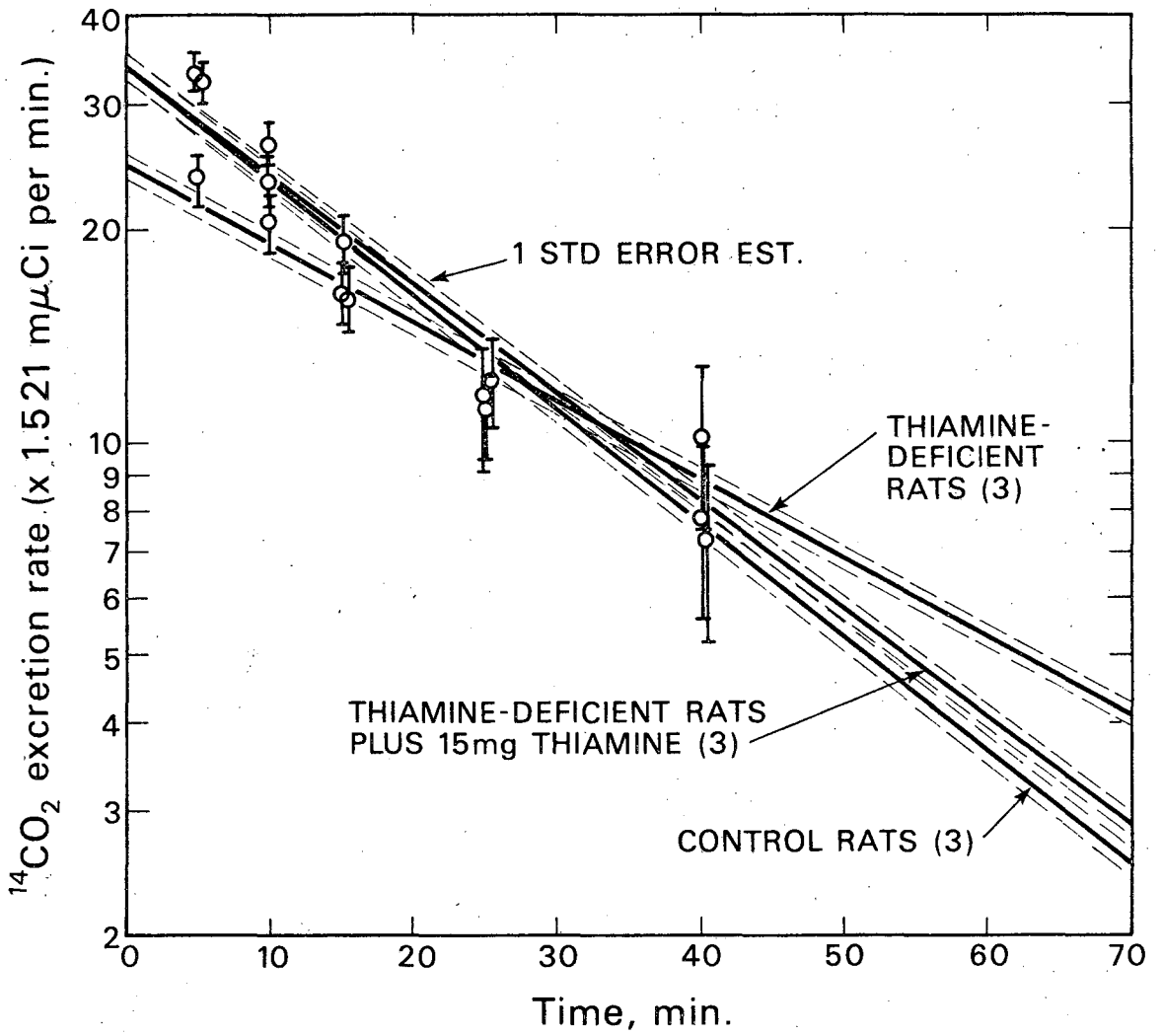

DBL 689-5427

Fig. 6

Table II

Slope ($T_{1/2}$) and integral ^{14}C excretion determined from $^{14}CO_2$ appearance in breath following IV administration of acetate-1-^{14}C in control and experimental rats (the number of animals in each group is noted in parentheses).

Category	Half-time $T_{1/2}$ (minutes) ± S.E.	^{14}C excretion in 60 minutes (%) ± S.E.
Normal rats (3)	18,474 ± 0.593	52.233 ± 4.193
Thiamine-deficient rats (3)	27.530 ± 1.497	46.720 ± 0.683
Thiamine-deficient rats 45 minutes after IV administration of 15 mg thiamine hydrochloride (3)	19.184 ± 0.477	55.645 ± 3.213
Thiamine-deficient rats 45 minutes after second daily dose of 15 mg thiamine hydrochloride (3)	21.973 ± 0.112	54.640 ± 6.884

the breath, it is possible that the abnormal $^{14}CO_2$ breath curves following administration of #1-^{14}C-pyruvate and acetate in thiamine-deficient animals were due to alterations in the CO_2-$H_2CO_3^-$ pools in thiamine-deficient rats rather than to alterations in specific metabolic steps related to $^{14}CO_2$ production. That this is not the case is demonstrated in data presented in Fig. 7 and Table III. This figure and table summarize data describing the appearance of $^{14}CO_2$ in the breath of control and thiamine-deficient rats given 1 μCi $H^{14}CO_3$ intravenously. Presentation and analysis of the data is identical to that of Fig. 4 and Table I. It appears from these data that thiamine deficiency does not remarkably alter CO_2-HCO_3^- pool kinetics (it may result in a small increase in integral excretion of $^{14}CO_2$ from the CO_2-H_2CO_3-HCO_3^-), however, this effect is opposite the effect noted with #1-^{14}C-labeled pyruvate and acetate. This result indicates that abnormalities in $^{14}CO_2$ appearance in the breath following administration of #1-^{14}C-pyruvate and acetate to thiamine-deficient animals could not result from alterations in CO_2-HCO_3^- pool kinetics.

2. Plasma Clearance of (Thiazole-2-^{14}C) Thiamine in Thiamine-Deficient Rats

To determine whether significant differences are present in thiamine kinetics, per se, between control and thiamine-deficient rats, the clearance of ^{14}C activity from the

plasma following IV administration of (thiazole-2-^{14}C) thiamine was studied. The results of such plasma thiamine clearance studies are presented for each of three thiamine-deficient and two control animals in Fig. 8. All animals in this study were of the same size and genetic background. Therefore the concentration of radioactivity in the plasma following IV injection of a standard dose (20 μCi) is an adequate reflection of the content of radioactivity in the initial distribution compartment of intravenously administered thiamine. It can be noted from Fig. 8 that at all times following IV administration of labeled thiamine the ^{14}C concentration in the plasma is lower in thiamine-deficient animals than in controls, but that the curves are otherwise roughly parallel. These results suggest that the initial distribution space of thiamine in thiamine-deficient animals is much larger than that in controls.

D. Discussion

In control rats approximately 65% of the ^{14}C administered as pyruvate-1-^{14}C appears in the breath as $^{14}CO_2$ within the first 60-minute period. This result is comparable to that obtained following IV administration of $H^{14}CO_3$ (i.e., 61%) and confirms that the largest component of pyruvate metabolism in vivo occurs by decarboxylation to form acetyl CoA rather than by pathways leading to glucogenesis. In control animals a smaller amount, only

$^{14}CO_2$ excretion following IV administration of $H^{14}CO_3$ in control and thiamine-deficient rats.

Figure 7 presents composite data of the rate of $^{14}CO_2$ production following IV administration of $H^{14}CO_3$ in four control and four thiamine-deficient rats. Vertical bars through each point define precision of position of the mean of excretion rates of $^{14}CO_2$ for each group of rats with 95% limits based on $t_{.95}\ S_{y.x}$. The broken lines above and below each curve are regression lines of ± 1 standard error of the estimate ($S_{x.y}$).

The ordinate represents $^{14}CO_2$ excretion rate expressed as x 1.521 mμCi/min and the abscissa as time in minutes following IV injection of $H^{14}CO_3$.

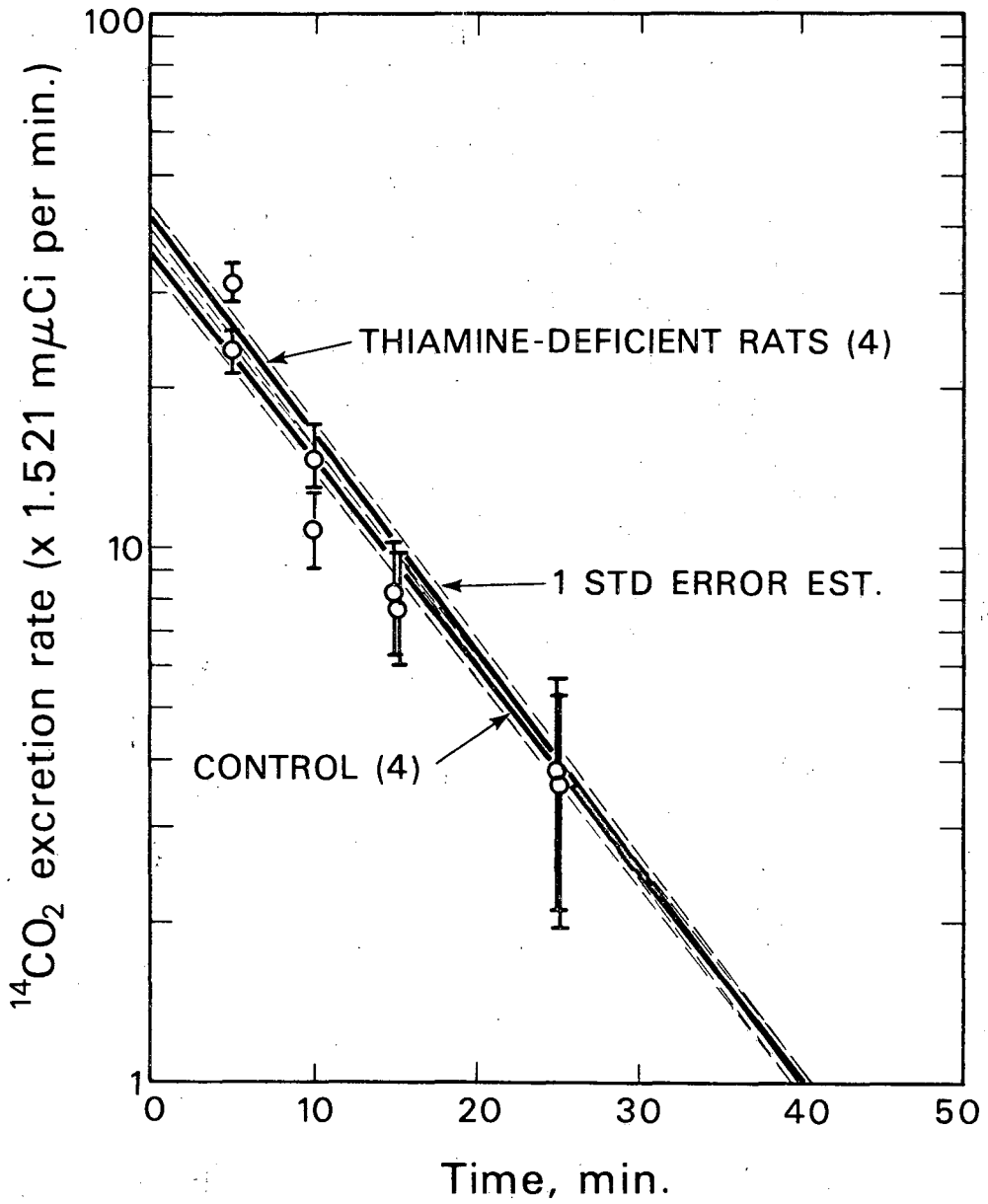

DBL 689-5426

Fig. 7

Slope ($T_{1/2}$) and integral ^{14}C excretion determined from $^{14}CO_2$ appearance in breath following IV administration of NaH $^{14}CO_3$ in control and experimental rats (the number of animals in each group is noted in parentheses).

Category	Half-time $T_{1/2}$ (minutes)	^{14}C excretion in 50 minutes (%) ± S.E.
Normal rats (4)	7.858	61.1227 ± 3.0906
Thiamine-deficient rats (4)	7.394	68.8246 ± 2.2626

Plasma clearance of (thiazole-2-^{14}C) thiamine hydrochloride in control and thiamine-deficient rats.

Figure 8 presents the clearance of ^{14}C activity from plasma following IV administration of (thiazole-2-^{14}C) thiamine hydrochloride in two control and three thiamine-deficient rats. The ordinate represents ^{14}C activity expressed as DPM/ml of plasma and the abscissa as time in minutes following IV injection of (thiazole-2-^{14}C) thiamine.

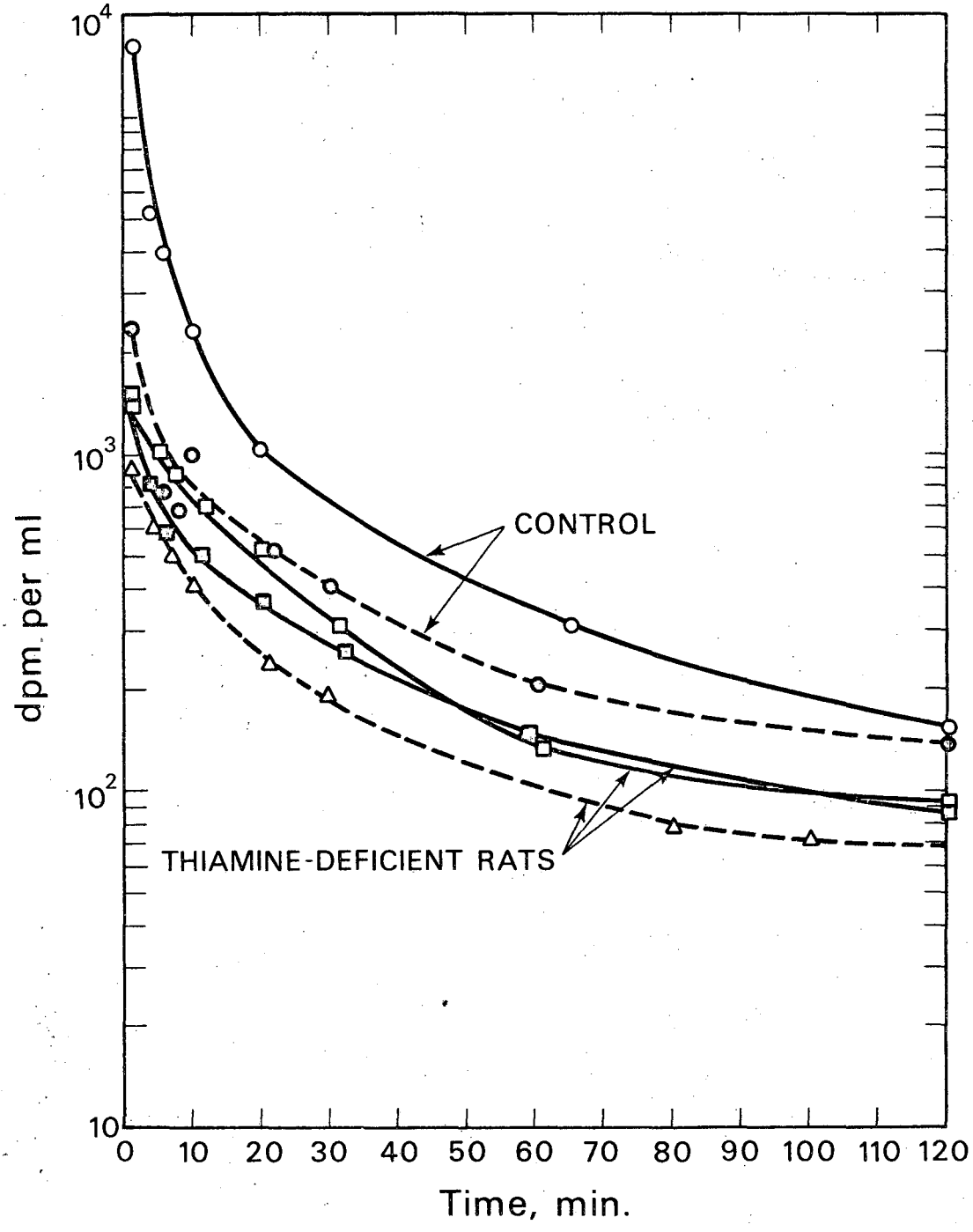

DBL 689-5425

Fig. 8

52% of the ^{14}C administered as acetate-1-^{14}C, could be accounted for as $^{14}CO_2$ during the initial 60 minutes following the intravenous administration of this material. Thus a small but significant amount of acetate appears to be fixed in slowly catabolized compounds (e.g., fatty acids), as opposed to direct oxidation to CO_2 in the TCA cycle.

In thiamine-deficient animals there was a delay in oxidation of both #1-^{14}C-labeled pyruvate and acetate to $^{14}CO_2$ (as evidenced by a prolonged $T_{1/2}$) as well as a diminished integral excretion of $^{14}CO_2$ in the $^{14}CO_2$ breath curves. Within 45 minutes after the intravenous administration of thiamine to thiamine-deficient rats, the pattern of appearance of $^{14}CO_2$ in the breath subsequent to the intravenous administration of #1-^{14}C labeled acetate was within normal limits. However, as long as 24 hours following the intramuscular injection of thiamine in thiamine-deficient rats, the pattern of appearance of $^{14}CO_2$ in the breath remained abnormal, and became normal only after a 48-hour period following two daily intramuscular injections of thiamine. This latter finding may be related to local binding of thiamine in the tissues surrounding the intramuscular injection site, with resulting diminution in the availability of thiamine for sites elsewhere in the body. Following intravenous administration there may be more generalized distribution of thiamine

throughout the body, making it more available for thiamine-dependent metabolic reactions. In particular, intravenous as opposed to intramuscular administration of thiamine may result in a greater delivery of thiamine to the liver, the site of a large fraction of pyruvate and acetate catabolism. An alternative explanation of the data is that the oxidative catabolism of the #1 carbon atom of pyruvate is more sensitive to thiamine deficiency than the oxidative catabolism of the #1 carbon atom of acetate.

That specific thiamine binding sites are relatively unsaturated in thiamine deficiency, as opposed to the non-deficient state, is further suggested by the studies of plasma thiamine clearance curves. Such curves in thiamine-deficient rats are below, but roughly parallel to, those seen in control animals. This result could be explained by postulating a larger initial distribution space for the ^{14}C-labeled thiamine in the thiamine-deficient animals than in the controls. This could be accounted for by postulating an increased rate at which thiamine equilibrates across cell membranes or by a larger quantity of unsaturated thiamine binding sites in thiamine-deficient animals than in control animals.

That the differences in $^{14}CO_2$ appearance in thiamine-deficient animals given #1-^{14}C pyruvate or acetate is not due to alterations of the bicarbonate pool is demonstrated by the finding of comparable $^{14}CO_2$ appearance curves

subsequent to the intravenous administration of ^{14}C-labeled bicarbonate in thiamine-deficient animals and controls.

The fact that alterations in the metabolism of pyruvate and acetate in the presence of thiamine deficiency can be detected in the intact animal by measurement of $^{14}CO_2$ production suggests the possible application of this approach to the early diagnosis of thiamine deficiency (beri-beri) in man. Such a human diagnostic procedure might consist of the measurement of $^{14}CO_2$ in the breath following administration of #1-^{14}C-labeled acetate or pyruvate, with subsequent repetition of the study after an intravenous administration of a therapeutic dose of thiamine. A significant increase in the slope of the $^{14}CO_2$ breath curve during the second study would suggest the presence of thiamine deficiency at the time of the initial study. The validity or possible usefulness of this approach in the early diagnosis of beriberi awaits study in human subjects.

E. Summary

In normal rats approximately 65% of ^{14}C administered as pyruvate-1-^{14}C appears in the breath as $^{14}CO_2$ within 60 minutes (comparable to the amount obtained following administration of $H^{14}CO_3^- \approx 61\%$), providing confirmation that *in vivo* pyruvate metabolism occurs almost exclusively via decarboxylation to acetyl CoA (a metabolic step requiring

the presence of thiamine pyrophosphate). On the contrary, only approximately 52% of ^{14}C administered as acetate-1-^{14}C appears in the breath as $^{14}CO_2$ within 60 minutes, suggesting that a small but measurable amount of acetate is "fixed" in more slowly catabolized compounds (e.g., fatty acids) as opposed to direct oxidation to CO_2 in the citric acid cycle.

In thiamine-deficient rats there is a significant delay in oxidation of both #1-^{14}C-pyruvate and acetate to $^{14}CO_2$. Within 45 minutes after IV injection of thiamine the $^{14}CO_2$ appearance curve following injection of acetate-1-^{14}C is within normal limits. In thiamine-deficient animals, $^{14}CO_2$ excretion following administration of $H^{14}CO_3^-$ is normal, but plasma clearance of ^{14}C-labeled thiamine is initially abnormally rapid, suggesting the presence in thiamine deficiency of unsaturated thiamine binding sites which equilibrate rapidly with plasma thiamine.

The $^{14}CO_2$ breath studies suggest the possibility of diagnosis of thiamine deficiency in man by determination of $^{14}CO_2$ appearance in the breath after administration of #1-^{14}C-pyruvate or acetate prior to, and subsequent to, the intravenous administration of thiamine. A significant increase in the rate of $^{14}CO_2$ production following administration of thiamine would suggest the presence of thiamine deficiency prior to thiamine administration.

IV. EFFECTS OF PHARMACOLOGICAL DOSES OF PYRIDOXINE ON TRYPTOPHAN CATABOLISM IN NORMAL RATS

A. Review of the problem

Pyridoxal phosphate is known to be a common coenzyme for a wide variety of biochemical reactions, including transaminations and decarboxylation (53,54). Additionally, previous studies demonstrated that either pyridoxine or pyridoxal phosphate increased the uptake of several amino acids (i.e., L-glycine, L-methionine, α-aminobutyric acid, γ-aminobutyric acid, and glutamate) into Ehrlich mouse-ascites carcinoma cells under either aerobic (55,56) or anaerobic (57,58) conditions. Similar results have been shown in vitamin B6-deficient rats treated with either L-penicillamine (59) or deoxypyridoxine (60). Moreover, pyridoxal phosphate and pyridoxine counteracted the inhibitory effect of 2,4-dinitrophenol (DNP) or intestinal absorption of L-methionine and L-histidine (61).

Little information is available concerning how pharmacological doses of pyridoxine may effect either the enhancement of cellular uptake of amino acids or other pyridoxal-phosphate dependent processes in the intact animals. Information on these points might provide a basis for understanding such clinical observations as the improvement of the "pyridoxine-responsive-anemia" following massive pyridoxine therapy (61).

In this study, appearance of $^{14}CO_2$ in the breath was measured following the intravenous administration of

L-tryptophan-1-^{14}C, L-histidine (imidazole-2-^{14}C), L-methionine-CH_3-^{14}C, and $NaH^{14}CO_3$ to control rats and to rats receiving pharmacological doses of pyridoxine.

B. Preparation of experimental animals

Inbred male Buffalo rats (Simonsen Laboratory, Gilroy, Calif.) weighing 220 to 250 g were used in all experiments.

In the first series of studies, control breath $^{14}CO_2$ studies were performed on seven rats prior to administration of pyridoxine. Six of these rats subsequently received 100 mg pyridoxine hydrochloride [2-methyl-3-hydroxy-4,5 (dihydroxymethyl) pyridine hydrochloride] (Eli Lilly and Co., Indianapolis, Indiana) intravenously 30 minutes prior to a repeat breath $^{14}CO_2$ study. In each $^{14}CO_2$ study, all rats received 5 μCi of L-tryptophan-1-^{14}C (carboxyl-labeled, specific activity: 20.42 mCi/mM, New England Nuclear Corp., 575 Albany Street, Boston, Massachusetts 02118) intravenously after light anesthesia with diethyl ether. The second study was performed 3 to 4 days after the initial control study.

In the second series of studies, the effect of pharmacological doses of pyridoxine on histidine catabolism was determined. The control group consisted of three rats. Three to four days after the initial control study, these rats were given pyridoxine in a fashion described above. In each study the rat received intravenously 2.5 μCi of L-histidine (imidazole-2-^{14}C) (specific activity: 57.8 mCi/mM,

Amersham/Searle Corporation).

In the third series of studies, the effect of pharmacological doses of pyridoxine on methionine catabolism was determined. Three rats were studied prior to and subsequent to injection of pyridoxine in the same procedure as described above. In each study the rat received intravenously 7 μCi of L-methionine-CH_3-^{14}C (specific activity: 14.77 mCi/mM, New England Nuclear Corp., same address as noted above).

In the fourth series of studies, the effect of pyridoxine one bicarbonate pool turnover was determined. Three rats were studied prior to and subsequent to the intravenous injection of pyridoxine. In each study the rat received 1 μCi of $NaH^{14}CO_3$ (specific activity: 21.5 mCi/mM, New England Nuclear Corp.) intravenously. For the bicarbonate pool turnover studies, the gas flow rate through the system was maintained at 3 liters/min. At this gas flow rate the mean washout time of the apparatus was less than 1 minute.

C. Results

Figures 9, 10, and 11 present curves showing the rate of $^{14}CO_2$ appearance in the breath of control and pyridoxine-treated rats subsequent to the intravenous administration of L-tryptophan-1-^{14}C, L-methionine-CH_3-^{14}C, and L-histidine (imidazole-2-^{14}C) respectively. The ordinate represents the rate of $^{14}CO_2$ excretion expressed as percent of administered ^{14}C excreted as $^{14}CO_2$ per minute on a

logarithmic scale and the abscissa as time in minutes on a linear scale following the intravenous administration of the ^{14}C-labeled materials. Each point represents the mean of excretion rates of $^{14}CO_2$ in the breath for each group of rats. The vertical bars at each time point define one standard error of the mean values for each group. It is clear that there is a qualitative difference between $^{14}CO_2$ breath curves of control rats and those of pyridoxine-treated rats subsequent to the intravenous administration of the ^{14}C-labeled tryptophan. After the injection of the ^{14}C-labeled histidine and methionine in pyridoxine-treated rats, no difference occurred in $^{14}CO_2$ appearance.

For data analysis, two parameters were used for each curve. The first parameter is the time at which the maximum rate of $^{14}CO_2$ excretion in the breath occurred ($T_{max.}$). The second parameter is the integral excretion of $^{14}CO_2$ during the initial 65 minutes after injection of ^{14}C-labeled tryptophan and during the initial 60 minutes after injection of either ^{14}C-labeled histidine or ^{14}C-labeled methionine. This latter parameter is a measure of the fraction of the ^{14}C involving the in vivo oxidation resulting in $^{14}CO_2$ production. Table VI digitally summarizes the data presented in Figs. 9 through 11. Figure 12 describes the rate of $^{14}CO_2$ appearance in the breath of control and pyridoxine-treated rats subsequent to the administration of $NaH^{14}CO_3$. Each point at 5, 10, 15, and 25 minutes

Fig. 9 presents composite data of the rate of $^{14}CO_2$ excretion following IV administration of L-tryptophan-1-^{14}C in seven controls and six rats treated with 100 mg pyridoxine HCl. The ordinate represents $^{14}CO_2$ excretion rate expressed as percent ^{14}C/min. and the abscissa as time in minutes following IV injection of L-tryptophan-1-^{14}C. Vertical bars through each point define ± 1 standard error of the mean of excretion rates of $^{14}CO_2$ for each group of rats.

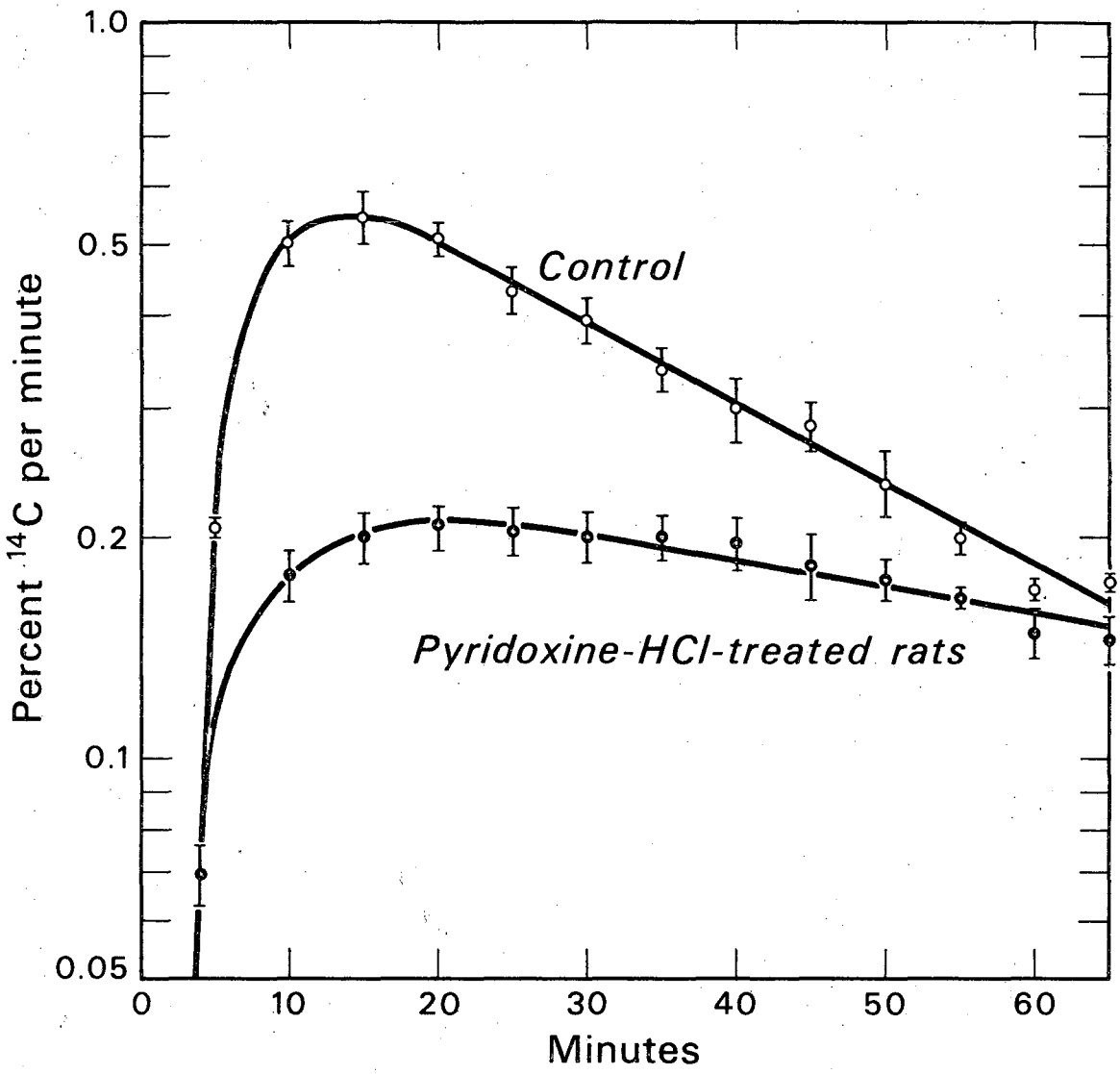

DBL 691-4510

Fig. 9

Fig. 10 presents composite data of the rate of $^{14}CO_2$ excretion following administration of L-methionine-CH_3-^{14}C in three control rats and three pyridoxine-treated rats. The ordinate represents $^{14}CO_2$ excretion rate expressed as percent ^{14}C/min. and the abscissa as time in minutes following IV injection of L-methionine-CH_3-^{14}C. Vertical bars through each point define ± 1 standard error of the mean of excretion rates of $^{14}CO_2$ for each group of rats.

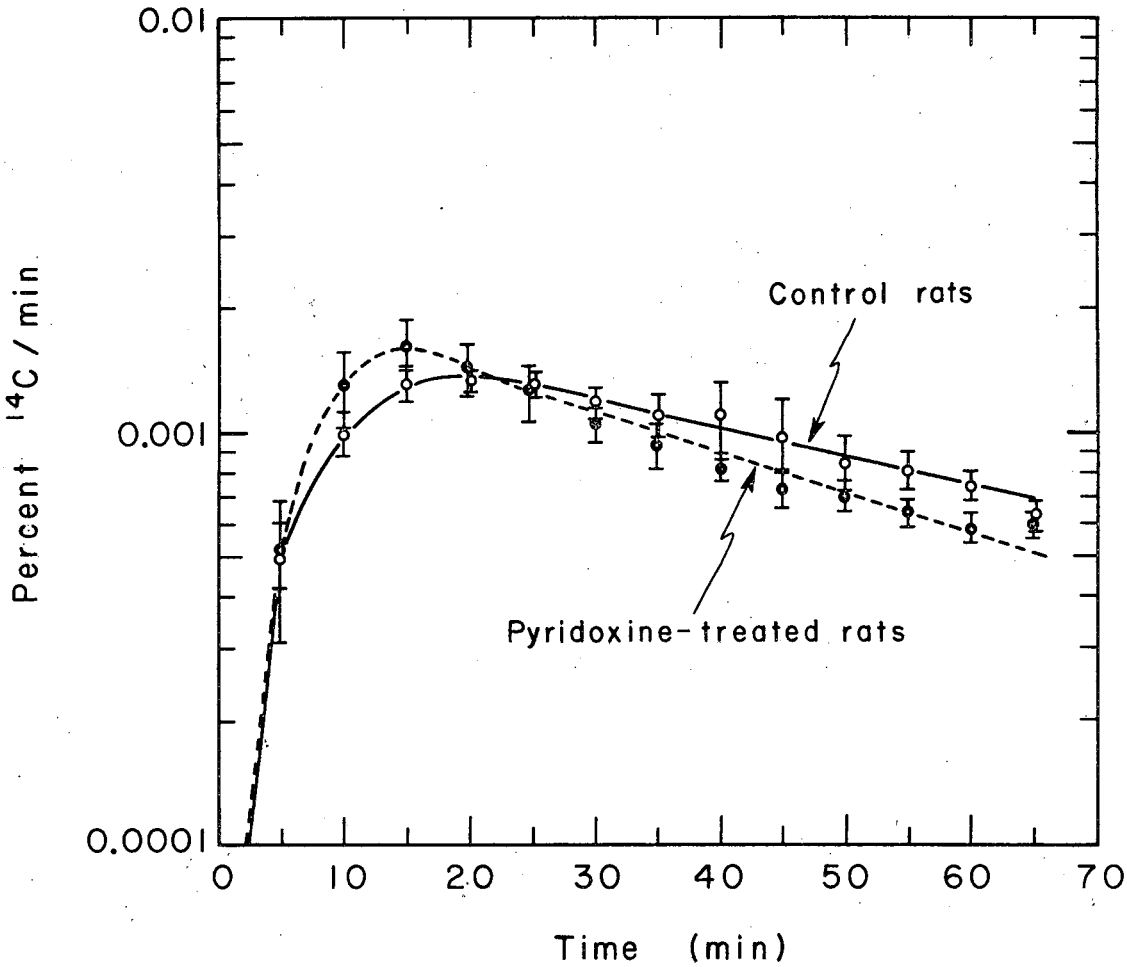
0.01
0.001
0.0001
Percent ^{14}C / min
Control rats
Pyridoxine-treated rats
0
10
20
30
40
50
60
70
Time (min)
XBL691-1731

Fig. 10

Fig. 11 presents composite data of the rate of $^{14}CO_2$ excretion following administration of L-histidine (imidazole-2-^{14}C) in three control rats and three pyridoxine-treated rats. The ordinate represents $^{14}CO_2$ excretion rate expressed as percent ^{14}C/min. and the abscissa as time in minutes following IV injection of L-histidine (imidazole-2-^{14}C). Vertical bars through each point define ± 1 standard error of the mean of excretion rates of $^{14}CO_2$ for each group of rats.

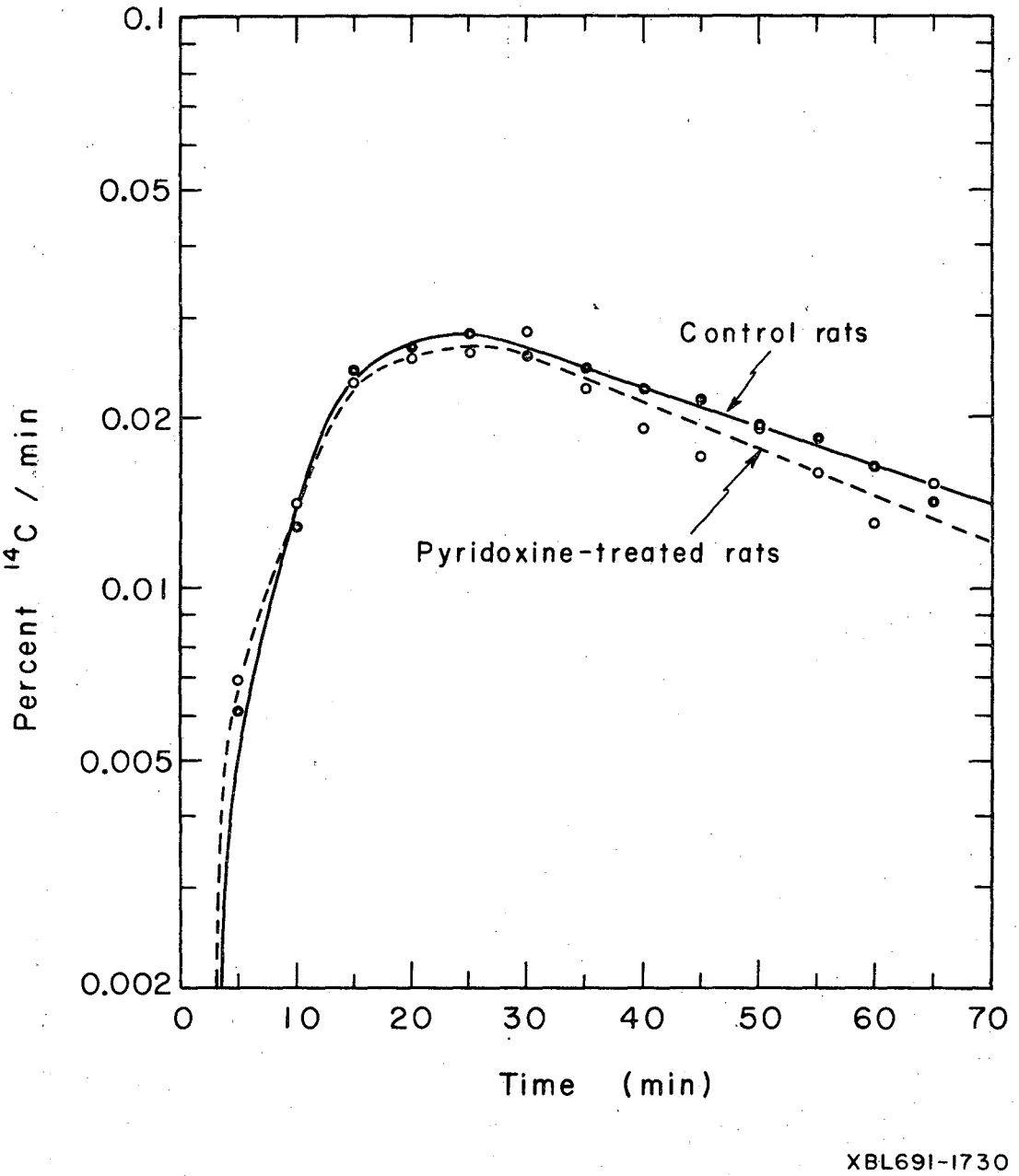
0.1
0.05
0.02
0.01
0.005
0.002
Percent ^{14}C / min
Control rats
Pyridoxine-treated rats
0
10
20
30
40
50
60
70
Time (min)
XBL691-1730

Fig. 11

represents the mean of excretion rate of $^{14}CO_2$ in the breath for each group of rats. Vertical bars through each point define precision of the mean with 95% limits based on $t_{.95}\ S_{y.x.}$ ($S_{y.x.}$ = standard error of the estimate). The zero time intercept (A) and the slope of the regression function (B) were determined by the least-squares best fit of the data to the function

$$Y = A + [B \pm S_{b(x).(y)}]\ X.$$

The broken lines immediately above and below each curve are regression lines of $\pm$ 1 standard error of the estimate ($S_{x.y.}$). In this analytic procedure the slopes of the $^{14}CO_2$ curves are analyzed at 5 minutes after intravenous injection of $NaH^{14}CO_3$. The slope (expressed as $T_{1/2}$) and integral amount ^{14}C excreted in the breath (expressed as %) during the initial 50 minutes of bicarbonate study for each group of rats are summarized in Table V.

D. Discussion

In these studies, we demonstrate a significant and selective effect of pharmacological doses of pyridoxine on the pattern of $^{14}CO_2$ production from the *in vivo* oxidation of L-tryptophan-1-^{14}C in normal rats. Such effects were not seen in pyridoxine-treated rats injected with L-histidine (imidazole-2-^{14}C), L-methionine-CH_3-^{14}C, or $NaH^{14}CO_3$. The alterations in the appearance of $^{14}CO_2$ from labeled tryptophan in pyridoxine-treated rats may be due to either alterations in its catabolism (such as possible enhancement

Fig. 12 presents composite data of the rate of $^{14}CO_2$ excretion following IV administration of $H^{14}CO_3$ in three controls and three pyridoxine-treated rats. Vertical bars through each point defines precision of position of the mean of excretion rates of $^{14}CO_2$ for each group of rats with 95% limits based on $t_{.95}\ S_{y.x.}$. The broken lines above and below each curve are regression lines of ± 1 standard error of the estimate ($S_{y.x.}$).

The ordinate represents $^{14}CO_2$ excretion rate expressed as percent ^{14}C/min. and the abscissa as time in minutes following IV administration of $H^{14}CO_3$.

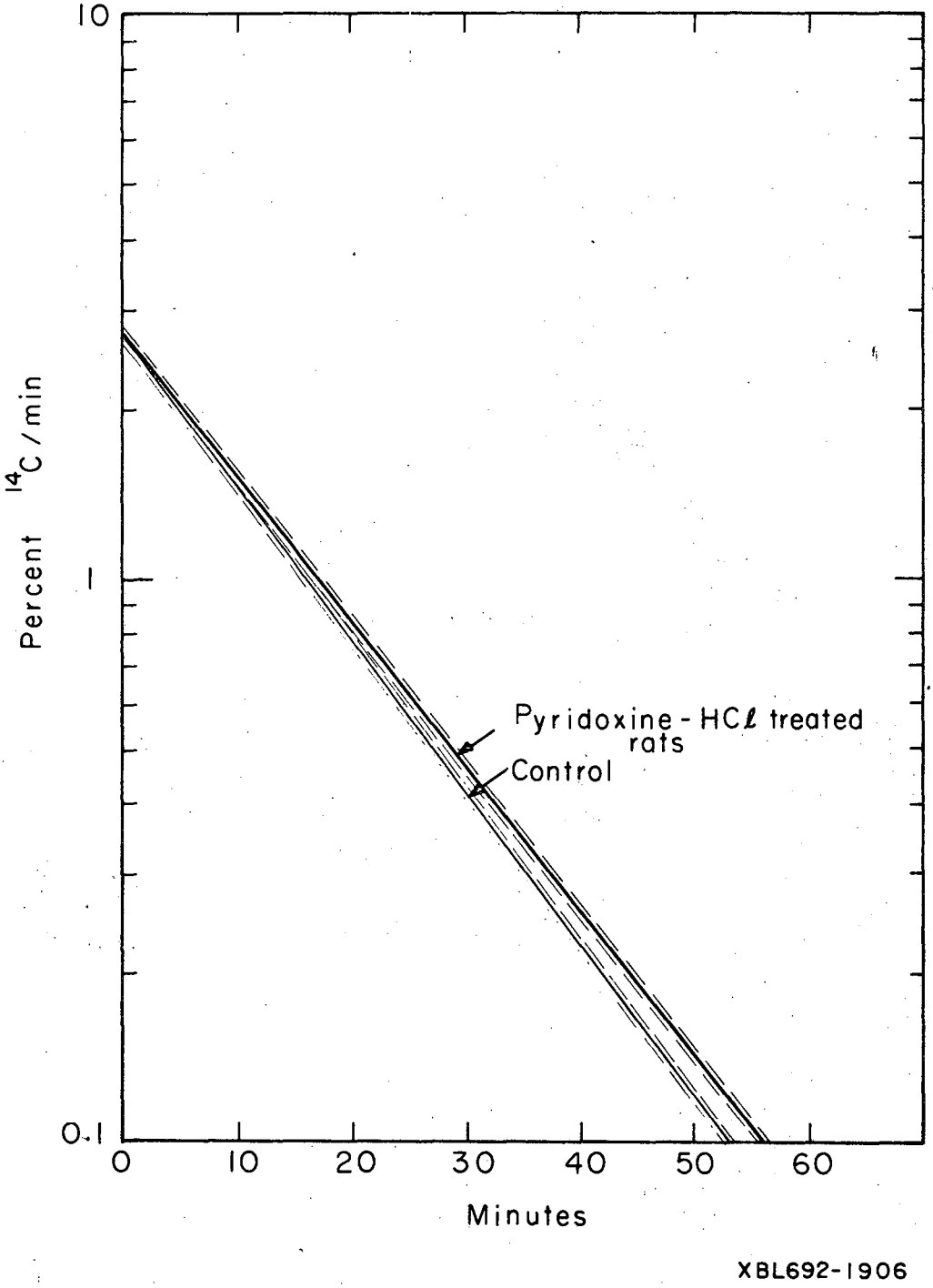
10
1
0.1
Percent ^{14}C / min
0
10
20
30
40
50
60
Minutes
Pyridoxine - HCl treated rats
Control
XBL692-1906

Fig. 12

Table IV

T_{max} and integral ^{14}C excretion determined from $^{14}CO_2$ appearance in breath following the intravenous administration of L-tryptophan-1-^{14}C, L-methionine-CH_3-^{14}C or L-histidine (imidazole-2-^{14}C) in control and pyridoxine-treated rats (the number of animals in each group is noted in parentheses).

Category	T_{max} (minutes) ± S.E.	^{14}C excretion in the breath during initial 60 or 65 minutes (%) ± S.E.
L-tryptophan-1-^{14}C		
Control (7)	13.92 ± 0.95	20.99 ± 1.98
Rats 30 minutes after IV administration of 100 mg pyridoxine HCl (6).	23.50 ± 1.03	11.50 ± 1.69
L-methionine-CH_3-^{14}C		
Control (3)	16.00 ± 1.04	0.71 ± 0.08
Rats 30 minutes after IV administration of 100 mg pyridoxine HCl (3)	20.33 ± 5.67	0.83 ± 0.09
L-histidine (imidazole-2-^{14}C)		
Control (3)	26.33 ± 1.85	1.54 ± 0.14
Rats 30 minutes after IV administration of 100 mg pyridoxine HCl (3)	25.67 ± 1.59	1.71 ± 0.11

of the formation of nicotinic acid with resulting decreased rate of conversion of tryptophan to serotonin) or increased physical transport of tryptophan across the cell membrane. The latter possibility is supported by the data obtained by M. Lin and H. S. Winchell in an *in vitro* study using dog bone-marrow cells incubated with L-tryptophan-3-^{14}C and L-histidine (imidazole-2-^{14}C) in basal medium of Eagle, with or without pyridoxal. This study demonstrated an expansion of the intracellular pool size of tryptophan, a change which could explain the delayed excretion of $^{14}CO_2$ in the breath of pyridoxine-treated rats in the present studies.

The mechanism of increased physical transport of tryptophan and histidine across the cell membranes in the presence of pyridoxine may be related to the formation of the Schiff bases involving those amino acids, pyridoxal, and a metal ion (63).

In addition, it is clear that rats treated with pharmacological doses of pyridoxine do not show significant alterations in CO_2-H_2CO_3-HCO_3 pool kinetics detected by the breath analysis.

E. Summary

In these studies, we demonstrated a selective effect of pharmacological doses of pyridoxine on the $^{14}CO_2$ production in the breath of normal rats subsequent to intravenous administration of the ^{14}C-labeled tryptophan.

Table V

Slope ($T_{1/2}$) and integral ^{14}C excretion determined from $^{14}CO_2$ appearance in breath following administration of $^{14}CO_3$ in control and pyridoxine-treated rats (the number of animals in each group is noted in parentheses).

Category	Half-time $T_{1/2}$ (minutes)	^{14}C excretion in 50 minutes (%) ± S.E.
Control (3)	7.88	64.24 ± 3.07
Rats 30 minutes prior to IV administration of 100 mg pyridoxine HCl (3)	8.98	62.80 ± 2.18

In normal rats given pharmacological doses of pyridoxine subsequent to injection of the ^{14}C-labeled histidine and methionine, these determinations were unchanged in comparison with control values. These results indicated that pharmacological doses of pyridoxine either increased selectively the rate of physical transport of tryptophan to intracellular sites of catabolism with a resultant enlarged intracellular pool size of this amino acid, or they altered the fractional turnover rates involved in tryptophan catabolism.

Treatment of rats with pharmacological doses of pyridoxine did not result in any alterations in CO_2-H_2CO_3-HCO_3, histidine, and methionine kinetics detectable by these in vivo studies.

V. ALTERATIONS IN HISTIDINE CATABOLISM IN NORMAL RATS GIVEN PHARMACOLOGICAL DOSES OF FOLIC ACID AND CYANOCOBALAMIN

A. Review of the problem

The #2 carbon atom of the imidazole ring of histidine is uniquely catabolized to CO_2 by passage through the "monocarbon pool" associated with a reduced form of folic acid (83). The rate of oxidation of this carbon atom to CO_2 has been shown to be markedly diminished in either folic acid or cyanocobalamin (vitamin B12)-deficient rats (84), and in folic acid deficient human subject (23,24).

In cyanocobalamin-deficient human subjects the rate of CO_2 production from the imidazole #2-carbon atom site of histidine appears to be normal (23,24). This paper demonstrates significant alterations in histidine catabolism in normal rats given pharmacological doses of either folic acid or cyanocobalamin.

B. Preparation of experimental animals

Normal inbred Buffalo rats (Simonsen Laboratory, Gilroy, California) fed S-L white diet (protein, 24.00%; fat, 6.85%; fiber, 3.14%; calcium, 0.73%; phosphorus, 0.52%; ash, 4.69%, vitamins A, D, Riboflavin, pantothenic acid, niacin, choline), weighing 240 to 245 g were divided into control, folic acid-treated, and cyanocobalamin-treated groups. The control group consisted of ten rats which received no prior treatment. The group receiving cyanocobalamin consisted of four rats given 250 µg of cyanocobalamin intravenously 60 minutes prior to the study (Rubramin, E. R. Squibb and Sons, N. Y.). The group receiving folic acid consisted of six rats which were given 15 mg of folic acid subcutaneously 60 minutes prior to the study (Folvite, Lederle Laboratories Division, American Cyanamid Company, Pearl River, N. Y.). At the initiation of each study, each rat, under light anesthesia with diethyl ether, received 2.5 µCi of L-histidine (imidazole-2-^{14}C) intravenously (specific activity: 57.8 mCi/mM,

Amersham/Searle Corporation). Immediately after such injection the animal was placed in a device which measured the $^{14}CO_2$ excretion rate.

C. Results

Figure 13 presents composite data of the rate of $^{14}CO_2$ production following intravenous administration of L-histidine (imidazole-2-^{14}C) in ten control rats, four rats given 250 μg cyanocobalamin intravenously 60 minutes prior to the study, and six rats given 15 mg folic acid subcutaneously 60 minutes prior to the study. The ordinate represents percent of administered ^{14}C excreted as $^{14}CO_2$ per minute, and the abscissa represents time in minutes following intravenous injection of L-histidine (imidazole-2-^{14}C). Each point represents the mean of the $^{14}CO_2$ excretion rate for each group of animals at the given time, and the lengths of the vertical bars through each point represent one standard error of the mean for each group.

It can be seen that qualitative differences exist between control curves and those obtained in either cyanocobalamin- or folate treated rats. For comparison of $^{14}CO_2$ breath curves, two parameters have been utilized for each curve. The first parameter is the time at which the maximum rate of $^{14}CO_2$ excretion in the breath occurs ($T_{max.}$), and the second parameter is the cumulative percentage of ^{14}C appearing as $^{14}CO_2$ within the initial 60 minutes subsequent to the intravenous administration of the ^{14}C-

Figure 13 presents composite data of the rate of $^{14}CO_2$ production following intravenous administration of L-histidine (imidazole-2-^{14}C) in ten control rats, four rats given 250 µg cyanocobalamin intravenously 60 minutes prior to the study, and six rats given 15 mg folic acid subcutaneously 60 minutes prior to the study. The ordinate represents percent of administered ^{14}C excreted as $^{14}CO_2$ per minute and the abscissa represents time in minutes following intravenous injection of L-histidine (imidazole-2-^{14}C). Each point represents the mean of the $^{14}CO_2$ excretion rate for each group of animals at the given time, and the length of the vertical bars through each point represents one standard error of the mean for each group.

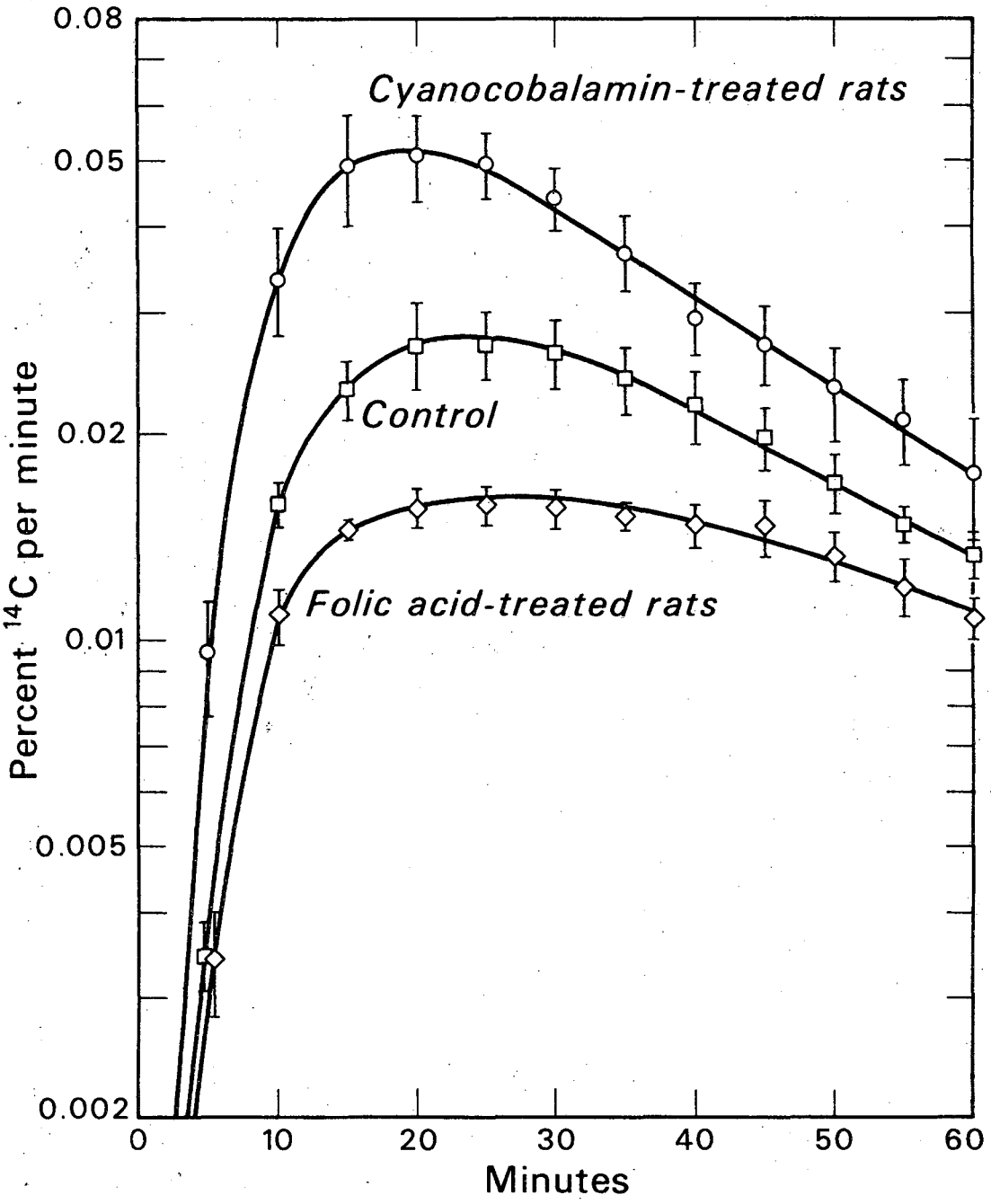

XBL 6812-6437

Fig. 13

labeled histidine. Table XIII presents values for the mean and standard error of the mean (S.E.) for each of these two parameters as determined in each individual study. From Fig. 13 and Table XIII we may conclude that normal rats pretreated with pharmacological doses of cyanocobalamin show a greater initial excretion rate of $^{14}CO_2$ and a shorter time before the maximum rate of $^{14}CO_2$ excretion is reached (T_{max}) than normal untreated rats, whereas normal rats pretreated with pharmacological doses of folic acid show a slower initial excretion rate of $^{14}CO_2$ and a longer T_{max} than normal untreated rats.

D. Discussion

These results demonstrate that pharmacological doses of cyanocobalamin increase the rate and amount of oxidation of the imidazole #2-carbon atom site of histidine to CO_2 in vivo, whereas pharmacological doses of folic acid have the opposite effect. Kinetically stated, these results mean that the fractional turnover rate of the rate-limiting processes involved in the oxidation of this carbon atom of intravenously administered histidine and the fraction of this carbon atom oxidized to CO_2 are increased by pharmacological doses of cyanocobalamin and decreased by pharmacological doses of folic acid. It is possible that this may result from alterations in physical transport of administered histidine to intracellular sites of catabolism such as might occur secondary to alteration in the kinetics of cell-membrane transport of histidine.

Table XIII

Changes in the time at which the maximum rate of excretion of $^{14}CO_2$ in expired breath occurred (T_{max}) and cumulative percentage of $^{14}CO_2$ excreted in breath during the initial 60 minutes following IV administration of L-histidine (imidazole-2-^{14}C) in control rats and rats given either folic acid or cyanocobalamin. The mean value and standard error of the mean for T_{max} and percent ^{14}C excreted in 60 minutes are given. (The number of animals in each group of rats is noted in parentheses).

Category	T_{max} (minutes) ± S.E.	^{14}C excretion in 60 minutes (%) ± S.E.
Control (10)	23.10 ± 0.77	1.02 ± 0.10
15 mg folic acid administered subcutaneously 60 minutes prior to study (6)	28.58 ± 1.16	0.72 ± 0.02
250 µg cyanocobalamin administered intravenously 60 minutes prior to study (4)	19.12 ± 1.38	1.84 ± 0.26

This possibility is presently being investigated in our laboratory. It is also possible that the results obtained may be due to alterations in the biochemical kinetics involved in histidine catabolism. It has been shown previously that high levels of folic acid inhibit dihydrofolic acid reductase in vitro (85). If the turnover rate of tetrahydrofolic acid (THF) moieties is sufficiently rapid to exhaust significantly any preformed THF within 1 hour, then this may explain our results following administration of high doses of folic acid. From evidence in cyanocobalamin-deficient subjects it has been postulated that cyanocobalamin influences the utilization of methylated tetrahydrofolic acid (86). If these results are due to cyanocobalamin-induced acceleration of catabolism of the imidazole #2-carbon atom of histidine after its attachment to tetrahydrofolate, then such an effect is not maximal at physiological levels of cyanocobalamin.

E. Summary

Following administration of histidine (imidazole-2-^{14}C) to normal rats given pharmacological doses of cyanocobalamin, the initial rate and amount of $^{14}CO_2$ excreted in the breath is significantly increased, whereas in normal rats given pharmacological doses of folic acid these measurements are decreased in comparison with normal untreated rats. These results indicate that

pharmacological doses of cyanocobalamin increase and folic acid decrease either the rate of physical transport of histidine to intracellular sites of catabolism of the fractional rate describing the actual biochemical steps of individual reactions involved in such catabolism.

VI. IN VIVO INACTIVATION OF FOLIC ACID BY IONIZING RADIATION

A. Review of the Problem

Sources of monocarbon fragments are the methyl group of methionine, betaine, and choline; the formaldehyde and formate groups arising from glycine and serine; and the formimino group of formimino glutamic acid arising from the catabolism of histidine. Folic acid, in its reduced form of tetrahydrofolic acid, is the carrier of monocarbon fragments. Monocarbon fragments are essential for nucleic acid synthesis, being incorporated into the 2 and 8 positions of purines, and as the source of the methyl group of thymine (Fig. 14).

Recent studies have revealed that irradiation of folic acid with ultraviolet results in its rapid inactivation, as measured by microbiological assay (64,65). Concentrations of both folic acid and citrovorum factor were markedly decreased in spleen 6 to 8 hours after whole-body irradiation with 400 to 600 R, and in liver and testis 6 days after local irradiation with 3000 R (66). Recent studies obtained by Winchell and Vimokesant (67) demonstrated that the de novo synthesis, using ^{14}C-formate and

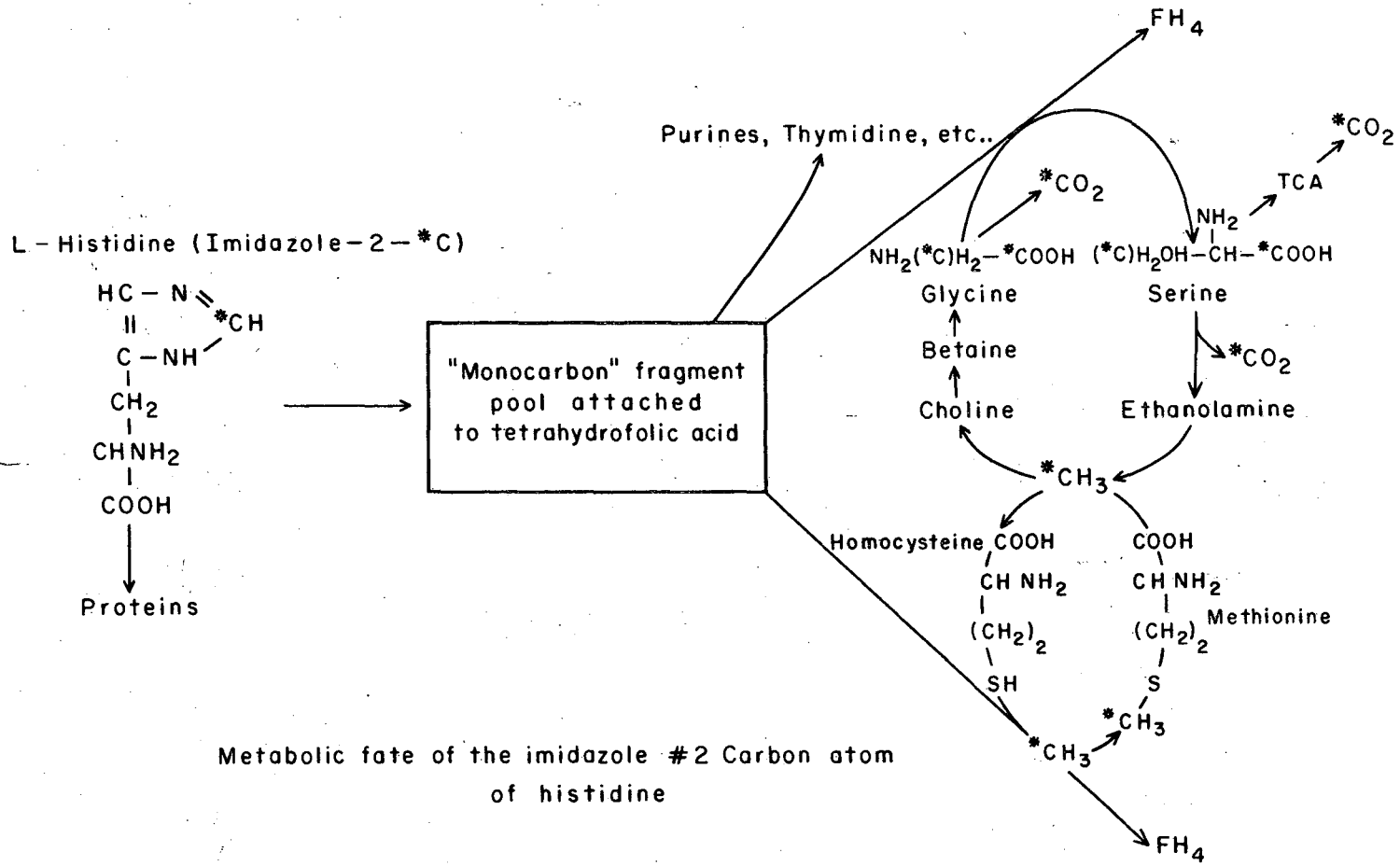

Metabolic fate of the imidazole #2 Carbon atom of histidine

Fig. 14

L-serine-3-^{14}C, was more radiosensitive than the incorporation of the base ^{3}H-thymidine into DNA thymine. Fish and Pollycove demonstrated that decreased availability of tetrahydrofolic acid *in vivo* resulted in a characteristic diminution in the appearance of $^{14}CO_2$ in the breath subsequent to intravenous administration of L-histidine (imidazole-2-^{14}C) (23,24). In the present study, we demonstrate a similar finding in irradiated rats subsequent to the intravenous injection of L-histidine (imidazole-2-^{14}C), and we suggest that such decreased $^{14}CO_2$ production in the breath may be due to either an *in vivo* radiation inactivation of tetrahydrofolic acid or the enzymatic processes responsible for its production. In additional studies, L-methionine-CH_3-^{14}C, L-glycine-1-^{14}C, L-serine-3-^{14}C, and ^{14}C-formate were injected into irradiated rats to determine whether the results obtained could be explained as nonspecific effects on cells or whether they specifically indicated radiation effects on monocarbon transport.

A second set of studies was performed in which large doses of methotrexate were administered to normal rats in an attempt to simulate the effects of ionizing radiation.

A third set of experiments was performed to determine the effect of radiation on hepatic binding of methotrexate-3', 5-'^{3}H. This latter measurement was felt to be a measure of folic acid reductase activity (68).

B. Preparation of experimental animals

1. Effects of radiation on oxidation of monocarbon fragment precursors to CO_2

Inbred male Buffalo rats (Simonsen Laboratory, Gilroy, California) weighing 240 to 330 g were used in all experiments. These animals had free access to food and water during the period of study.

a. L-histidine (imidazole-2-^{14}C)

Twelve male Buffalo rats weighing 285 to 330 g were used in this study. Pairs of animals were studied in groups receiving sham irradiation and exposure to 200, 400, and 600 R of x rays. Sham irradiated animals were placed in the same condition configuration in x ray field for the same time periods as those receiving x irradiation. The source of x rays for these experiments was an x ray machine (philips, Holland, type 11645, C13832) operated at 150 kVp and 15 mA and with an inherent filtration of 1 mm of aluminum and 1 mm of copper. The target-animal distance was 10 inches. The dose rates, measured in air, were 15 to 27 r/min. Animals were studied at 16 minutes and then at 2, 5, 8, 11, 15, 23, and 30 days after the irradiation or sham-irradiation procedures. In each study, the rat received 5 μCi of L-histidine (imidazole-2-^{14}C) intravenously (specific activity: 51.8 mCi/mM, Nuclear Chicago, 333 East Howard Avenue, Des Plaines, Illinois 60018).

b. L-methionine-CH_3-^{14}C

Seven male Buffalo rats were divided into two group of three sham-irradiated and four irradiated rats. The irradiated rats were subdivided further into two pairs of rats exposed to 400 and 600 r of x rays. Studies were performed at 20 minutes and then at 2, 5, 9, 16, and 21 days after sham-irradiation or irradiation exposures. Each rat received 14 µCi of L-methionine-CH_3-^{14}C intravenously (specific activity: 14.77 mCi/mM, New England Nuclear Corp., 575 Albany street, Boston. Massachusetts 02118).

c. ^{14}C-formate

Twelve male Buffalo rats weighing 240 to 250 g were divided into two groups of six sham-irradiated rats and six rats given 400 and 600 r of x rays. The first experiments were studied at 20 minutes, and repeat studies were then performed at 2, 5, 9, 14, and 20 days after irradiation. In each study, the rat received 2.5 µCi of ^{14}C-formate intravenously (specific activity: 4.62 mCi/mM, New England Nuclear Corp.).

d. L-glycine-1-^{14}C

Sixteen male Buffalo rats were used in three experiments. The rats were divided into two group of seven sham-irradiated rats and nine irradiated rats studied in groups receiving 400 and 600 r of x rays. Irradiation procedure was similar to that described previously. Sham-irradiated and irradiated rats were studied at 20 minutes and then at

3, 5, 7, 12, and 20 days after irradiation or sham-irradiation procedures. In each study, the rat received 2.5 μCi of L-glycine-1-^{14}C intravenously (specific activity: 5.0 mCi/mM, Nuclear Chicago).

e. L-serine-3-^{14}C

Eight male Buffalo rats were divided into sham-irradiated and irradiated groups. Sham-irradiated and irradiated rats were studied in pairs after sham irradiation or irradiation and then studies were repeated at 3, 5, 9, 14, and 21 days later. In each study, the rat, after anesthetization with diethyl ether, received 2.5 μCi of L-serine-3-^{14}C intravenously (specific activity: 8.5 mCi/mM, Nuclear Chicago).

2. Methotrexate studies

a. cold methotrexate

Eight male Buffalo rats weighing 240 to 250 g were divided into two groups of four control and four methotrexate-treated rats. Each methotrexate-treated rat received 2.5 mg of methotrexate (4-amino-N^{10}-methyl pteroyglutamic acid, Lederle Laboratories Division, American Cyanamid Company, Pearl River, N.Y.) intravenously, 3 hours prior to the intravenous administration of 2.5 μCi of L-histidine (imidazole-2-^{14}C). A measure of $^{14}CO_2$ production has been performed by the same procedure as described above. Repeat studies had been performed at 3 days after methotrexate treatment.

b. <u>influence of radiation on hepatic bindings of methotrexate-3', 5'-^{3}H</u>

Seven male Buffalo rats weighing 230 to 245 g were assembled into two groups of three control and four irradiated rats. Rats of the irradiated group were exposed to x radiation and produced by a 200 kVp machine, at 15 mA and with an inherent filtration equivalent to 1 mm of aluminum and 1 mm of copper. The target-animal distance was 30 cm. The dose rate, measured in air, was 46 r/min, and the total doses given were 2000 and 3000 r.

Two hours after irradiation, each rat of the control and irradiated groups received 100 μCi of methotrexate-3', 5'-^{3}H (specific activity: 250 mCi/mM, Nuclear Chicago) diluted with 10 mg of cold methotrexate (4-amino-N^{10}-methyl Pteroyglutamic acid, Lederle Laboratories Division, American Cyanamid Company, Pearl River, N.Y.) intravenously under light ether anesthesia. One hour after the intravenous injection of the ^{3}H-labeled methotrexate, the rats were sacrificed. The liver was removed and washed with saline. All surgical operations and irradiations were carried out between 10:35 a.m. and 2:30 p.m. The livers were homogenized in saline in a Waring Blendor. After three washings with saline, the homogenates were dried at 60°C and weighed to obtain the total dry liver weight. Samples of each were weighed and the aliquots were then digested in 3 ml of Nuclear Chicago solubilizer (0.6 n

solution in toluene) which was added to 18 ml of scintillation liquid made of 30% methanol in toluene containing 4 g of naphthalene 2,5-diphenyloxazole (PPO, Scintillation Grade, Packard Instrument Company, Downers Grove, Ill.) and 100 mg of 1,4 bis-(2-(5-phenyloxazolyl)-benzene (POPOP, scintillation grade, same address as above) per liter. The ^{3}H activity in the solution was determined by a Nuclear Chicago Model 725 liquid scintillation counter. Internal standardization was obtained with a radioactive solution standard (C_6H_5-CH_3-^{3}H) in toluene (specific activity: 3.042×10^5 dpm/ml, Nuclear Chicago). Counting efficiency was 1.7389% ± 0.1360, and background was generally 23.2 counts/min.

C. Results

1. Effects of radiation on oxidation of monocarbon fragment precursors to CO_2

a. L-histidine (imidazole-2-^{14}C)

Figure 15 presents representative curves depicting the rate of $^{14}CO_2$ appearance in the breath of pairs of normal animals (upper curve) and in rats 8 days after exposure to 400 r (lower curve) following the intravenous administration of L-histidine (imidazole-2-^{14}C). The ordinate represents rate of $^{14}CO_2$ appearance in the breath expressed as % ^{14}C per minute and the abscissa as time in minutes following intravenous injection of the ^{14}C-labeled histidine. It can be seen that there is a qualitative difference between

the two curves.

Figure 16 presents the composite data of the serial change in T_{max} (expressed as minutes), subsequent to the IV administration of the ^{14}C-labeled histidine to sham irradiated rats and rats receiving various doses of x rays.

No change was seen in T_{max} in serial studies performed in six sham irradiated controls following the IV administration of histidine (imidazole-2-^{14}C). The maximum range of T_{max} in these animals was from 12 to 12.5 minutes. Irradiated rats showed early significant prolongation in T_{max} within 16 minutes following irradiation. The maximum prolongation in T_{max} was reached at 5 to 8 days, returning to near normal by the fifteenth postirradiation day (50).

Figure 17 presents the results of the cumulative excretion of $^{14}CO_2$ in the breath during the initial 80 min subsequent to the intravenous administration of the ^{14}C-labeled histidine in irradiated rats. It can be seen that the cumulative excretion of $^{14}CO_2$ in the breath diminished during the fifth to eighth day following irradiation, but returned to near the normal range by the fifteenth day.

The data used in Figs. 16 and 17 are summarized in Table VI.

b. L-methionine-CH_3-^{14}C

Figure 18 presents representative curves showing the rate of appearance of $^{14}CO_2$ in the breath of three control

Fig. 15. Pattern of $^{14}CO_2$ excretion rates in the breath of pairs of normal rats (open circles) and in rats 8 days after exposure to 400 R (closed circles). The percentage of administered ^{14}C appearing the breath as $^{14}CO_2$ per minute is plotted on the ordinate, and time after intravenous administration of histidine (imidazole-2-^{14}C) is plotted on the abscissa. Each point represents the mean value of data from a pair of rats.

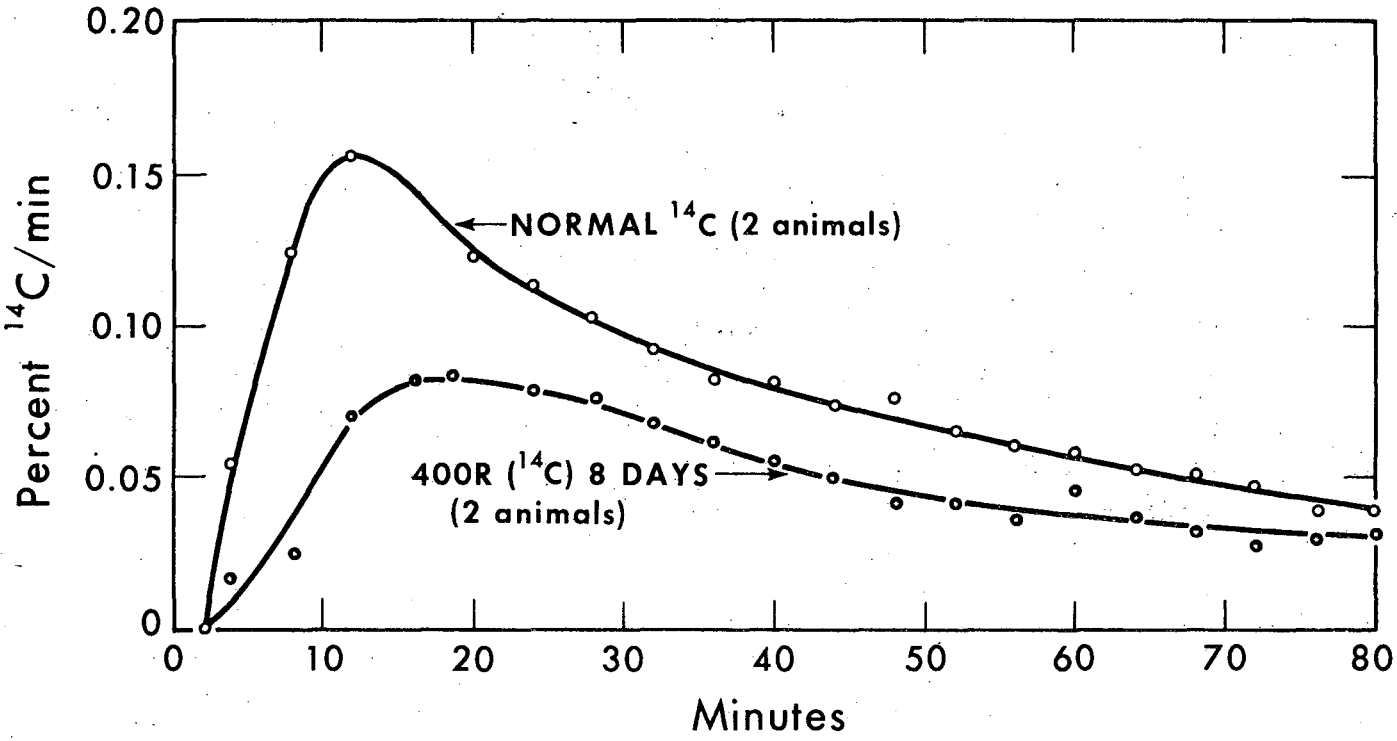

XBL 677-4329

Fig. 15

rats (upper curve) and two rats two days after exposure to 600 R (lower curve) subsequent to the intravenous administration of L-methionine-CH_3-^{14}C. The ordinate represents $^{14}CO_2$ excretion rate expressed as mμCi per minute the the abscissa as time in minutes following intravenous injection of the ^{14}C-labeled methionine. In the normal curve, each point represents the mean of the rate at the given time, and the vertical bars through each point represents 1 standard error for the mean of this group. It is clear there is a qualitative difference between the $^{14}CO_2$ breath curves.

Figure 19 presents composite data of the serial change in T_{max} (expressed as minutes) In control and irradiated rats subsequent to the intravenous administration of the ^{14}C-labeled methionine. Irradiated rats showed a significant prolongation in T_{max} on the second and fifth postirradiation days, and the T_{max} returned to the normal range by the ninth day.

Figure 20 presents the cumulative percent of $^{14}CO_2$ excretion of control and irradiated rats during the 60 min after intravenous injection of L-methionine-CH_3-^{14}C. There is a significant decrease of the cumulative excretion of $^{14}CO_2$ in rats given 400 R at 5 and 9 days, returning to the normal range by the sixteenth day. A markedly diminished $^{14}CO_2$ production in rats given 600 R was noted as early as 20 minutes after irradiation, and this decrease

Fig. 16. Changes in the time at which maximum rate of $^{14}CO_2$ excreted in the breath occurred (T_{max}) after intravenous administration of histidine (imidazole-2-^{14}C) in irradiated and control rats. Each line represents the mean value of data from a pair of rats. The T_{max} is plotted on the ordinate, and time after irradiation is plotted on the abscissa. Results in irradiated rats are shown in the heavier upper curves, and results in the sham-irradiated controls are shown in the lighter lower curves. The 0-day value for each study represents values obtained 16 minutes after the irradiation or sham-irradiation procedure.

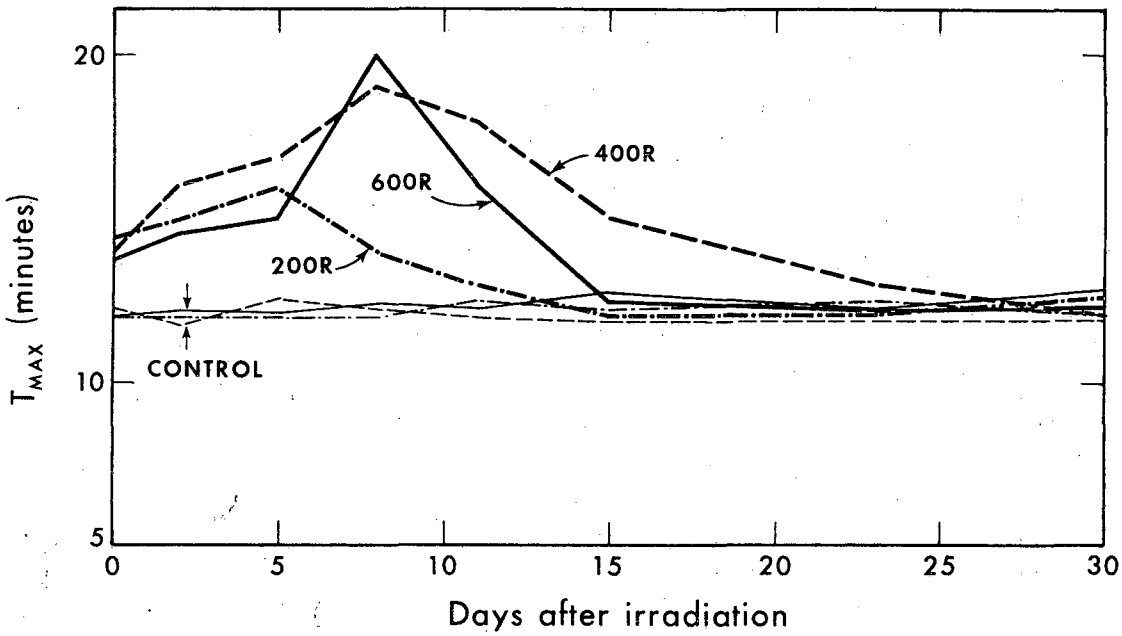

XBL 674-1330

Fig. 16

Fig. 17. Changes in the cumulative percentage of $^{14}CO_2$ excreted in the breath during the 80 minutes following intravenous administration of histidine (imidazole-2-^{14}C) in irradiated rats. Cumulative percentage of $^{14}CO_2$ excreted in 80 minutes is plotted on the ordinate, and days after irradiation is plotted on the abscissa. Each line represents the mean value of data from a pair of rats. The 0-day value for each study represents values obtained 16 minutes after the irradiation or sham-irradiation procedure.

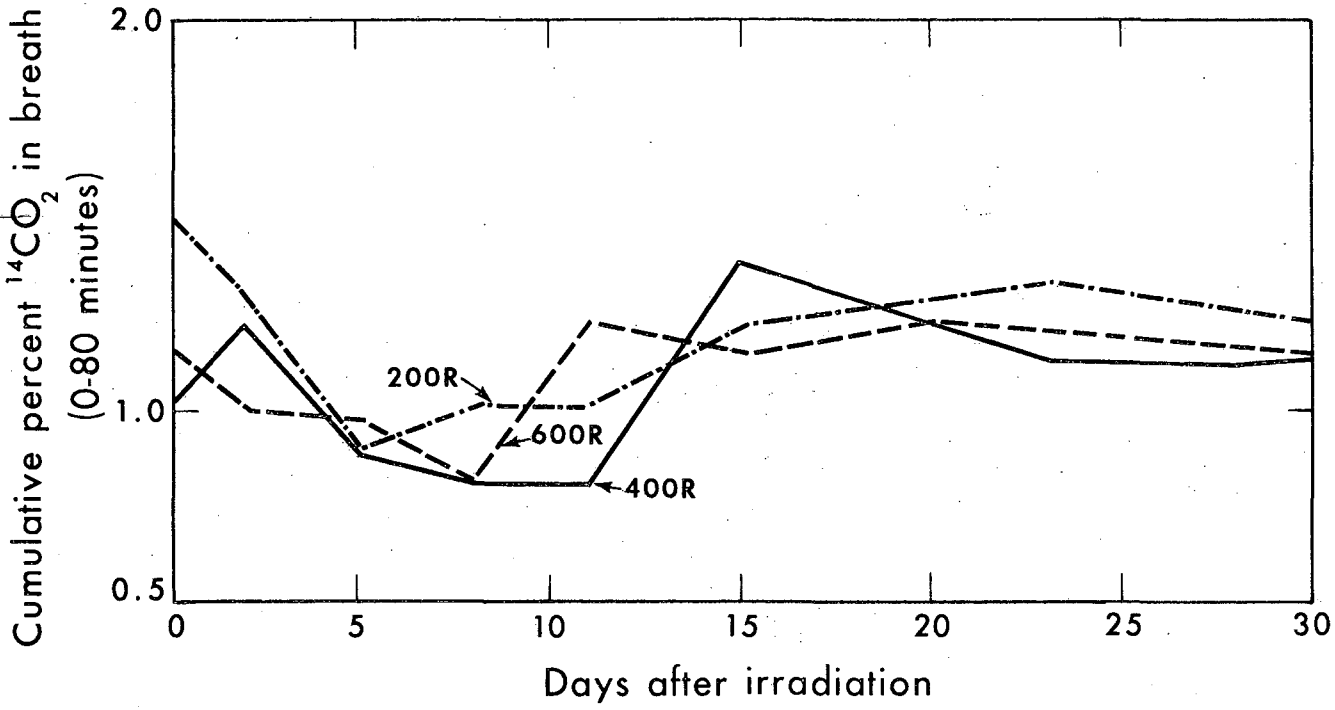

XBL 678-4495

Fig. 17

Table VI

Changes in T_{max} and Cumulative ^{14}C Excretion in Breath

Category	Time of study after irradiation or sham irradiation	T_{max} (minutes)	^{14}C (% excretion in 80 minutes)
Normal animals (6)	16 minutes, 2,5,8, 11,15,23, and 30 days	12-12.5 (total range)	1.177 ± = 0.008
Irradiated animals			
200 R (2)	16 minutes	14.5	1.522
	2 days	15	1.304
	5 days	16	0.891
	8 days	14	1.030
	11 days	13	1.034
	15 days	12	1.212
	23 days	12	1.318
	30 days	12	1.211
400 R (2)	16 minutes	14	1.007
	2 days	15	1.221
	5 days	17	0.885
	8 days	19	0.801
	11 days	18	0.805
	15 days	15	1.394
	23 days	13	1.116
	30 days	12	1.121
600 R (2)	16 minutes	14	1.165
	2 days	14.5	1.077
	5 days	15	0.980
	8 days	20	0.819
	11 days	16	1.238
	15 days	12.5	1.114
	23 days	12	1.223
	30 days	12	1.117

This table presents the values of the time at which maximum excretion of $^{14}CO_2$ in the breath (T_{max}) occurred and the cumulative ^{14}C excreted in the breath of rats after intravenous administration of histidine (imidazole-2-^{14}C). No significant change in these parameters was seen in serial studies performed at various stated times following sham irradiation of control animals. Values for T_{max} in this control group fell within the range of 12.0 to 12.5 minutes while values for ^{14}C excretion in the breath within 80 minutes were 1.177 ± 0.008% (S.E.). The number of animals in each category is noted in parentheses.

Fig. 18. Pattern of $^{14}CO_2$ excretion rates in the breath of three normal rats (upper curve) and in two rats two days after exposure to 600 R (lower curve). The percentage of administered ^{14}C appearing in the breath as $^{14}CO_2$ per minute is plotted on the ordinate, and time after intravenous administration of L-methionine-CH_3-^{14}C is plotted on the abscissa. Each point represents the mean of the $^{14}CO_2$ excretion rate for each group of animals at the given time. The length of the vertical bars through each point represents one standard error of the mean for the group of control rats.

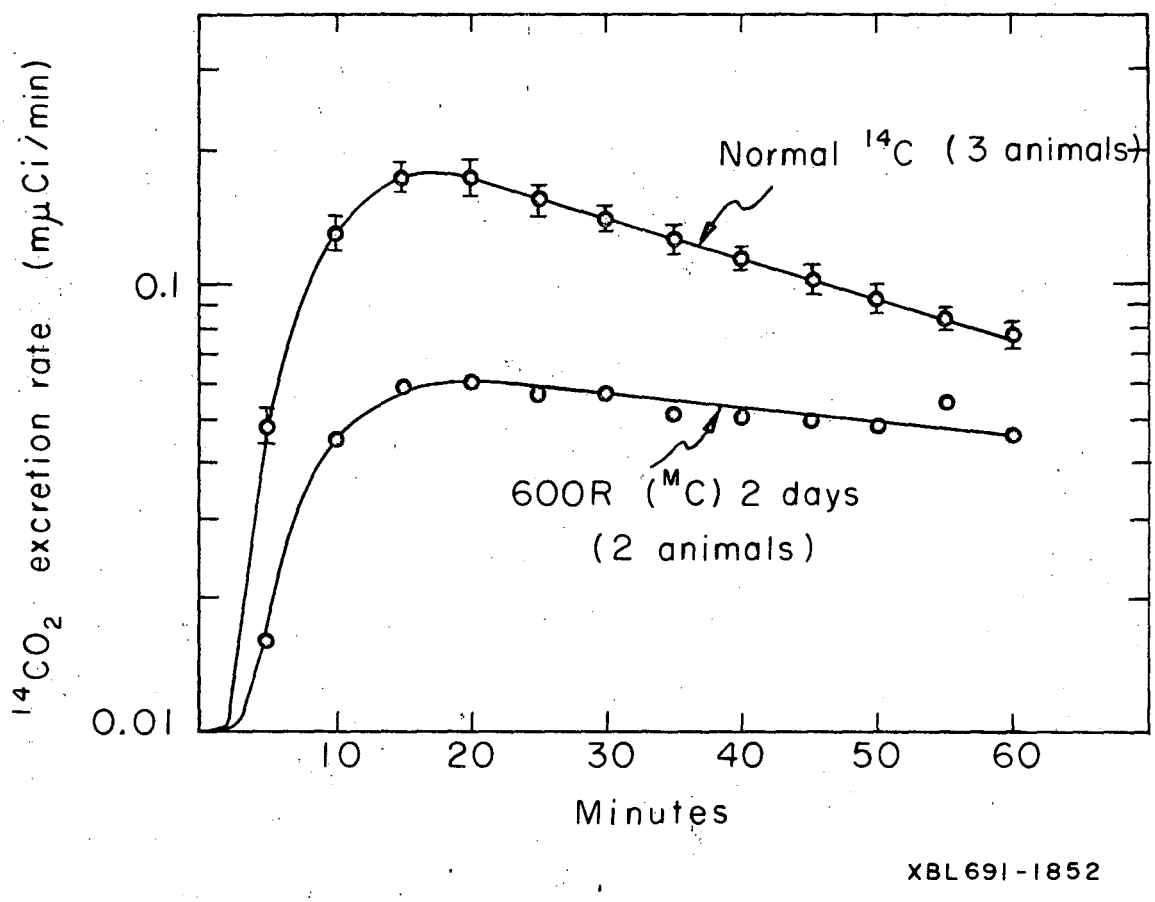
$^{14}CO_2$ excretion rate (mμCi/min)
0.1
0.01
Normal ^{14}C (3 animals)
600R (^{M}C) 2 days
(2 animals)
10
20
30
40
50
60
Minutes
XBL691-1852

Fig. 18

continued at least until the sixteenth postirradiation day.

Table VII summarizes data presented in Figs. 19 and 20.

c. ^{14}C-formate

Figure 21 presents the single exponential regression function with 95% confidence limits for the downslope of the $^{14}CO_2$ breath curves in four control rats (dotted line) and two irradiated rats 5 days after exposure to 600 R (solid line) following the intravenous administration of ^{14}C-formate. The ordinate presents the rate of $^{14}CO_2$ excretion expressed as mμCi per minute and the abscissa as time in minutes following the intravenous injection of ^{14}C-formate. Each point, at 5, 15, 25, and 40 min represents the mean of excretion rates of $^{14}CO_2$ for the control group. Vertical bars at each point define precision of position of the mean of $^{14}CO_2$ excretion rates with 95% limits based on $t_{.95}\ S_{y.x.}$ ($S_{y.x.}$ = one standard error of the estimate). The broken lines above and below each curve are regression lines of ± 1 standard error of the estimate. It is clear that there is significant difference between the two curves.

Figure 22 presents the serial changes in the half time of such curves subsequent to the administration of ^{14}C-formate to pairs of rats receiving various doses of x irradiation at 20 min, and 2, 5, 9, 13, and 19 days after irradiation. Irradiated rats given 600 R showed early significant prolongation of $T_{1/2}$ within 20 min following

Fig. 19. Changes in T_{max} of the $^{14}CO_2$ breath curves after intravenous administration of L-methionine-CH_3-^{14}C in irradiated rats and sham-irradiated rats. Each line represents the mean value of data from a pair of irradiated rats or a group of control rats. The T_{max} is plotted on the ordinate, and time after irradiation is plotted on the abscissa. Results in irradiated rats are shown by the broken curves, and results in the sham-irradiated controls are shown by the solid curve. The 0-day value for each study represents values obtained 20 min after the irradiation or sham-irradiation procedure.

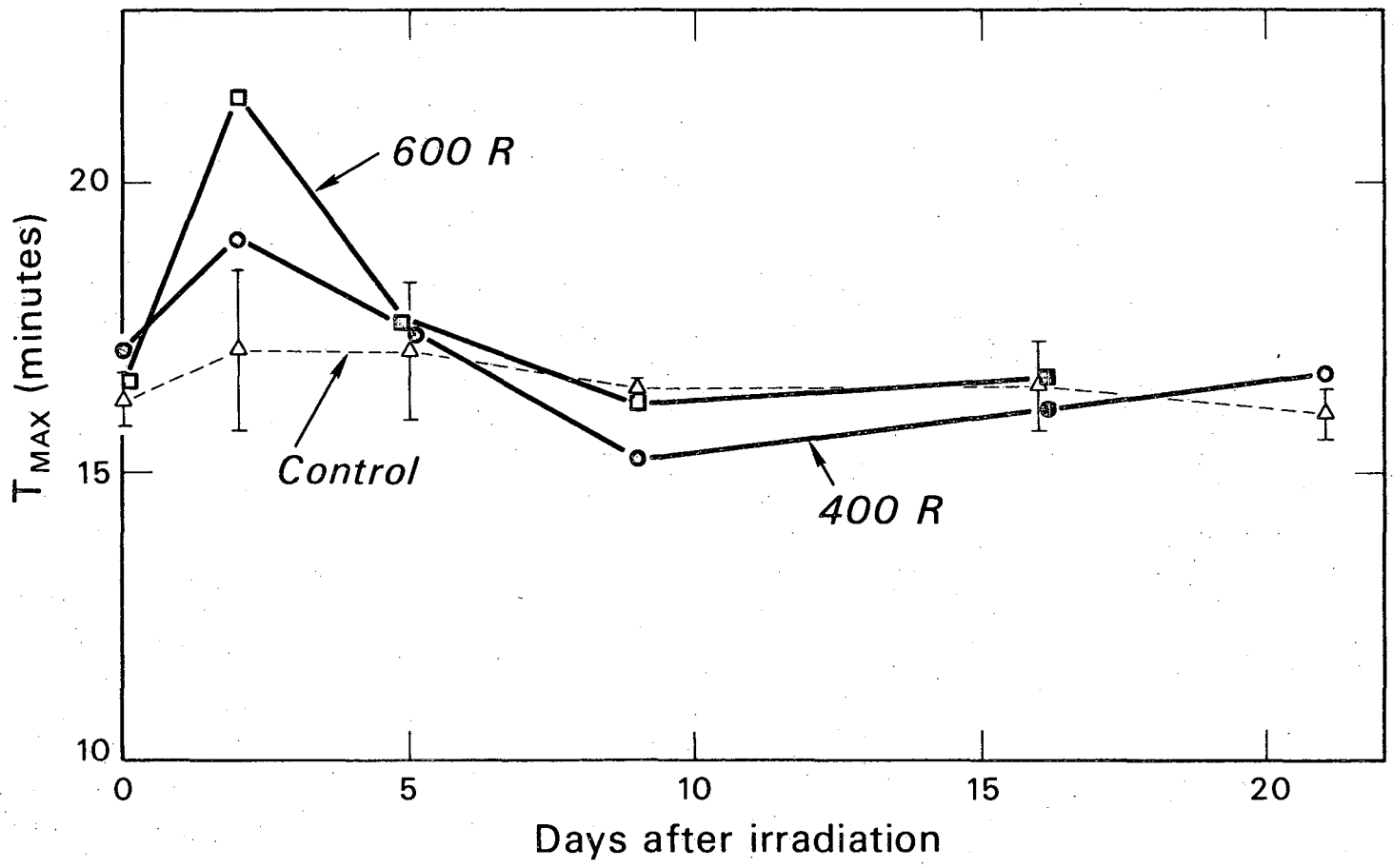

DBL 692-4556

Fig. 19

Fig. 20. Changes in the cumulative percentage of $^{14}CO_2$ excreted in the breath during the initial 60 min following intravenous administration of L-methionine-CH_3-^{14}C in irradiated rats and sham-irradiated rats. The cumulative percentage of $^{14}CO_2$ excreted in 60 min is plotted on the ordinate, and days after irradiation is plotted on the abscissa. Each line represents the mean value of data from a pair of irradiated rats or a group of three control rats. The 0-day value for each study represents values obtained 20 min after the irradiation or sham-irradiation procedure. At the given time, the length of the vertical bars through each point represents 1 standard error of the mean for the group of control rats.

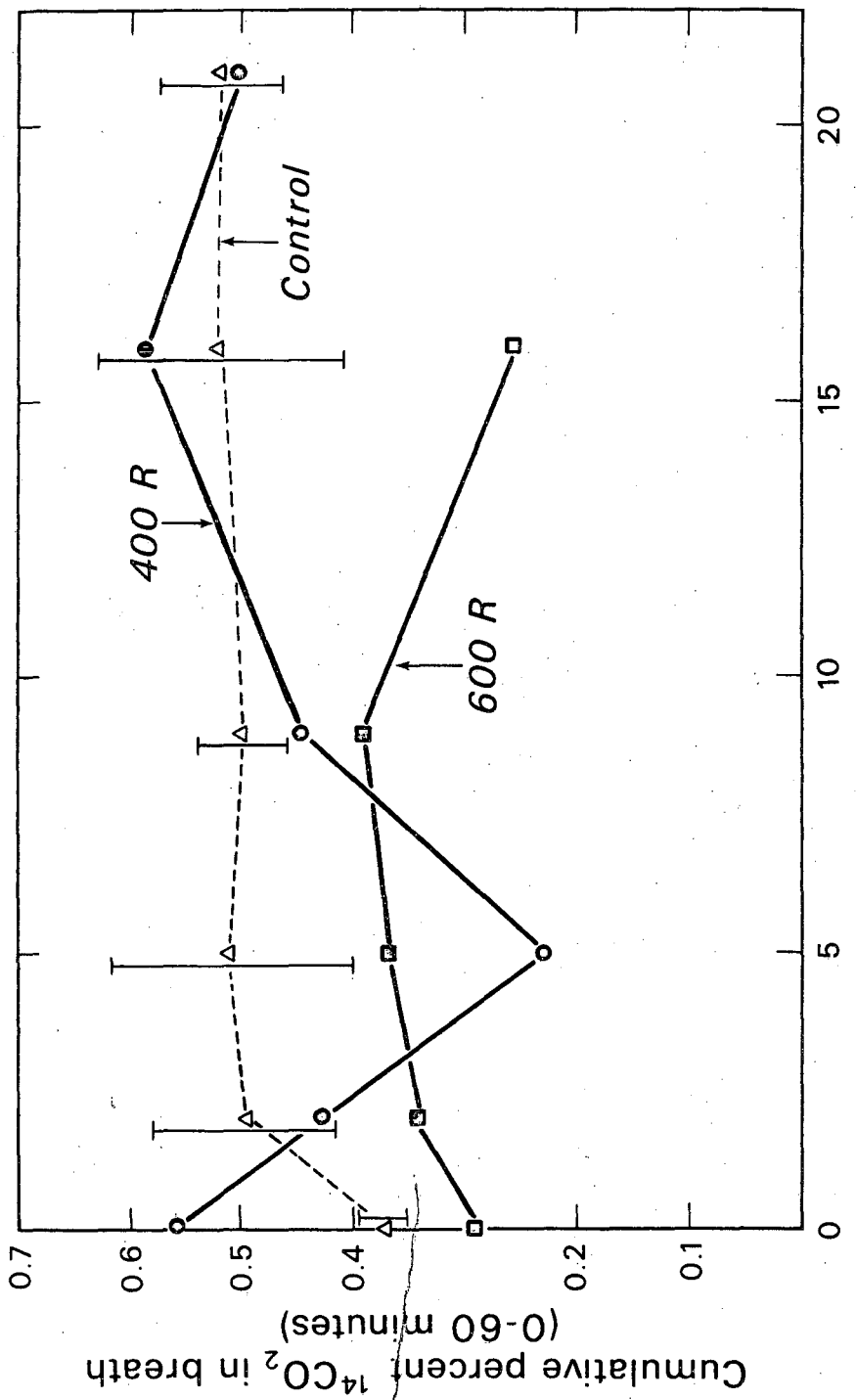

DBL 692-4562

Fig. 20

Table VII

Table VII. T_{max} and integral ^{14}C excretion determined from $^{14}CO_2$ appearance in breath following intravenous administration of L-methionine-CH_3-^{14}C in control and irradiated rats (the number of animals in each group of rats is noted in parentheses).

Category	Time of study after irradiation or sham irradiation	T_{max} (min)	^{14}C excretion in 60 min (%)
Control animals (3)	20 min, 2,5,9,16, and 21 days	16.34 ± (S.E. = 0.49)	0.49 ± (S.E. = 0.04)
Irradiated rats			
400 R (2)	20 min	17	0.57
	2 days	18.25	0.43
	5 days	17.25	0.23
	9 days	15.75	0.45
	16 days	16.25	0.59
	21 days	16.75	0.50
600 R (2)	20 min	16.5	0.29
	2 days	21.75	0.34
	5 days	17.25	0.37
	9 days	16.25	0.39
	16 days	15.27	0.26

irradiation. The maximum prolongation of $T_{1/2}$ was reached at 2 to 5 days, but it returned to near normal by the ninth day after irradiation.

Figure 23 presents the results of integral ^{14}C excretion (from 0 to ∞) after the intravenous injection of ^{14}C-formate in irradiated rats. It is clear that the integral ^{14}C excretion in the breath of irradiated rats given 600 R decreased during the initial 2 to 5 days, returning to near normal by the ninth day after irradiation. Table VIII summarizes data presented in Figs. 22 and 23.

d. L-glycine-1-^{14}C and L-serine-3-^{14}C

Figure 24 presents serial T_{max} of $^{14}CO_2$ breath curves of control and irradiated rats subsequent to the intravenous injection of L-glycine-1-^{14}C at 20 min, and then at 3, 7, 12, and 20 days after irradiation. Figure 24 presents results of the cumulative excretion of $^{14}CO_2$ in the breath during the initial 60 min following the administration of the ^{14}C-labeled glycine in irradiated rats. It can be seen that there is no significant change in T_{max} and cumulative excretion of $^{14}CO_2$ in irradiated rats. Table IX summarizes data presented in Figs. 24 and 25. Figure 26 presents serial T_{max} of $^{14}CO_2$ breath curves of control and irradiated rats subsequent to the administration of L-serine-3-^{14}C at 20 min and 2, 5, 9, 13, and 19 days after radiation exposure. Figure 27 presents results of the cumulative excretion of $^{14}CO_2$ in the breath during the

Fig. 21. Single exponential regression function with 95% confidence limits for the downslope of the $^{14}CO_2$ breath curves in control rats (dotted lines) and two irradiated rats five days after exposure to 600 R (solid line) following the intravenous administration of ^{14}C-formate. The ordinate represents the rate of $^{14}CO_2$ excretion expressed as mμCi per minute and the abscissa as time in min following the intravenous injection of ^{14}C-formate. Vertical bars through each point define precision of position of the mean of excretion rates of $^{14}CO_2$ for each group of rats with 95% limits based on $t_{.95}\ S_{y.x}$. The broken lines above and below each curve are regression lines of ± 1 standard error of the estimate.

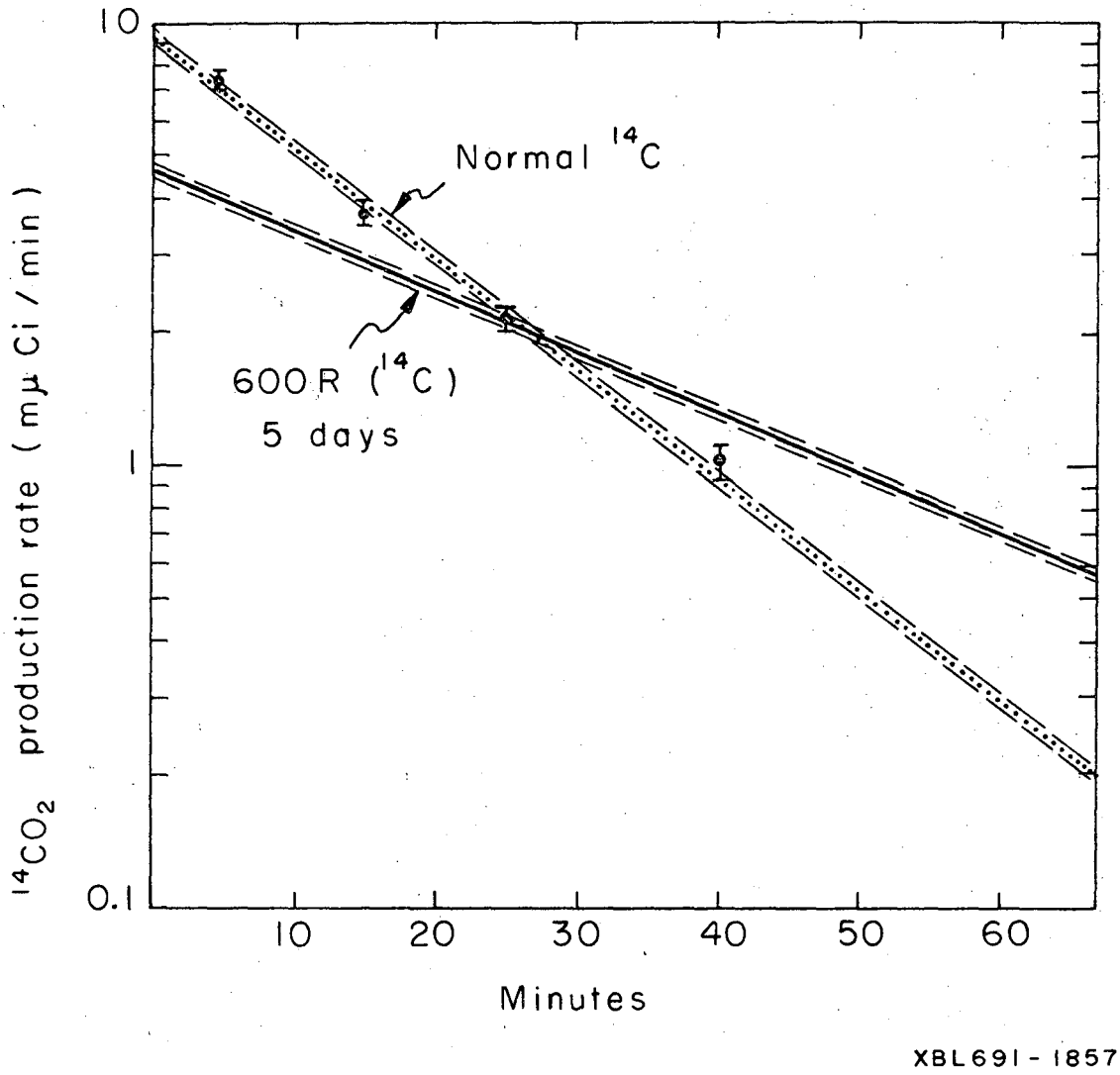
10
1
0.1
Normal ^{14}C
600R (^{14}C)
5 days
$^{14}CO_2$ production rate (mμ Ci / min)
10
20
30
40
50
60
Minutes
XBL691-1857

Fig. 21

Fig. 22. Changes in the half-time ($T_{1/2}$) of the $^{14}CO_2$ breath curves after intravenous administration of ^{14}C-formate in irradiated and control rats. Each point represents the mean value of data from a pair of rats. $T_{1/2}$ is plotted on the ordinate, and time after irradiation is plotted on the abscissa. Results in irradiated rats are shown in the solid lines, and results in sham-irradiated rats are shown in the broken lines. The 0-day value for each study represents values obtained 20 min after the irradiation or sham-irradiation procedure.

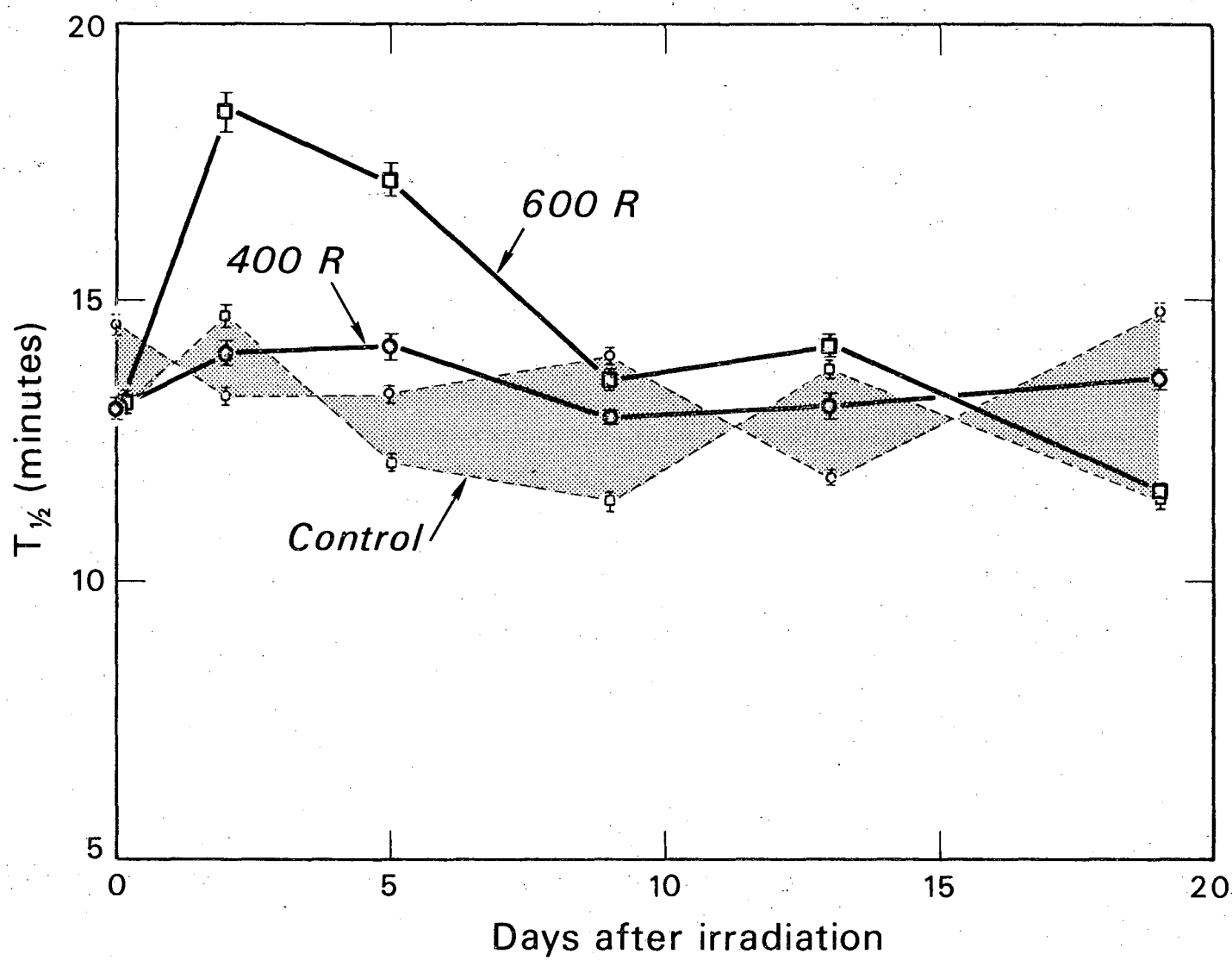
20
15
10
5
0
5
10
15
20
T½ (minutes)
Days after irradiation
600 R
400 R
Control
DBL 692-4557

Fig. 22

Fig. 23. Changes in the integral ^{14}C excretion $(0 \rightarrow \infty)$ in the breath following intravenous administration of ^{14}C-formate in irradiated and sham-irradiated rats. Integral ^{14}C excretion (%) is plotted on the ordinate, and days after irradiation is plotted on the abscissa. Each line represents the mean value of data from a pair of rats. Results in irradiated rats are shown in solid lines and results in sham-irradiated controls are shown in the broken lines. The 0-day value for each study represents values obtained 20 min after the irradiation or sham-irradiation procedure. Vertical bars through each point define the standard error of the mean of the excretion rates of $^{14}CO_2$ for the group of control and irradiated rats.

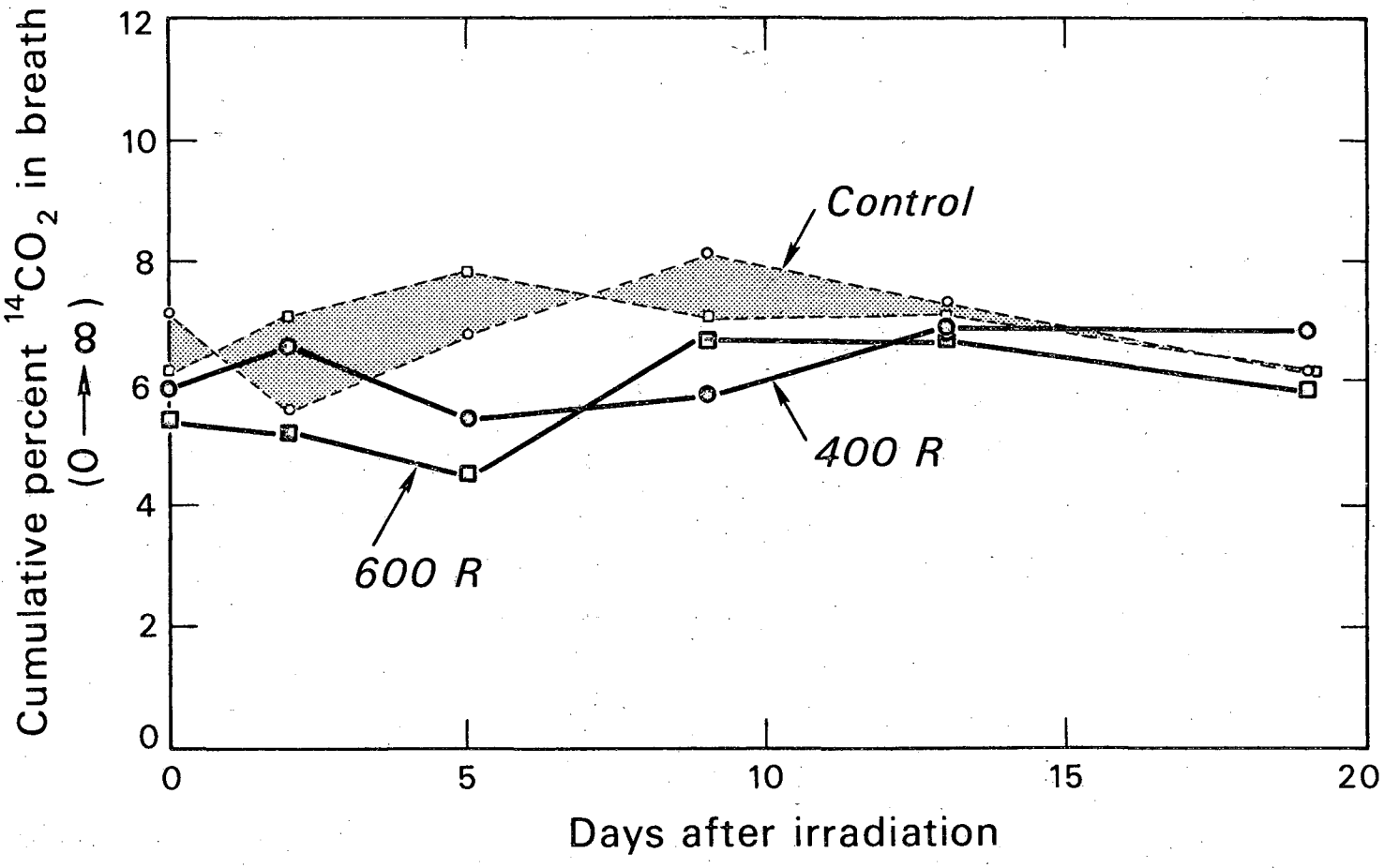

DBL 692-4559

Fig. 23

Table VIII.

Changes in $T_{1/2}$ and integral ^{14}C excretion determined from $^{14}CO_2$ appearance in breath following intravenous administration of ^{14}C-formate in control and irradiated rats (the number of animals in each group of rats is noted in parentheses).

Category	Time of study after irradiation or sham irradiation	Half-time ($T_{1/2}$) (min ± S.E.)	Integral ^{14}C excretion ($0 \rightarrow \infty$) (% ± S.E.)
Control rats (4)	20 min, 2, 5, 9, 13, and 19 days	12.81 ± 0.13	6.92 ± 0.10
Irradiated rats 400 R (2)	20 min	13.12 ± 0.16	6.00 ± 0.01
	2 days	14.14 ± 0.23	6.65 ± 0.01
	5 days	14.27 ± 0.20	5.42 ± 0.08
	9 days	12.98 ± 0.17	5.87 ± 0.07
	13 days	13.12 ± 0.24	5.92 ± 0.07
	19 days	13.68 ± 0.18	6.86 ± 0.07
600 R (2)	20 min	13.09 ± 0.17	6.86 ± 0.09
	2 days	16.37 ± 0.34	5.30 ± 0.08
	5 days	17.20 ± 0.29	4.58 ± 0.08
	9 days	13.69 ± 0.18	6.74 ± 0.09
	13 days	14.27 ± 0.20	6.73 ± 0.07
	19 days	11.60 ± 0.11	5.84 ± 0.06

Fig. 24. Serial T_{max} of $^{14}CO_2$ breath curves after intravenous administration of L-glycine-1-^{14}C in irradiated and control rats. Each line represents the mean value of data from a pair of rats. The T_{max} is plotted on the ordinate, and time after irradiation is plotted on the abscissa. Results in irradiated rats are shown in the solid lines, and results in the sham-irradiated controls are shown in the broken lines. The 0-day value for each study represents values obtained 20 min after the irradiation or sham-irradiation procedure.

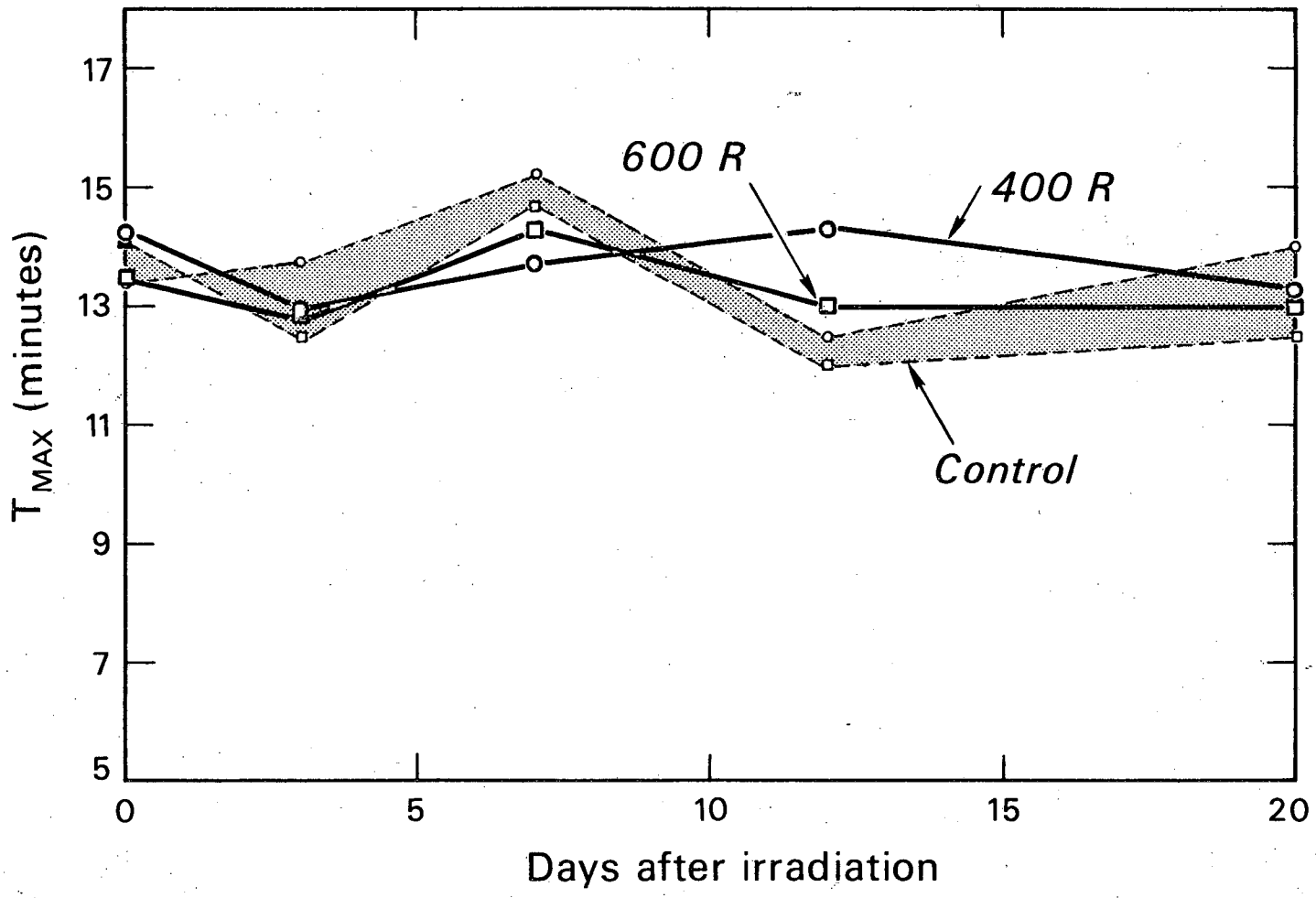

DBL 692-4560

Fig. 24

Fig. 25. Cumulative percentage of $^{14}CO_2$ excreted in the breath during the initial 60 min following intravenous administration of L-glycine-1-^{14}C in irradiated and sham irradiated rats. Cumulative percentage of $^{14}CO_2$ excreted in 60 min is plotted on the ordinate, and days after irradiation is plotted on the abscissa. Results in irradiated rats are shown in the solid lines, and results in sham-irradiated controls are shown in the broken lines. The 0-day value for each study represents values obtained 20 min after the irradiation or sham-irradiation procedure.

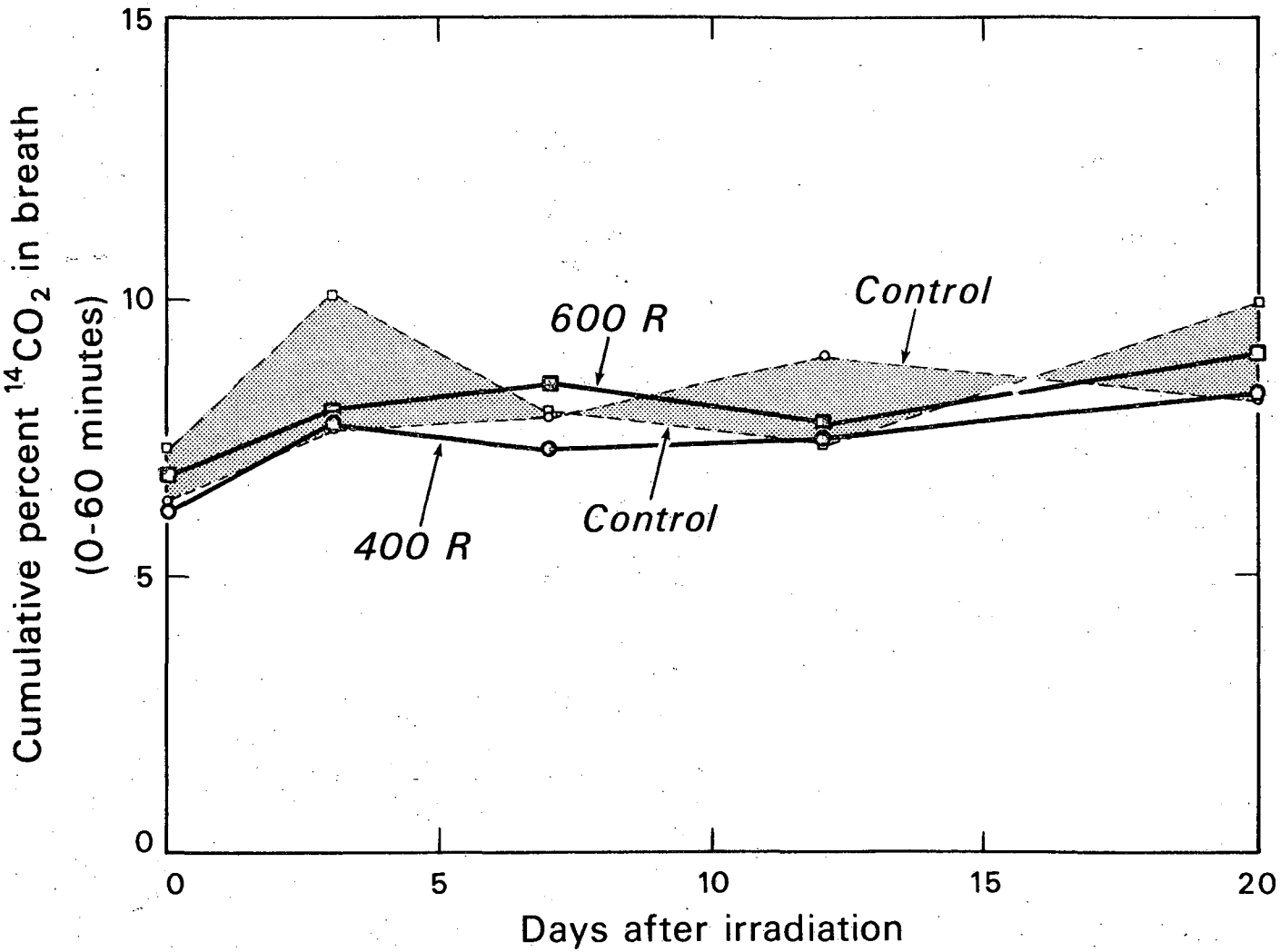

DBL 692-4564

Fig. 25

Table IX.

Serial T_{max} and integral ^{14}C excretion determined from $^{14}CO_2$ appearance in breath following intravenous administration of L-glycine-1-^{14}C in control and irradiated rats (the number of animals in each group of rats is noted in parentheses).

Category	Time of study after irradiation or sham irradiation	T_{max} (min ± S.E.)	^{14}C excretion in 60 min (% ± S.E.)
Control rats (4)	20 min	13.87 ± 0.77	6.85 ± 0.63
	3 days	13.12 ± 1.12	8.91 ± 0.73
	7 days	15.00 ± 0.46	7.98 ± 0.35
	12 days	12.25 ± 0.25	7.68 ± 1.14
	20 days	13.25 ± 0.94	9.25 ± 0.92
Irradiated rats			
400 R (2)	20 min	14.25	6.30
	3 days	13	7.87
	7 days	13.75	7.41
	12 days	14.25	7.59
	20 days	13.25	8.45
600 R (2)	20 min	13.50	6.98
	3 days	13.00	8.07
	7 days	14.25	8.55
	12 days	13.00	7.69
	20 days	13.00	9.17

Fig. 26. Serial T_{max} of the $^{14}CO_2$ breath curves after intravenous administration of L-serine-3-^{14}C in irradiated and control rats. Each line represents the mean value of data from a pair of irradiated rats or a group of control rats. T_{max} is plotted on the ordinate, and time after irradiation is plotted on the abscissa. Results in irradiated rats are shown in the solid lines, and results in the sham-irradiated rats are shown in the broken line. The vertical bars at each point define 1 standard error of the mean of $^{14}CO_2$ excretion rate. The 0-day value for each study represents values obtained 20 min after irradiation or sham-irradiation procedure.

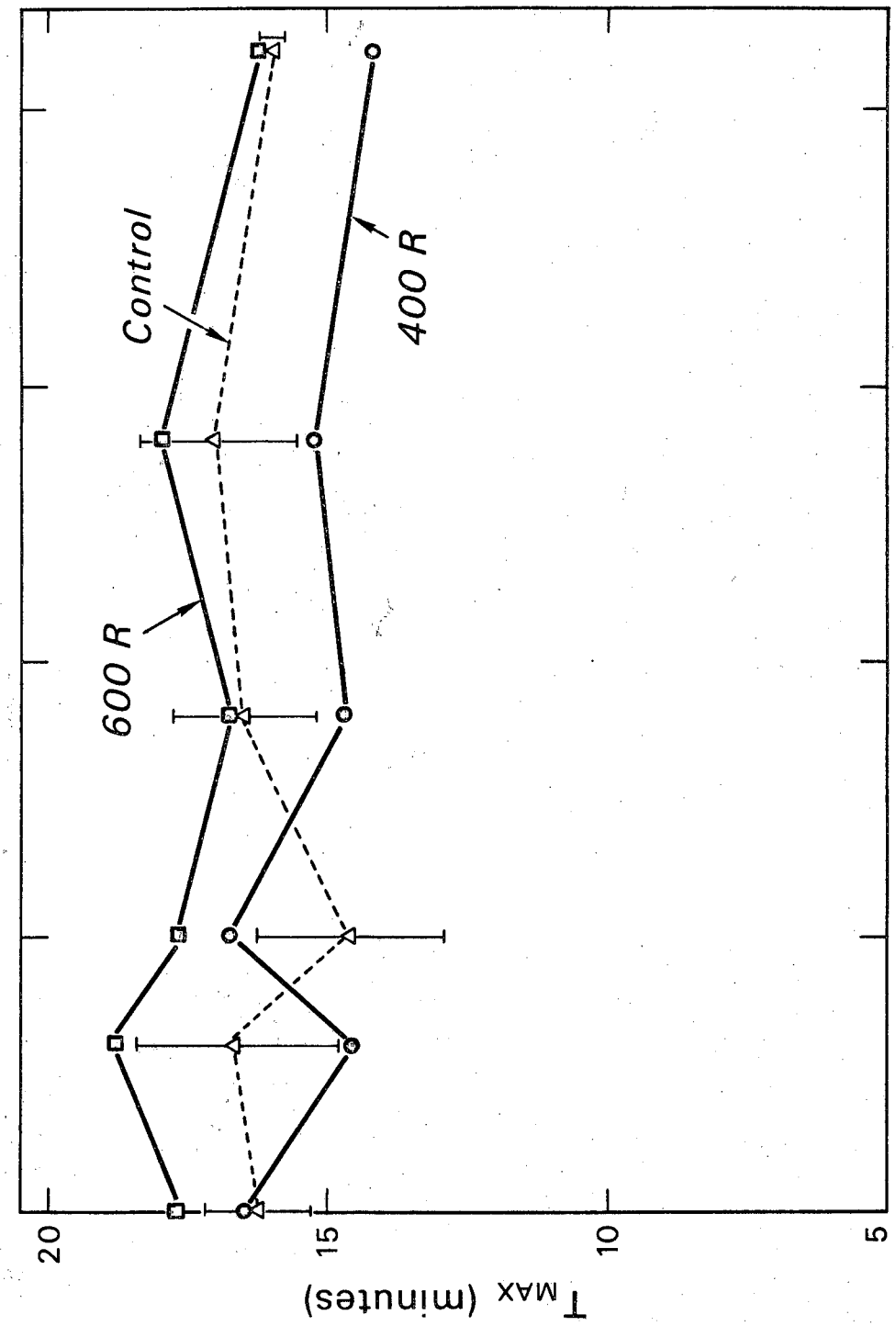

DBL 692-4561

Fig. 26

Fig. 27. Cumulative percentage of $^{14}CO_2$ excreted in the breath during the initial 60 min following intravenous administration of L-serine-3-^{14}C in irradiated and sham-irradiated rats. Cumulative percentage of $^{14}CO_2$ excreted in 60 min is plotted on the ordinate, and days after irradiation is plotted on the abscissa. Results in irradiated rats are shown in the broken lines, and results in the sham-irradiated rats are shown in the solid lines. Each line represents the mean value of data from a pair of irradiated rats or a group of control rats. The 0-day value for each study represents values obtained 20 min after the irradiation or sham-irradiation procedure.

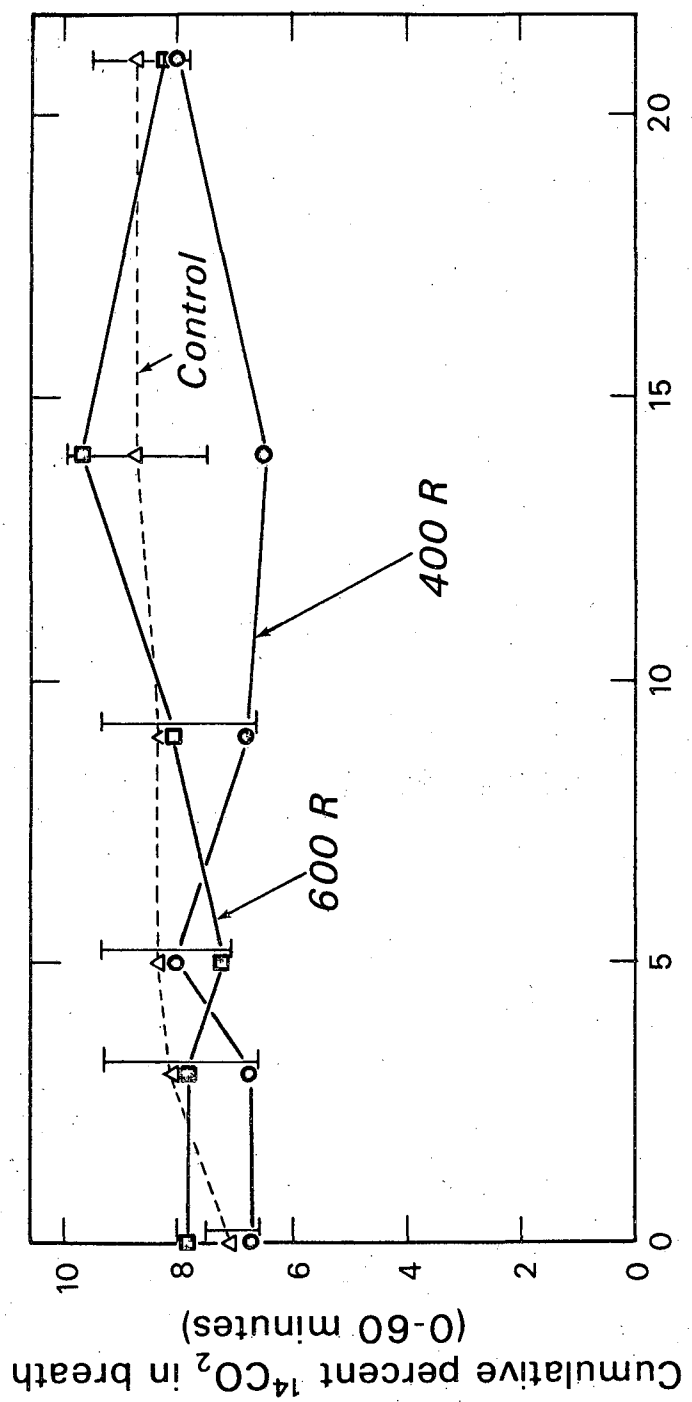

DBL 692-4563

Fig. 27

Table X.

T_{max} and integral ^{14}C excretion determined from $^{14}CO_2$ appearance in the breath following intravenous administration of L-serine-3-^{14}C in control and irradiated rats (the number of animals in each group of rats is noted in parentheses).

Category	Time of study after irradiation or sham-irradiation	T_{max} (min ± S.E.)	Integral ^{14}C excretion in 60 min (% ± S.E.)
Control rats (4)	20 min	16.25 ± 0.92	7.14 ± 0.42
	3 days	16.75 ± 1.90	8.18 ± 0.90
	5 days	14.62 ± 1.25	8.36 ± 0.33
	9 days	16.50 ± 1.36	8.19 ± 1.06
	14 days	17.00 ± 1.43	8.79 ± 0.95
	21 days	16.00 ± 0.20	8.75 ± 0.64
Irradiated rats			
400 R (2)	20 min	16.50 –	7.44
	3 days	14.50	6.78
	5 days	16.75	8.10
	9 days	14.75	6.85
	14 days	15.25	6.60
	21 days	14.25	8.09
600 R (2)	20 min	17.75	7.90
	3 days	18.75	7.84
	5 days	17.75	7.33
	9 days	16.75	8.10
	14 days	18.00	9.70
	21 days	16.25	8.38

initial 60 min following the injection of the ^{14}C-labeled serine in irradiated rats. It is clear that there is no significant change in T_{max} and cumulative excretion of $^{14}CO_2$ in irradiated rats. Table X summarizes data presented in Figs. 26 and 27.

2. Methotrexate studies

a. cold methotrexate

Figure 28 presents composite data of the rate of $^{14}CO_2$ production following intravenous administration of L-histidine (imidazole-2-^{14}C) in four control rats and four rats given 2.5 mg methotrexate intravenously three hours and three days prior to the study. The ordinate represents the rate of $^{14}CO_2$ excretion expressed as mμCi/min, and the abscissa represents time in min following the intravenous administration of L-histidine (imidazole-2-^{14}C). Each point represents the mean of the $^{14}CO_2$ excretion rate for each group of rats at the given time, and the lengths of the vertical bars through each point represent 1 standard error of the mean for each group.

It can be seen that there is no qualitative difference between control curves and those obtained in methotrexate-treated rats. No significant changes in T_{max} and cumulative excretion of $^{14}CO_2$ in the breath during the initial 60 min were noted in methotrexate-treated rats as compared with the controls.

Table XI summarizes the data presented in Fig. 28.

Fig. 28. Composite data of the rate of $^{14}CO_2$ excretion following intravenous administration of L-histidine (imidazole-2-^{14}C) in four control rats and four rats 3 hours and 3 days after intravenous injection of 2.5 mg methotrexate. The ordinate represents $^{14}CO_2$ excretion rate expressed as muCi/min and the abscissa as time in min following intravenous administration of the ^{14}C-labeled histidine. Vertical bars through each point defines 1 standard error of the mean of excretion of $^{14}CO_2$.

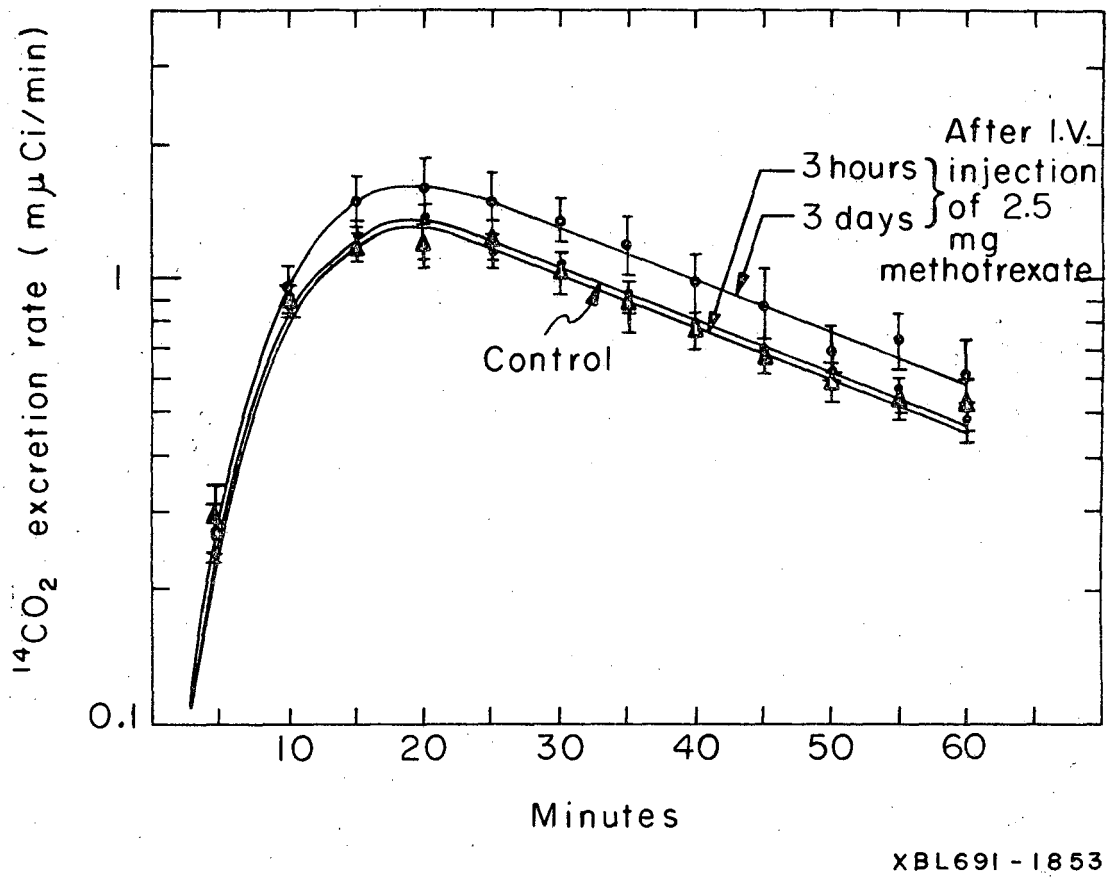
$^{14}CO_2$ excretion rate (mμCi/min)
1
0.1
10
20
30
40
50
60
Minutes
After I.V. injection of 2.5 mg methotrexate
3 hours
3 days
Control
XBL691-1853

Fig. 28

Table XI.

T_{max} and integral ^{14}C excretion determined from $^{14}CO_2$ appearance in breath following IV administration of L-histidine (imidazole-2-^{14}C) in control and methotrexate-treated rats (the number of animals in each group is noted in parentheses).

Category	T_{max} (min ± S.E.)	^{14}C excretion in 60 min (% ± S.E.)
Normal rats (4)	20.76 ± 0.52	1.01 ± 0.05
Rats 3 hours after IV administration of 2.5 mg methotrexate (4)	18.75 ± 2.69	0.97 ± 0.10
rats 3 days after initial administration of methotrexate (4)	20.37 ± 0.75	1.20 ± 0.17

Table XII.

Binding capacity of folate reductase to methotrexate-3', 5'-^{3}H expressed in terms of DPM per mg of dry weight of rat liver in three control and four rats exposed to 2000 and 3000 R of x rays (the number of animals in each group of animals is noted in parentheses).

Category	DPM/mg of dry weight of rat liver
Control animals (3)	44.60 (± S.E. = 8.45)
Irradiated animals	
2000 R (2)	47.75
3000 R (2)	44.92

b. methotrexate-3',5'-^{3}H

Data on the hepatic binding of the intravenously administered methotrexate-3', 5'-^{3}H in three control rats and four rats exposed to 2000 and 3000 R of x rays is presented in Table XII. No significant difference in hepatic binding of labeled methotrexate was noted between control and irradiated rats.

D. Discussion

1. Effects of radiation on oxidation of monocarbon fragment precursors to CO_2

Previous studies demonstrated that ^{14}C atoms from ^{14}C-formate, L-histidine (imidazole-2-^{14}C), and L-methionine-CH_3-^{14}C are readily incorporated into the monocarbon fragment pool attached to tetrahydrofolic acid, from this point they may be either utilized in synthetic processes or rapidly oxidized to $^{14}CO_2$.

In the studies presented here, we demonstrated a difference in the pattern of $^{14}CO_2$ in the breath subsequent to the intravenous administration of L-histidine (imidazole-2-^{14}C), L-methionine-CH_3-^{14}C, and ^{14}C-formate between normal and irradiated rats. However, no significant effects were seen in the oxidation to $^{14}CO_2$ of L-glycine-1-^{14}C and L-serine-3-^{14}C in irradiated rats. This finding suggested that results obtained with histidine, methionine, and formate were relatively specific and not due to non-specific alterations in amino acid metabolism.

At various times following irradiation, the time at which the maximum rate of excretion of $^{14}CO_2$ in the breath occurs was prolonged, and there was a diminution of the total amount of the ^{14}C appearing in the breath during the initial 60 to 80 min of the study following injection of the ^{14}C-labeled histidine or methionine.

The half-time ($T_{1/2}$) of the single exponential regression function with 95% confidence limits for the downslope of $^{14}CO_2$ breath curves in irradiated rats was prolonged and there was a diminution of the integral ^{14}C excretion from 0 to ∞ in the breath following the injection of ^{14}C-formate.

The effect described is seen within 16 to 20 min after irradiation and therefore cannot be ascribed to delayed nonspecific effects of radiation on the animal's overall physiology. Also these effects cannot be due to alteration in absorption of folic acid from the intestinal tract, since body stores of folic acid are sufficient to prevent the appearance of folic acid deficiency for many months following complete removal of this material from the diet (69). The pattern of appearance of $^{14}CO_2$ in the breath of irradiated rats was similar to the pattern seen in folic-acid-deficient subjects subsequent to the intravenous administration of L-histidine (imidazole-2-^{14}C) (24,25) and L-methionine-CH_3-^{14}C (7). The abnormal appearance of $^{14}CO_2$ in the breath subsequent to the intravenous

administration of L-histidine (imidazole-2-^{14}C) is considered to be pathognomonic of tetrahydrofolic acid in man by Fish and Pollycove (70), since they have not observed similar changes due to other causes. Thus, it is tempting to postulate that the decreased $^{14}CO_2$ appearance in the breath subsequent to the intravenous administration of L-histidine (imidazole-2-^{14}C), L-methionine-CH_3-^{14}C, and ^{14}C-formate may be related to inactivation of tetrahydrofolic acid or the processes responsible for its production. The former possibility was consistent with the finding that pteroyglutamic acid was irradiated with ultraviolet light; it was rapidly inactivated and degraded in aqueous solutions (64). Folic acid has been shown to be degraded by x irradiation, and the main part of degradation to be involved in the p-amino-benzoic acid moiety (71). Folic acid and citrovorum factor were significantly diminished a few hours after 400 to 600 R of x irradiation in spleen and from the 10th day on, in testis of rats (72).

Moreover, the production of tetrahydrofolic acid requires the availability of NADPH, which recently has been shown to be partially inactivated in rat liver following total body exposure to 800 R (73). Recent works of Winchell and Vimokesant demonstrated that the de novo synthesis of thymine and adenine utilizing ^{14}C-formate was more radiosensitive than the incorporation of ^{3}H-thymidine into DNA thymine, and both the synthesis of thymidine,

thymine, and the purine, adenine, were significantly inhibited by radiation exposure (67). In this work, they also postulated that the marked radiosensitivity of the synthesis of these bases, which required a common pathway via monocarbon transport, involved radiation inactivation of tetrahydrofolic acid or of the enzymatic processes required for its production.

The #1 carbon atom of glycine or the #3 carbon atom of serine may arise from monocarbon fragments from the monocarbon pool but their subsequent oxidation to CO_2 is essentially independent of any further passage of this carbon atom through the monocarbon pool.

A decrease of $^{14}CO_2$ excretion in the breath of irradiated rats subsequent to the intravenous administration of ^{14}C-formate would not be expected to be due to any alterations of the physical transport of this compound across the cell membrane, because the oxidation of formate to CO_2 proceeds very rapidly, and thus its transport across the cell membrane must be equally rapid. It is known that ^{14}C atoms from ^{14}C-formate enter the monocarbon pool attached to tetrahydrofolic acid. That radiation affects the pattern of $^{14}CO_2$ excretion in the breath of irradiated rats subsequent to the intravenous injection of ^{14}C-formate suggests that the major pathway of the <u>in vivo</u> oxidation of format must proceed by passage through the monocarbon pool. This result suggests that ^{14}C-formate

might be useful in the study of folic acid deficiency in human subjects, as are L-histidine (imidazole-2-^{14}C) and L-methionine-CH_3-^{14}C which have been used previously for this purpose.

2. Methotrexate studies

a. cold methotrexate

It is generally known that chronic administration of several folate antigonists causes severe inhibition of formation of folic acid reductase (74-76), thus inhibiting the formation of tetrahydrofolic acid. Fish and Pollycove (70) have shown a significantly decreased $^{14}CO_2$ appearance in the breath subsequent to the intravenous administration of L-histidine (imidazole-2-^{14}C) in patients subsequent to chronic treatment with amethopterin. In this study, we fail to demonstrate the effect of a single dose of methotrexate on $^{14}CO_2$ excretion in the breath of normal rats subsequent to the intravenous injection of L-histidine (imidazole-2-^{14}C). It is possible that the body's folic acid stores provide protective against a single dose of methotrexate, but not against multiple doses (77,80). This possibility is supported by the finding that dihydrofolic acid reductase levels were actually increased in leucocytes and erythrocytes from dogs (81) or from patients with or without hematological diseases (82) subsequent to the injection of single doses of methotrexate. Our present results may also be related to the fact that it is not

possible to provoke megaloblastic anemia in rats by treatment with methotrexate, and thus rats may have inherent resistance to methotrexate as compared with other species.

b. methotrexate-3', 5'-^{3}H

It has now been demonstrated that methotrexate inhibits folic acid reductase by actual binding with this enzyme. We therefore attempted to determine the effect of ionizing radiation on folic acid reductase levels by measuring the binding capacity of the folate reductase to methotrexate-3', 5'-^{3}H in irradiated rat liver. However, the results obtained showed that ionizing radiation had no effect on such binding capacity. It is possible that the technique used was limited by cell membrane transport of methotrexate rather than cellular content of folic acid reductase. It is also possible, that ionizing radiation did not influence the ability of folic acid reductase to bind methotrexate, but the folic acid reductase may still have been functionally inactivated.

E. Summary

These studies showed a decrease of the initial rate and amount of $^{14}CO_2$ excretion in the breath of rats given various doses of x rays following intravenous administration of L-histidine (imidazole-2-^{14}C), L-methionine-CH_3-^{14}C, and ^{14}C-formate. No significant alteration in $^{14}CO_2$ production was noted in irradiated rats subsequent to the intravenous injection of either L-glycine-1-^{14}C or L-serine-3-^{14}C.

These results suggested that ionizing radiation affected monocarbon fragment transport by inactivation of tetrahydrofolic acid or of the processes required for its production. The $^{14}CO_2$ production was unchanged in normal rats given single and massive doses of methotrexate subsequent to the intravenous injection of L-histidine (imidazole-2-^{14}C), and radiation failed to influence hepatic binding of ^{3}H-labeled methotrexate.

ACKNOWLEDGEMENTS

I wish to express my deep appreciation to Dr. H. S. Winchell for his help in directing the research involved, and for his personal guidance in preparing this dissertation. Without Dr. Winchell's deep interest in Nuclear Medicine, enthusiasm in teaching, and unsurpassed assiduousness this work could not have been accomplished. The association with Dr. Winchell in this enterprise has been personally most inspiring in every way.

I thank Dr. S. A. Landaw for his help in the operation of the apparatus in the beginning phases of this work, and Dr. Mary Anne Williams for her valuable suggestions in the preparation of this manuscript.

I appreciate Dr. E. L. Dobson for his valuable and helpful advice throughout my academic work.

I express my gratitude to Dr. John H. Lawrence and Dr. Hardin Jones for allowing me to study at the Donner Laboratory.

I express my gratitude to Mrs. Nancy N. Finley and Miss Barbara Shipley, and all technicians in the Donner Laboratory who cooperated with me throughout this work.

I thank the editors in the publications section and Mrs. Mary Harmon for their help in preparing this thesis, and for preliminary typing.

Thanks of a special sort are due to the International Atomic Energy Agency, the National Academy of Sciences, and the American Medical Association for fellowships during my stay in the United States of America.

The work was done under the auspices of the United States Atomic Energy Commission.

VII. Appendix 1

Effects of large doses of unlabeled L-methionine on $^{14}CO_2$ production in rats given L-histidine (imidazole-2-^{14}C), L-serine-3-^{14}C, formimino-^{14}C L-glutamic acid, and ^{14}C-formate

A. Review of the problem

In previous studies, competition between several amino acids for intestinal absorption has been proposed (87-93). This competition was not found in kidney tissue (94). Methionine was found to cause a large inhibition in the uptake of many amino acids in brain slices of rats (95). In folic-acid and vitamin-B12-deficient rats given massive doses of L-methionine, the amount of $^{14}CO_2$ production from the #2 carbon of the imidazole ring of histidine was shown to be significantly increased (84).

In the study presented here, we demonstrate significant alterations in the catabolism of L-histidine, L-serine, and formimino glutamic acid in normal rats given loading doses of L-methionine, by the measurement of $^{14}CO_2$ production in methionine-treated rats subsequent to the intravenous administration of L-histidine (imidazole-2-^{14}C), L-serine-3-^{14}C, and formimino-^{14}C L-glutamic acid.

B. Preparation of experimental animals

Inbred male Buffalo rats (Simonsen Laboratory, Gilroy, California) weighing 240 to 245 g were used in all experiments.

L-histidine (imidazole-2-^{14}C)

In the first series of studies, 35 rats were divided into two groups of 13 methionine-treated rats and 22 control rats and rats given no treatment prior to the administration of the ^{14}C-labeled histidine. Methionine-treated rats were subdivided further into two subgroups of animals. Four rats in the first subgroup received 40 mg of L-methionine (General Biochemicals, Laboratory Park, Chagrin Falls, Ohio) mixed homogenously with 2.5 μCi of L-histidine (imidazole-2-^{14}C) (specific activity: 267 μCi/mg, Nuclear Chicago Corp., Des Plaines, Ill.) intravenously. Ten rats in the second subgroup were given 40 mg of L-methionine 10, 40, and 120 min prior to the intravenous injection of 2.5 μCi of L-histidine (imidazole-2-^{14}C).

In each study, each rat received 2.5 μCi of L-histidine (imidazole-2-^{14}C) intravenously under light anesthesia with diethyl ether, and the appearance of $^{14}CO_2$ in the breath was determined.

^{14}C-formimino L-glutamic acid

In the second series of studies, eight male Buffalo rats were divided into two group of four control rats and

four methionine-treated rats. Each experimental rat received 40 mg of L-methionine 10 to 40 min prior to the intravenous administration of 10 μCi of ^{14}C-formimino L-glutamic acid (specific activity: 1.0 mCi/10.1 mg, New England Nuclear Corp., 575 Albany Street, Boston, Massachusetts 02118) intravenously.

L-serine-3-^{14}C

In the third series of studies, 12 male Buffalo rats were divided into two groups of six control and six methionine-treated rats. Experimental rats were given 40 mg of L-methionine 10 to 40 min prior to the intravenous administration of 2.5 μCi of L-serine-3-^{14}C (specific activity: 8.5 mCi/mM, Nuclear Chicago, 333 Howard Avenue, Des Plaines, Ill. 60018) intravenously.

^{14}C-formate

In the fourth series of studies, six male Buffalo rats were divided into two groups of three control rats and three methionine-treated rats. Each experimental rat was given 40 mg of methionine 10 min prior to intravenous injection of 0.5 μCi of ^{14}C-formate (specific activity: 1.00 mCi/14.5 mg, New England Nuclear Corp.).

C. Results

L-histidine (imidazole-2-^{14}C)

Figure 29 presents curves of composite data expressing the rate of $^{14}CO_2$ appearance in the breath of control rats and rats either given homogeneous mixture

of L-methionine and L-histidine (imidazole-2-^{14}C), or L-methionine prior to the intravenous injection of L-histidine (imidazole-2-^{14}C). The ordinate represents $^{14}CO_2$ excretion rate expressed as mμCi per min on a logarithmic scale and the abscissa as time in min on a linear scale. Each point represents the mean of the $^{14}CO_2$ excretion rate for each group of animals at the given time, and the length of the vertical bars through each point represents 1 standard error of the mean for each group.

It is clear that there was significantly decreased $^{14}CO_2$ production in the rate treated with methionine 10 to 40 min prior to the intravenous injection of the ^{14}C-labeled histidine. The cumulative excretion of $^{14}CO_2$ during the initial 90 min returned to the normal range in rats given 40 mg of L-methionine 120 min prior to the administration of the ^{14}C-labeled histidine. However, no significant difference was noted between $^{14}CO_2$ breath curves of control rats and those given a homogeneous mixture of methionine and L-histidine (imidazole-2-^{14}C).

Formimino-^{14}C L-glutamic acid

Figure 30 presents composite data of $^{14}CO_2$ breath curves of control and methionine-treated rats. There is a slight difference between $^{14}CO_2$ curves of control rats and those of methionine-treated rats.

L-serine-3-^{14}C

Figure 31 presents the composite data depicting the rate of $^{14}CO_2$ excretion in the breath of six control rats and six rats given 40 mg of L-methionine 10 and 40 min prior to the intravenous administration of L-serine-3-^{14}C. The significantly decreased $^{14}CO_2$ appearance in the breath of methionine-treated rats was seen at 10 min prior to the intravenous administration of L-serine-3-^{14}C, returning to the normal range at 40 min prior to the injection of the ^{14}C-labeled serine.

^{14}C-formate

Figure 32 presents composite data of $^{14}CO_2$ breath curves of control rats and methionine-treated rats. There is no significant difference between $^{14}CO_2$ curves of control rats and those of methionine-treated rats.

Table XIV summarizes data presented in Figs. 29 through 32.

D. Discussion

The studies presented here demonstrate that large doses of L-methionine decrease the amount of oxidation of the #2 carbon of the imidazole ring of histidine, the #3 carbon of serine, and probably the carbon atom of the formimino glutamic acid to CO_2 *in vivo*, whereas loading doses of L-methionine do not influence on the oxidation of ^{14}C-formate. These results suggest that L-methionine may inhibit the physical transport of L-histidine and L-serine

Fig. 29. Composite data of the rate of $^{14}CO_2$ appearance in the breath following IV administration of L-histidine (imidazole-2-^{14}C) 10, 40, and 120 min subsequent to the intravenous injection of 40 mgs of L-methionine. The ordinate represents percent of administered ^{14}C excreted as $^{14}CO_2$ per minute and the abscissa represents time in min following intravenous injection of the ^{14}C-labeled histidine. Each point represents the mean of the $^{14}CO_2$ excretion rate for each group of animals at the given time, and the length of the vertical bar through each point represents 1 standard error of the mean.

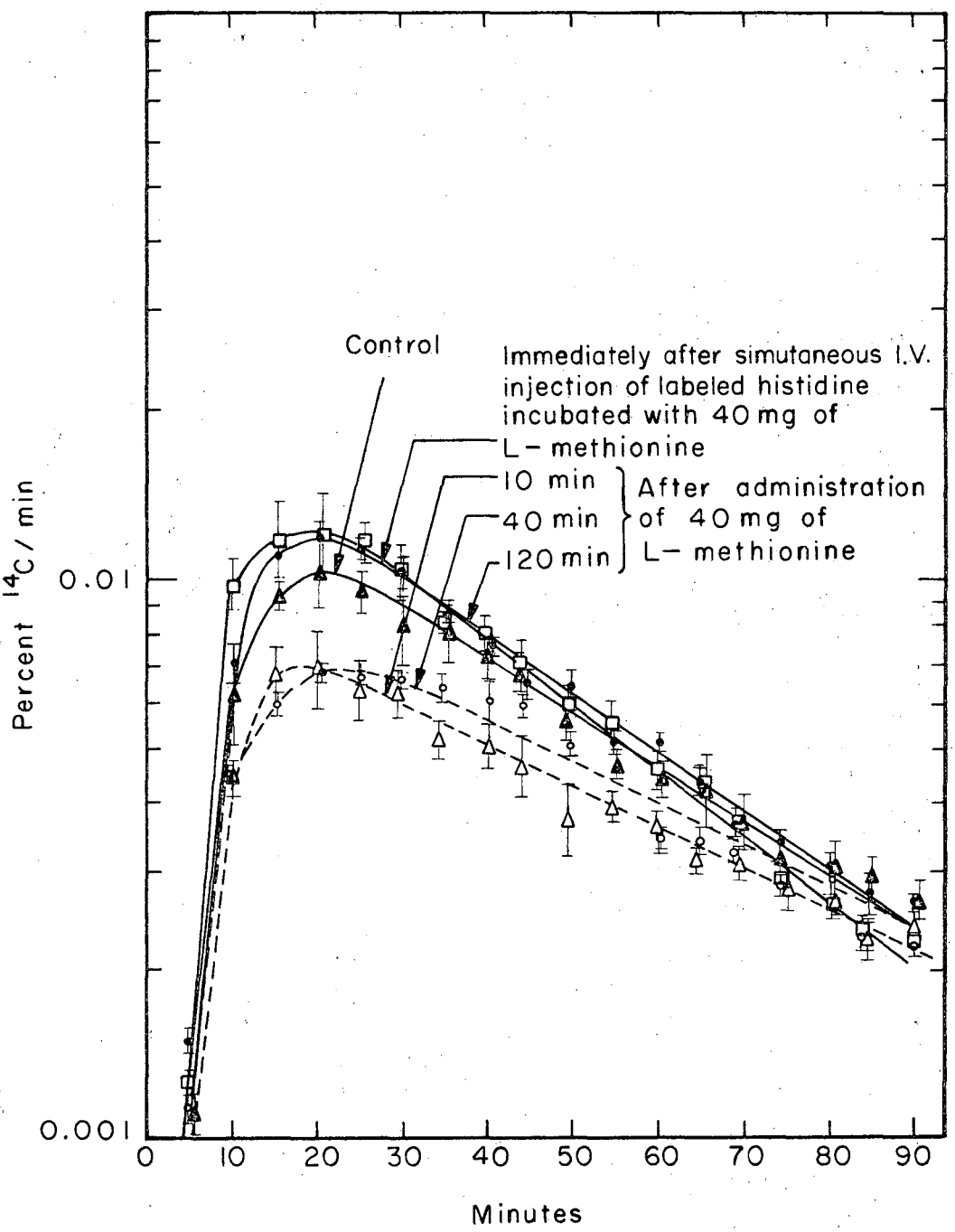
Control
Immediately after simutaneous I.V. injection of labeled histidine incubated with 40 mg of L- methionine
10 min
40 min
120 min
After administration of 40 mg of L- methionine
Percent ^{14}C / min
0.01
0.001
0
10
20
30
40
50
60
70
80
90
Minutes
XBL 692-1952

Fig. 29

Fig. 30. Composite data of the rate of $^{14}CO_2$ appearance in the breath following the IV administration of formimino-^{14}C L-glutamic acid 10 and 40 min subsequent to the administration of 40 mg of L-methionine.

The ordinate represents percent of administered ^{14}C excreted as $^{14}CO_2$ per min and the abscissa represents time in min following intravenous injection of the ^{14}C-labeled formimino glutamic acid. Each point represents the mean of the $^{14}CO_2$ excretion rate for each group of animals at the given time, and the length of the vertical bar through each point represents 1 standard error of the mean.

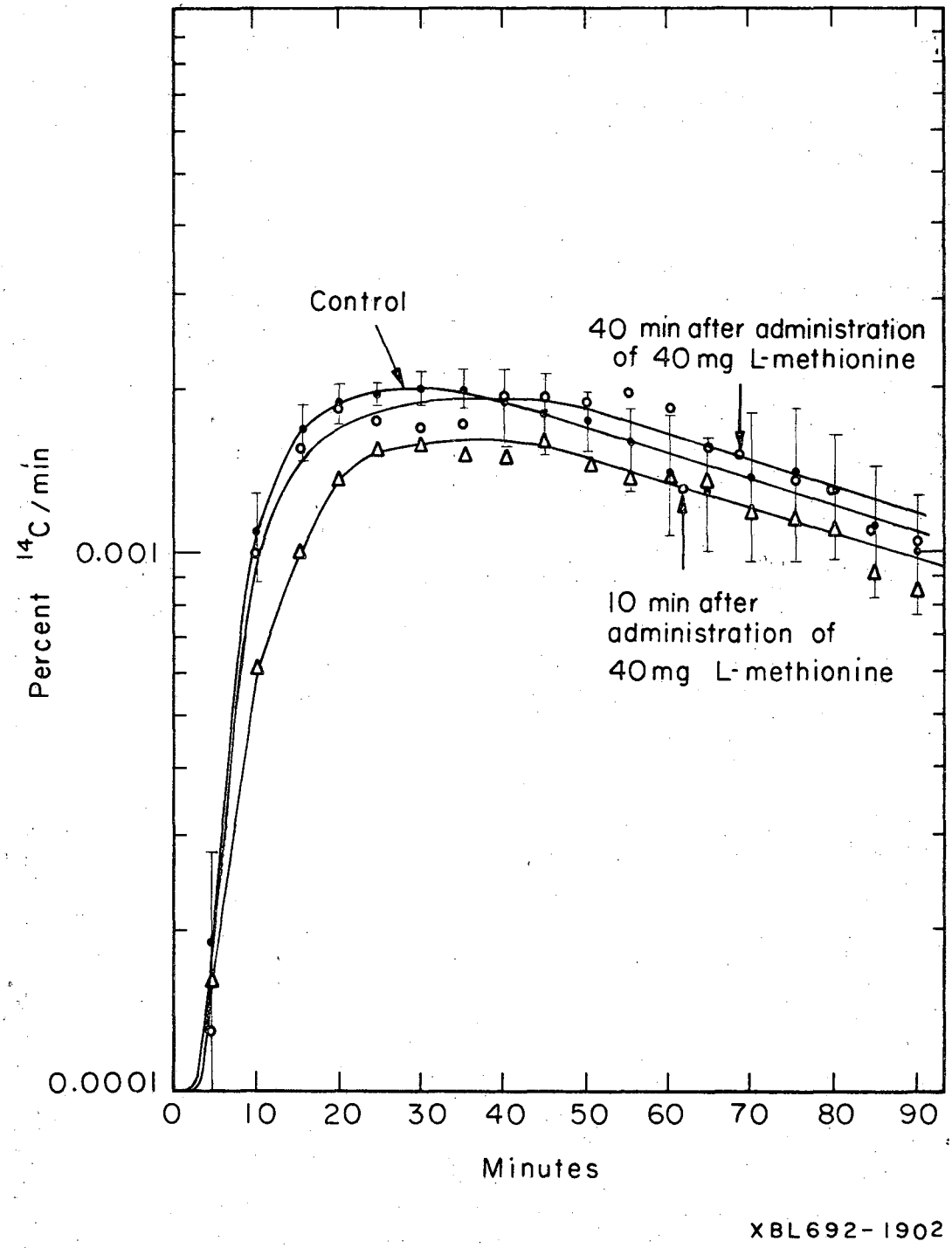
Control
40 min after administration
of 40 mg L-methionine
10 min after
administration of
40mg L-methionine
Percent ^{14}C/min
0.001
0.0001
0
10
20
30
40
50
60
70
80
90
Minutes
XBL692-1902

Fig. 30

Fig. 31. Composite data of the rate of $^{14}CO_2$ appearance in the breath following the IV administration of L-serine-3-^{14}C 10 and 40 min subsequent to the IV injection of 40 mg of L-methionine.

The ordinate represents percent of administered ^{14}C excreted as $^{14}CO_2$ per min and the abscissa represents time in min following intravenous injection of the ^{14}C-labeled serine. Each point represents the mean of the $^{14}CO_2$ excretion rate for each group of animals at the given time, and the length of the vertical bar through each point represents 1 standard error of the mean.

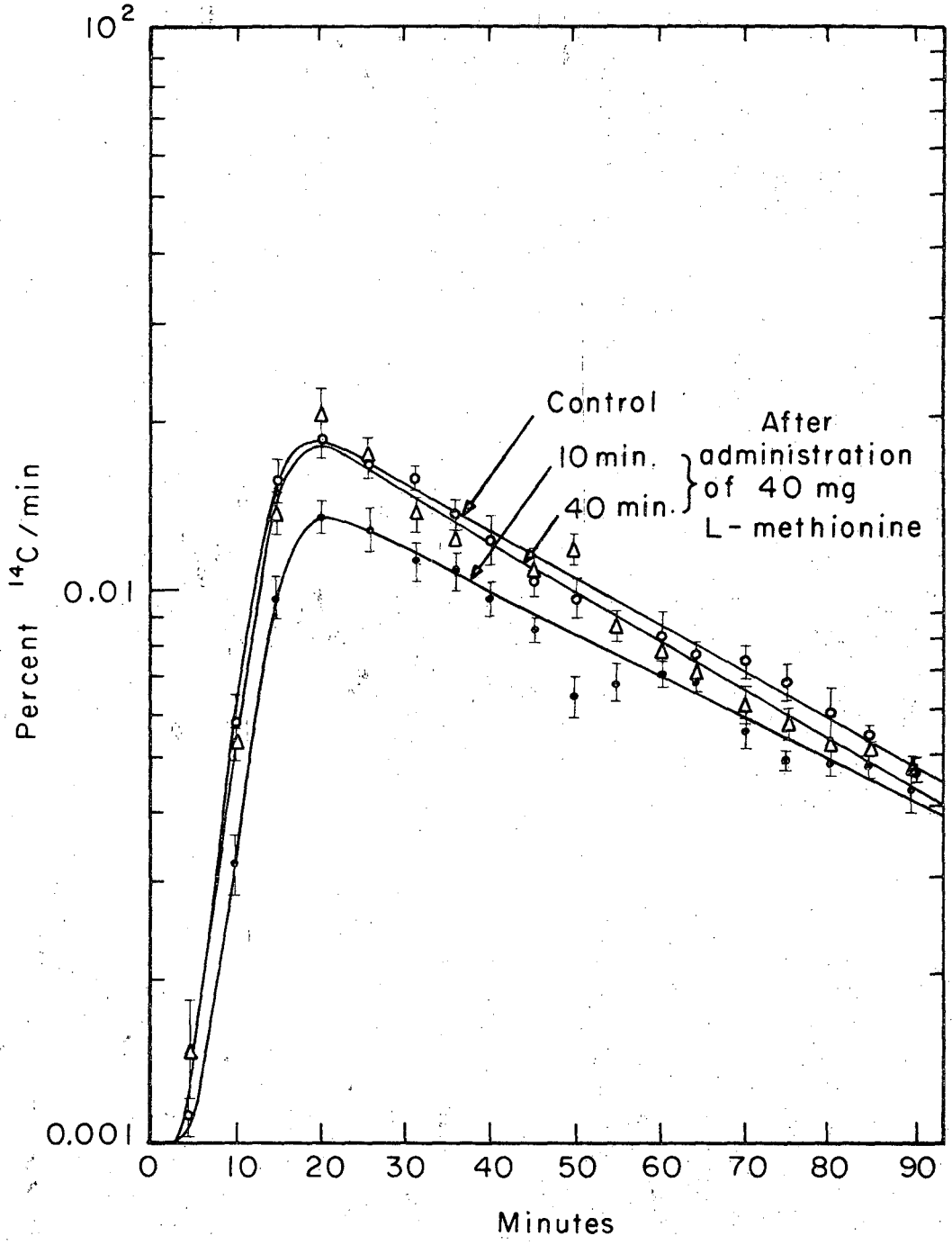
10^2
0.01
0.001
Percent ^{14}C/min
Control
10 min.
40 min.
After administration of 40 mg L-methionine
0
10
20
30
40
50
60
70
80
90
Minutes
XBL692-1903

Fig. 31

Fig. 32. Composite data of the rate of $^{14}CO_2$ appearance in the breath following the IV administration of ^{14}C-formate 10 min subsequent to the IV injection of 40 mg of L-methionine.

The ordinate represents percent of administered ^{14}C excreted as $^{14}CO_2$ per min and the abscissa represents time in min following intravenous injection of the ^{14}C-formate. Each point represents the mean of the $^{14}CO_2$ excretion rate for each group of animals at the given time, and the length of the vertical bar through each point represents 1 standard error of the mean.

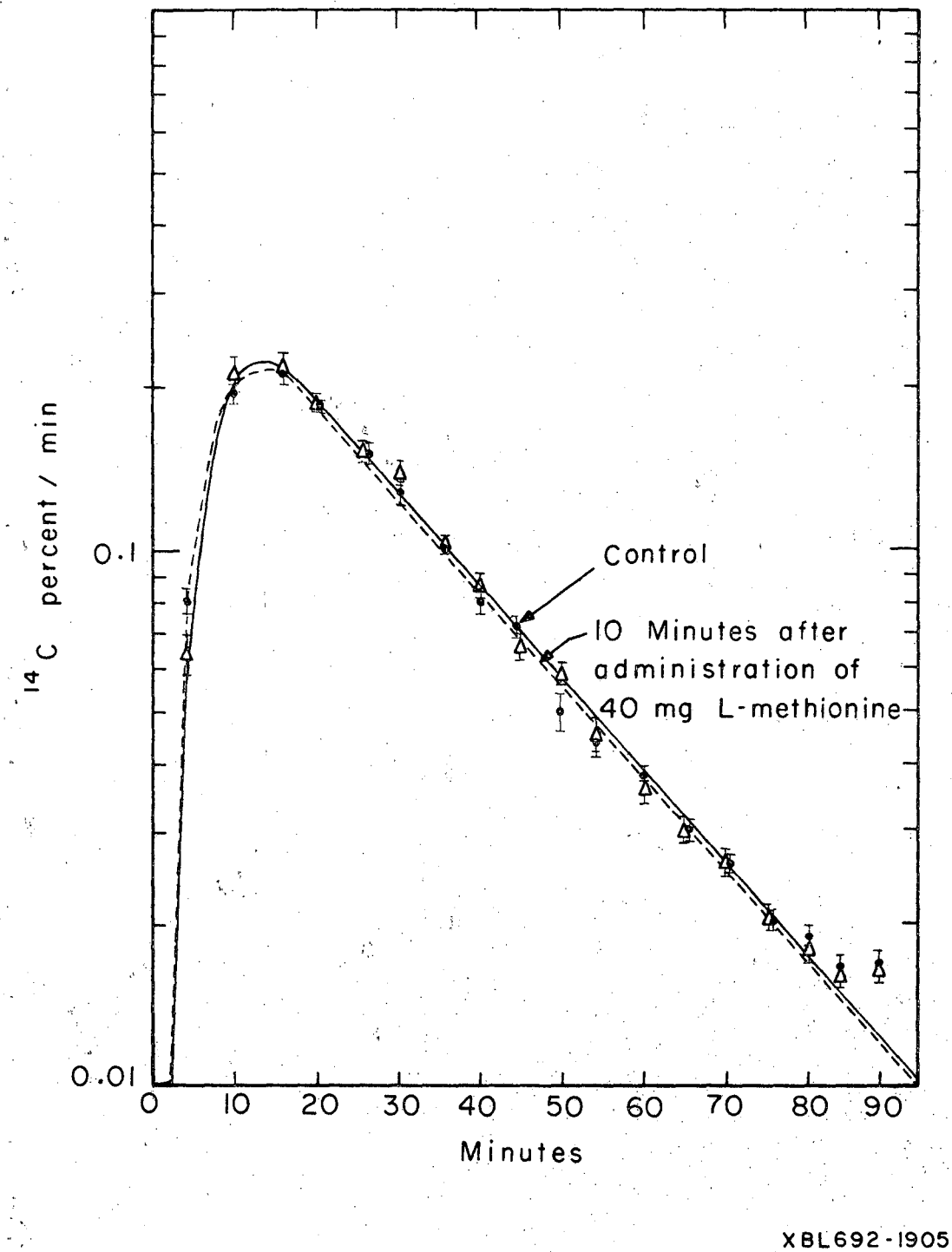
^{14}C percent / min
0.1
0.01
0
10
20
30
40
50
60
70
80
90
Minutes
Control
10 Minutes after
administration of
40 mg L-methionine
XBL692-1905

Fig. 32

Table XIV

T_{max} and integral ^{14}C excretion determined from $^{14}CO_2$ appearance in breath following IV administration of L-histidine (imidazole-2-^{14}C), formimino-^{14}C glutamic acid, L-serine-3-^{14}C, and ^{14}C-formate in control and methionine-treated rats (the number of animals in each group is noted in parentheses).

Table XIV

Category	T_{max} (min ± S.E.)	^{14}C excretion in 90 min (% ± S.E.)
L-histidine (imidazole-2-^{14}C)		
Control rats (22)	21.54 ± 0.57	1.20 ± 0.65
Rats given simultaneous IV injection of the ^{14}C-labeled histidine incubated with 40 mg L-methionine (4)	22.75 ± 1.65	1.06 ± 0.11
Rats 10 min after IV administration of 40 mg L-methionine (3)	21.50 ± 2.18	0.77 ± 0.18
Rats 40 min after IV administration of 40 mg L-methionine (3)	20.12 ± 0.83	0.86 ± 0.05
Rats 120 min after IV administration of 40 mg L-methionine (3)	19.00 ± 0.76	1.14 ± 0.16
Formimino-^{14}C L-glutamic acid		
Control rats (6)	28.25 ± 4.61	0.39 ± 0.07
Rats 10 min after IV administration of 40 mg L-methionine (2)	37.5	0.31
Rats 40 min after IV administration of 40 mg L-methionine (2)	34.25	0.38
L-serine-3-^{14}C		
Control rats (6)	16.83 ± 1.48	9.03 ± 0.72
Rats 10 min after IV administration of 40 mg L-methionine (3)	16.67 ± 1.01	6.70 ± 0.34
Rats 40 min after IV administration of 40 mg L-methionine (3)	14.17 ± 0.60	8.65 ± 0.50

Table XIV continued

Category	T_{max} (min ± S.E.)	^{14}C excretion in 90 min (% ± S.E.)
^{14}C-formate		
Control rats (3)	12.67 ± 1.20	7.57 ± 0.27
Rats 10 min after IV administration of 40 mg L-methionine (3)	13.33 ± 0.17	7.65 ± 0.36

across the cell membrane. The alterations in formimino glutamic acid may be due to either an inhibition of a physical transport of this amino acid or an inhibition of biochemical processes involved in the oxidation of mono-carbon fragments attached to tetrahydrofolic acid. In contrast, L-methionine in loading doses has no effect on formate. Our data are consistent with the previous findings, which demonstrated decreased uptakes of several amino acids by L-methionine for Ehrlich ascites tumor cells (87,94), for rat brain slices (95), and for intestinal absorption in normal hamsters (88) and rats (89). Moreover, our results are strongly supported by recent data obtained by Lin and Winchell (96) in this Laboratory confirming that L-methionine apparently depressed the intracellular uptakes of L-histidine and L-serine in equilibrium state. They utilized dog bone marrow cells incubated in basal medium of Eagle in the presence of L-histidine (imidazole-2-^{14}C) or L-serine-3-^{14}C in the presence and absence of L-methionine. The intracellular uptakes of the above amino acids, which were analyzed, according to the compartment theory, demonstrated that fractional turnover rate of intracellular pool, and the influx constant, fractional efflux constant, and fractional utilization rate constant of those amino acids were definitely depressed by large doses of L-methionine. Recent studies by Stahelin and Winchell (97) in this Laboratory showed that administration

of large doses of L-methionine to folic-acid-deficient persons caused abnormal mentation in these patients. These induced behavioral changes may be due to a strong inhibition of L-methionine on the uptakes of other amino acids in various tissues, including brain tissue.

E. Summary

Following administration of L-histidine (imidazole-2-^{14}C), L-serine-3-^{14}C, and formimino-^{14}C L-glutamic acid to normal rats given large doses of L-methionine, the initial rate and amount of $^{14}CO_2$ excreted in the breath are significantly decreased whereas following administration of ^{14}C-formate $^{14}CO_2$ appearance is unchanged in methionine-treated rats. These results indicate the presence of *in vivo* competition for physical transport across cell membranes of these amino acids. The $^{14}CO_2$ breath-analysis technique should be useful in future study of competition for metabolism between various materials.

VIII. Appendix 2

Effects of sodium iodide on $^{14}CO_2$ production in normal rats given L-tyrosine-1-^{14}C, L-histidine (imidazole-2-^{14}C), and L-methionine-CH_3-^{14}C

A. Review of the problem

The action of iodine on thyroid metabolism is complex and still incompletely understood. Large doses of inorganic iodide have been shown to inhibit the formation of organic iodide in both in vivo and in vitro studies (98-99) by blocking the iodination of L-tyrosine or by the coupling mechanism involved in the conversion of diiodotyrosine to thyroxine (100-103) or both. This block is related to the level of plasma inorganic iodide (99). Barnes et al. demonstrated apparent decreased catabolism and utilization of tyrosine in hyperthyroidism by analysis of $^{14}CO_2$ breath curves and by analysis of plasma protein-^{14}C activity in hyperthyroid subjects subsequent to intravenous administration of L-tyrosine-1-^{14}C (104).

In this study, we demonstrated an *in vivo* effect of sodium iodide on the oxidation to CO_2 of the #1 carbon atom of L-tyrosine, the #2 carbon atom of the imidazole ring of L-histidine, and the carbon atom of the methyl group of L-methionine; the demonstration was by determination of $^{14}CO_2$ breath curves of normal rats given

large doses of sodium iodide before intravenous administration of L-tyrosine-1-^{14}C, L-histidine (imidazole-2-^{14}C), and L-methionine-CH_3-^{14}C.

B. Preparation of experimental animals

Inbred male Buffalo rats (Simonsen Laboratory, Gilroy, California) weighing 240 to 245 g were used in all experiments.

In the first series of studies, rats were divided into two groups of eight control and eight experimental rats treated with 10 to 15 mg of NaI. The appearance of $^{14}CO_2$ in the breath was measured subsequent to the intravenous administration of L-tyrosine-1-^{14}C in each of these animals. After these first experiments, five rats of the experimental group received 15 mg of sodium iodide (10 ml contains 1 g sodium iodide with sodium sulfite, 0.133% and monothioglycerol, 0.25%, Eli Lilly and Co., Indianapolis) intravenously and three rats of the experimental group received 10 mg of sodium iodide intravenously 60 min prior to performance of a repeat study. In each study the rat received 0.75 μCi of L-tyrosine-1-^{14}C (specific activity: 0.1 mCi/0.95 mg, New England Nuclear Corp., 575 Albany Street, Boston, Massachusetts, 02118) intravenously after light anesthesia with diethyl ether.

In a second series of experiments $^{14}CO_2$ appearance in the breath was measured subsequent to the intravenous administration of the ^{14}C-labeled histidine. The

experimental animals consisted of three control and three NaI-treated rats. In each study, the rat received 2 μCi of L-histidine (imidazole-2-^{14}C) (specific activity: 57.8 mCi/mM, Amersham/Searle Corporation) intravenously. In a third series of studies, two control and two sodium-iodide-treated rats were used. In each study, the rat received 10 μCi of L-methionine-CH_3-^{14}C (specific activity: 14.77 mCi/mM, New England Nuclear Corp., 575 Albany Street, Boston, Massachusetts 02118) intravenously and the $^{14}CO_2$ production was measured by the same procedure as described above.

C. Results

Figure 23 presents composite data of the rate of $^{14}CO_2$ appearance in the breath of eight control rats, five rats given 15 mg of sodium iodide, and three rats given 10 mg of sodium iodide intravenously 60 min prior to the intravenous administration of L-tyrosine-1-^{14}C.

It can be seen that there is a qualitative difference between $^{14}CO_2$ breath curves of control rats and those of rats given 15 mg of sodium iodide intravenously. However, no change of the $^{14}CO_2$ breath curves is noted in rats treated with 10 mg of sodium iodide. The cumulative percent of ^{14}C appearing as $^{14}CO_2$ in the breath during the initial 60 minutes subsequent to the intravenous administration of the ^{14}C-labeled tyrosine is decreased in rats given 15 mg of sodium iodide.

Fig. 33. Composite data of the rate of $^{14}CO_2$ appearance in the breath following intravenous administration of L-tyrosine-1-^{14}C 60 min after the intravenous injection of 10 to 15 mg sodium iodide.

The ordinate represents percent of administered ^{14}C excreted as $^{14}CO_2$ per min and the abscissa represents time in min following intravenous injection of the ^{14}C-labeled tyrosine. Each point represents the mean of the $^{14}CO_2$ excretion rate for each group of animals at the given time. The length of the vertical bar through each point represents 1 standard error of the mean.

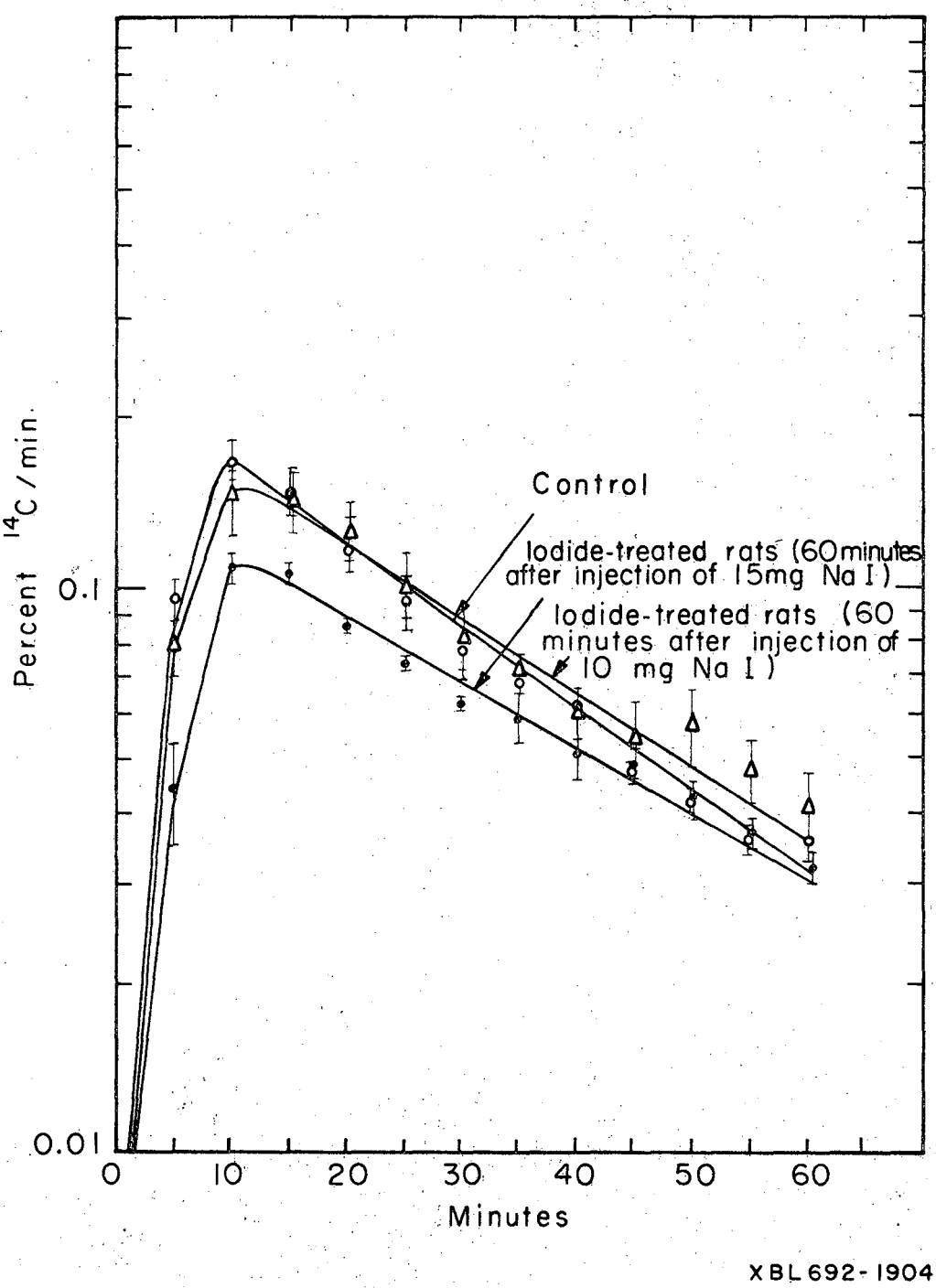
Percent ^{14}C / min.
0.1
0.01
Control
Iodide-treated rats (60minutes after injection of 15mg Na I)
Iodide-treated rats (60 minutes after injection of 10 mg Na I)
0
10
20
30
40
50
60
Minutes
XBL692-1904

Fig. 149

Similar results are summarized in Fig. 34, which presents the composite data of the rate of $^{14}CO_2$ excretion in the breath of three control rats and three rats given 15 mg of sodium iodide 60 min prior to the intravenous administration of the L-histidine (imidazole-2-^{14}C). Again, there is decreased $^{14}CO_2$ production noted in rats given sodium iodide following intravenous administration of the ^{14}C-labeled histidine. Fig. 35 presents the data obtained in rats treated with 15 mg of sodium iodide and in control rats subsequent to the intravenous administration of L-methionine-CH_3-^{14}C. It is seen that there is no difference between the $^{14}CO_2$ breath curves obtained in sodium-iodide-treated rats and those of the control rats.

Table XV summarizes values presented in Figs. 33 through 35.

D. Discussion

The results presented here demonstrate that large doses of sodium iodide decrease the amount of oxidation of the #1 carbon atom of L-tyrosine and the #2 carbon atom of the imidazole ring of L-histidine to CO_2 *in vivo*, whereas loading doses of sodium iodide have no effect on the carbon atom of the methyl group of L-methionine. These findings demonstrate that the fractional turnover rate limiting catabolic steps involved in the oxidation of carbon atoms of histidine and tyrosine is decreased by

Fig. 34. Composite data of the rate of $^{14}CO_2$ appearance in the breath after intravenous administration of L-histidine (imidazole-2-^{14}C) 60 min following intravenous injection of 15 mg sodium iodide.

The ordinate represents percent of administered ^{14}C excreted as $^{14}CO_2$ per min and the abscissa represents time in min following intravenous injection of the ^{14}C-labeled histidine. Each point represents the mean of the $^{14}CO_2$ excretion rate for the group of animals at the given time. The length of the vertical bar through each point represents 1 standard error of the mean.

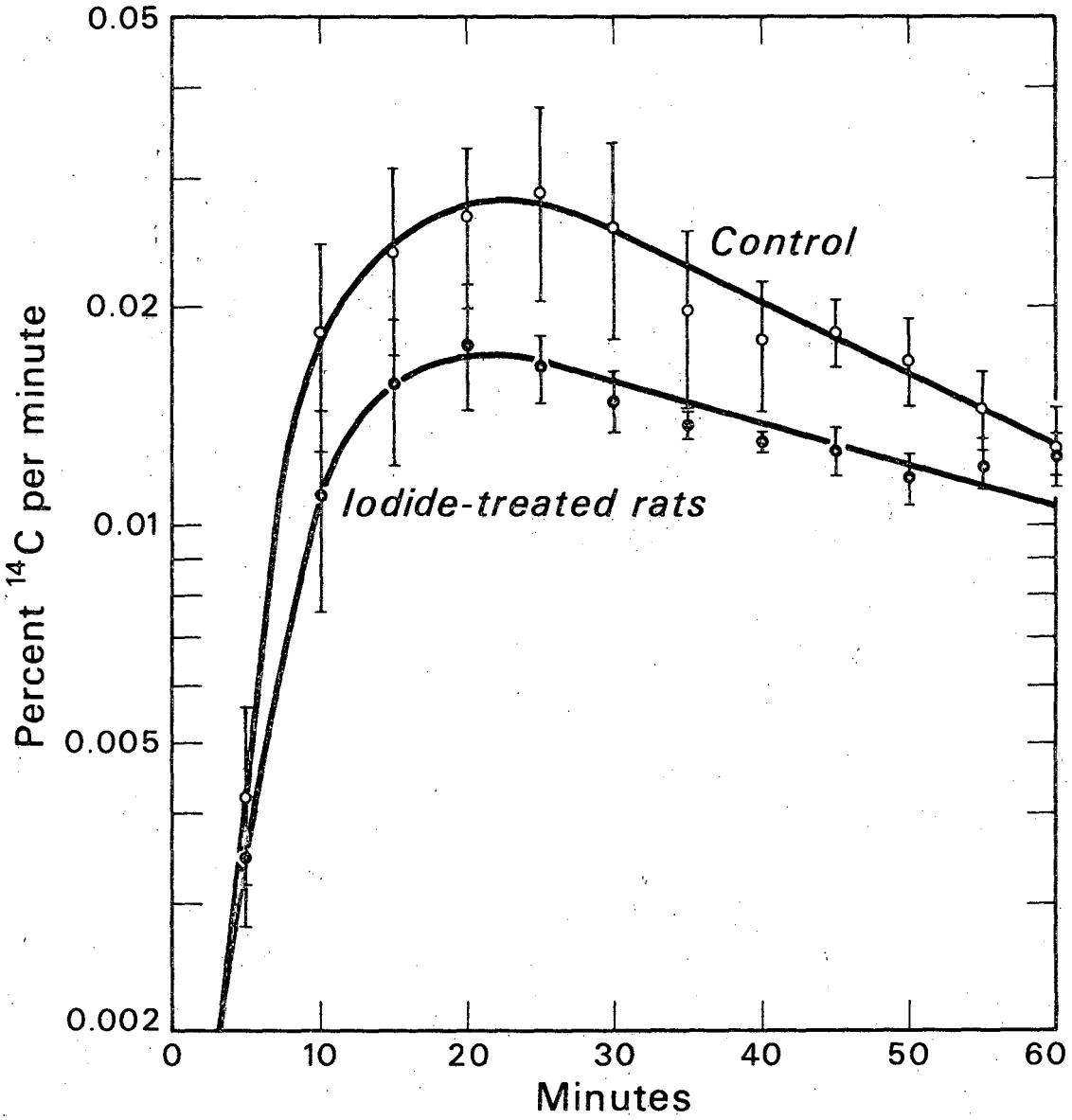
0.05
0.02
0.01
0.005
0.002
Percent ^{14}C per minute
Control
Iodide-treated rats
0
10
20
30
40
50
60
Minutes
DBL 691-4508

Fig. 34

Fig. 35. Composite data of the rate of $^{14}CO_2$ appearance in the breath following intravenous administration of L-methionine-CH_3-^{14}C 60 min after intravenous injection of 15 mg sodium iodide.

The ordinate represents percent of administered ^{14}C excreted as $^{14}CO_2$ per min and the abscissa represents time in min following intravenous injection of the ^{14}C-labeled methionine. Each point represents the mean of the $^{14}CO_2$ excretion rate for the group of animals at the given time.

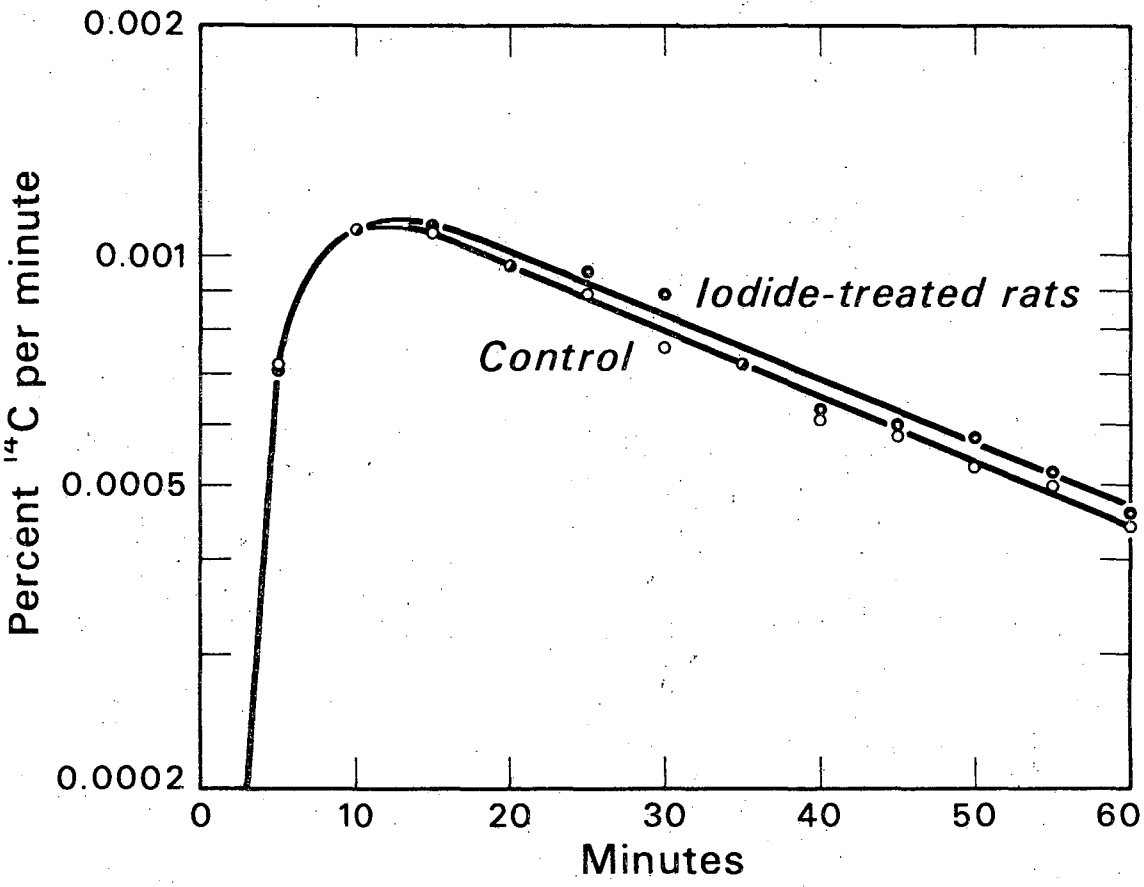
0.002
0.001
0.0005
0.0002
Percent ^{14}C per minute
Iodide-treated rats
Control
0
10
20
30
40
50
60
Minutes
DBL 691-4509

Fig. 35

Table XV

T_{max} and integral ^{14}C excretion determined from $^{14}CO_2$ appearance in breath following IV administration of L-tyrosine-1-^{14}C, L-histidine (imidazole-2-^{14}C), and L-methionine-CH_3-^{14}C.

Category	T_{max} (min ± S.E.)	^{14}C excretion in 60 min (% ± S.E.)
L-tyrosine-1-^{14}C		
Control rats (8)	9.68 ± 0.38	4.87 ± 0.31
Rats 60 min after IV administration of 15 mg NaI (5)	11.90 ± 0.76	3.64 ± 0.17
Rats 60 min after IV administration of 10 mg NaI (3)	10.66 ± 0.70	4.78 ± 0.70
L-histidine (imidazole-2-^{14}C		
Control rats (3)	23.17 ± 1.20	1.12 ± 0.25
Rats 60 min after IV administration of 15 mg NaI (3)	21.67 ± 3.68	0.68 ± 0.06
L-methionine-CH_3-^{14}C		
Control rats (2)	12	0.435
Rats 60 min after IV administration of 15 mg NaI (2)	14.5	0.460

large doses of sodium iodide. These results may be due either to alteration of biochemical processes of those amino acids or to their physical transport across the cell membrane. For the former possibility, large doses of sodium iodide may interfere with biochemical processes of tyrosine catabolism. This explanation is supported by the finding that large doses of iodine may inhibit the incorporation of iodine into organic combination in thyroid tissue, an action which is similar to that of an antithyroid compound (102). It is known that the catabolism of L-tyrosine and L-histidine occurs primarily in liver tissue. Similar information is not available for L-methionine. We may therefore suggest that large doses of sodium iodide might inhibit the physical transport of L-tyrosine and L-histidine across the cell membrane in liver tissue.

If the proposed hypothesis was correct, then it may be used to explain the inhibitory effect of iodide on the hyperfunctioning thyroid gland.

E. Summary

Following administration of L-tyrosine-1-^{14}C and L-histidine (imidazole-2-^{14}C) to normal rats given loading doses of sodium iodide, the initial $^{14}CO_2$ excretion in the breath is significantly decreased, whereas in normal rats given the same amount of sodium iodide the $^{14}CO_2$ excretion is unchanged subsequent to the administration of L-methionine-CH_3-^{14}C. These results suggest that large

doses of sodium iodide may inhibit the physical transport of L-tyrosine and L-histidine, but not L-methionine, across the cell membrane in liver tissue.

Bibliography

1. W. H. Sebrell and R. S. Harris. The Vitamins, Volumes I, II, III. Academic Press, Inc., N.Y., 1954.
2. P. Gyorgy. Vitamin Methods, Volumes I, II. Academic Press, Inc., N.Y., 1950.
3. W. H. Eddy, Vitaminology. The Williams and Wilkins Co., 1949.
4. S. A. Koser. Vitamin Requirements of Bacteria and Yeasts. Charles Thomas, Illinois, 1968.
5. A. A. Albanese. Newer Methods of Nutritional Biochemistry. Academic Press, N.Y., 1963, p. 257-260.
6. L. S. Goodman and A. Gilman. The Pharmacological Basis of Therapeutics. MacMillan Company, New York, 1965, p. 1420-1432.
7. B. M. Tolbert. Ionization chamber assay of radioactive gases. University of California Radiation Laboratory report UCRL-3499, March 1956.
8. B. M. Tolbert, M. Kirk, and E. M. Baker. Continuous $^{14}CO_2$ and CO_2 excretion studies in experimental animals. Am. J. Physiol. 185: 269-274 (1956).
9. C. H. Wang and D. L. Willis. A time course study of $^{14}CO_2$ production from rats metabolizing glucose-^{14}C substrate. In Radiotracer Methodology in Biological Sciences. Prentice-Hall, Inc., N.Y., 1965, p. 323-332.

10. C. H. Wang. Experimental design in animal rado-respirometry. In Symposium on Respiration Pattern Analysis in Intermediary Metabolism Study, June 1964, Berkeley, California.

11. B. M. Tolbert, M. Kirk, and F. Upham. Carbon-14 respiration pattern analyzer for clinical studies. Rev. Sci. Instr. 30: 116-120 (1959).

12. B. M. Tolbert. Instrument development and data handling in respiration $^{14}CO_2$ pattern analysis. In Symposium on Respiration Pattern Analysis in Intermediary Metabolism Study, June, 1964, Berkeley, California.

13. M. B. Fish. Human in vivo metabolism kinetics using endogenous $^{14}CO_2$ production. In Symposium on Radio-isotopes and Nuclear Radiation in Medicine, December, 1967, Berkeley, California.

14. G. V. Leroy, G. T. Okita, E. C. Tocus, and D. Charleston. Continuous measurement of specific activity of $^{14}CO_2$ in expired air. Intern. J. Appl. Radiation Isotopes 7: 273-286 (1960).

15. F. J. Domingues, K. J. Goldner, R. R. Baldwin, and J. R. Lowry. An instrument and technique for the continuous measurement of respiratory CO_2 patterns in metabolic tracer studies. Intern. J. Appl. Radiation Isotopes 7: 77-86 (1959).

16. L. L. Shane, H. S. Winchell, B. A. Shipley, and N. N. Finley. The influence of hydrocortisone upon histidine kinetics in the rat. Semiannual report-Biology and Medicine, Lawrence Radiation Laboratory Report UCRL-18347, Spring 1968, 53-58.

17. L. L. Shane, H. S. Winchell, N. N. Finley, B. A. Shipley, and J. H. Lawrence. Increased histidine turnover in rats following administration of glucagon. Lawrence Radiation Laboratory Report UCRL-18347, Spring 1968.

18. B. M. Tolbert, A. M. Hughes, M. R. Kirk, and M. Calvin. Effect of coenzyme A on the metabolic oxidation of labeled fatty acids: Rate studies, instrumentation, and liver fractionation. Arch. Biochem. Biophys. 60: 301-319 (1956).

19. B. M. Tolbert, J. H. Lawrence, and M. Calvin. Respiratory carbon-14 patterns and physiological state. In Proceedings of the Internation Conference on the Peaceful Uses of Atomic Energy, Geneva, 8 August, 1955.

20. T. W. Sargent, D. M. Israelstam, A. T. Shulgin, S. A. Landaw, and N. N. Finley. A note concerning the fate of the 4-methoxyl group in 3, 4-dimethoxy-phenethylamine (DMPEA). Biochem. Biophys. Research Commun. 29: 126-130 (1967).

21. M. Pollycove. Glucose kinetics and oxidation and the effects of insulin, tolbutamide, and phenethyl biguanide (DBT), in normal human subjects. In Symposium on Respiration Pattern Analysis in Intermediary Metabolism Study, June 16, 1964, Berkeley, California.

22. E. S. Gordon. Carbon-14 studies of glucose and fatty acid oxidation in human subjects. In Symposium on Respiration Pattern Analysis in Intermediary Metabolism Study, June 16, 1964, Berkeley, California.

23. M. B. Fish, M. Pollycove, and T. V. Feichtmeir. Differentiation betwen vitamin B12-deficient and folic acid-deficient anemias with ^{14}C-histidine. Blood 21: 447-461 (1963).

24. M. B. Fish, M. Pollycove, and T. V. Feichtmeir. Differential diagnosis of the megaloblastic anemias using ^{14}C-histidine, ^{14}C-proprionate and $^{14}CO_2$ breath analysis. In J. Sirchis, Biomedical Application of Labeled Molecules. Euratom, Belgium, 1964, p. 339-351.

25. M. Barnes, M. Fish, M. Pollycove, and H. S. Winchell. Abnormalities of in vivo tyrosine kinetics in human thyroid disease (Abstract). Clin. Research 14: 130 (1966).

26. M. B. Fish, Human in vivo metabolism kinetics using endogenous $^{14}CO_2$ production. In Symposium on Radioisotopes and Nuclear Radiation in Medicine, December 4-8, Berkeley, California.

27. D. M. Israelstam, A. Johnson, and H. S. Winchell. Methionine and Schizophrenia. J. Nucl. Med. 8: 325-326 (1967).

28. H. S. Winchell. Kinetics of the CO_2-HCO_3^- pool in man. (Abstract) Clin. Res. 17: 166 (1969).

29. S. A. Landaw and S. H. Winchell. Endogenous production of carbon-14-labeled carbon monoxide. An in vivo technique for the study of heme catabolism. J. Nucl. Med. 7: 696-707 (1966).

30. H. Jeffey and J. Alvarez. Liquid scintillation counting of carbon-14. Anal. Chem. 33: 612-615 (1961).

31. R. H. S. Thompson and R. E. Johnson. Bood pyruvate in vitamin B1 deficiency. Biochem. J. 29: 694-700 (1935).

32. G. D. Lu and B. S. Platt. Studies on the metabolism of pyruvic acid in normal and vitamin B1-deficient states. The effect of exercise on blood pyruvate in Vitamin B1 deficiency in man. Biochem. J. 33: 1538-1543 (1939).

33. B. S. Platt and G. D. Lu. Studies on the metabolism of pyruvic acid in normal and Vitamin B1-deficient states. The cumulation of pyruvic acid and other carbonyl compounds in beriberi and the effect of vitamin B1. Biochem. J. 33: 1525-1537 (1939).

34. G. D. Lu and D. M. Needham. The fate of injected pyruvate in the normal rabbit. Biochem. J. 33: 1544-1548 (1939).

35. C. C. Liang. Studies on experimental thiamine deficiency. Trends of keto acid formation and detection of glyoxylic acid. Biochem. J. 82: 429-434 (1961).

36. G. G. Banerji and L. J. Harris. Methods for assessing the level of nutrition. A carbohydrate tolerance test for vitamin B1. Biochem. J. 33: 1346-1355 (1939).

37. M. E. Shils, H. G. Day, and E. V. McCollum. The effect of thiamine deficiency in rats on the excretion of pyruvic acid and bisulfite-binding substances in the urine. J. Biol. Chem. 139: 145-161 (1941).

38. G. G. Banerji and J. Yudkin. The vitamin-B1 sparing action of fat and protein. The oxidation of pyruvate by the tissues of symptom-free rats on diets deficient in vitamin B1. Biochem. J. 36: 530-541 (1942).

39. R. M. Bucle. Blood pyruvic and α-ketoglutaric acids in thiamine deficiency. Metabolism 14: 141-149 (1964).

40. M. K. Horwitt and O. Kreisler. The determination of early thiamine-deficient states by estimation of blood lactic and pyruvic acids after glucose administration and exercise. J. Nutrition 37, 411-427 (1949).

41. W. N. Pearson and W. J. Darby, Jr. Catabolism of ^{14}C-labeled thiamine by the rat as influenced by dietary intake and body thiamine stores. J. Nutrition 93: 491-498 (1967).

42. R. A. Neal and W. N. Pearson. Studies of thiamine metabolism in the rat. Isolation and identification of 2-methyl-4-amino-5-pyrimidine carboxylic acid as a metabolite of thiamine in rat urine. J. Nutrition 83: 351-357 (1964).

43. M. Balaghi and W. N. Pearson. Comparative studies of the metabolism of ^{14}C-pyrimidine-labeled thiamine, ^{14}C-thiazole-labeled thiamine, and $_{35}S$-labeled thiamine in the rat. J. Nutrition 91: 9-19 (1967).

44. M. Balaghi and W. N. Pearson. Metabolism of physiological doses of thiazole-2-^{14}C-labeled thiamine by the rat. J. Nutrition 89: 265-270 (1966).

45. P. T. McCarthy, L. R. Cerecedo, and E. V. Brown. The fate of thiamine-$_{35}S$ in the rat. J. Biol. Chem. 209: 611-618 (1954).

46. M. J. Verrett and L. R. Cerecedo. Metabolism of thiamine-$_{35}S$ in the rabbit. Proc. Soc. Exptl. Biol. Med. 98: 509-513 (1958).

47. W. N. Pearson and W. J. Darby, Jr. Catabolism of ^{14}C-labeled thiamine by the rat as influenced by dietary intake and body thiamine stores. J. Nutrition 93: 491-498 (1967).

48. J. M. Iacono and B. C. Johnson. Thiamine metabolism. I. The metabolism of thiazole-2-^{14}C-thiamine in the rat. J. Am. Chem. Soc. 79: 6321-6324 (1957).

49. M. A. Williams, L. C. Chu, D. J. McIntosh, and I. Hindenberg. Effects of dietary fat level on pantothenate depletion and liver fatty acid composition in the rat. J. Nutrition 94: 377-382 (1968).

50. T. Ngo, H. S. Winchell, and S. Landaw. Altered in vivo metabolism of histidine (imidazole-2-^{14}C) in irradiated rats. Rad. Research, 34: 390-395 (1968).

51. T. M. Ngo, H. S. Winchell, M. A. Williams, N. N. Finley, and J. H. Lawrence. Decreased $^{14}CO_2$ production in thiamine-deficient rats given #1-^{14}C pyruvate and acetate: A possible mean for early diagnosis of beriberi? Submitted to J. Nucl. Med.

52. T. M. Ngo, H. S. Winchell, and J. H. Lawrence. Alterations in histidine catabolism in normal rats given pharmacological doses of folic acid and cyancobalamin. Submitted to Proc. Soc. Exptl. Biol. Med.

53. R. S. Harris, I. G. Wool, and J. A. Loraine. Vitamin and Hormones. Academic Press, N. Y., and London, 1964, 387-883.

54. E. E. Snell. Chemical structure in relation to biological activities of vitamin B6 in Vitamins and Hormones. Academic Press, N.Y., and London, 1958, p. 77-125.

55. T. R. Riggs and L. M. Walker. Diminished uptake of ^{14}C-α-amino-isobutyric acid by tissues of vitamin B6-deficient rats. J. Biol. Chem. 233: 132-137 (1958).

56. H. N. Christensen, T. R. Riggs, and B. A. Coyne. Effects of pyridoxal and indoleacetate on cell uptake of amino acids and potassium. J. Biol. Chem. 209: 413-427 (1954).

57. D. L. Oxender and H. N. Christensen. Transcellular concentrations as a consequence of intracellular accumulation. J. Biol. Chem. 234: 2321-2324 (1959).

58. P. R. Pal and H. N. Christensen. Uptake of pyridoxal and pyridoxal phosphate by Ehrlich ascites tumor cells. J. Biol. Chem. 236: 894-897 (1961).

59. H. Akedo, T. Sugawa, S. Yoshikawa, and M. Suda. Intestinal absorption of amino acids. I. The effect of vitamin B6 on the absorption of L-amino acids through the intestine. J. Biol. Chem. 47: 124-130 (1960).

60. F. A. Jacobs, L. J. Coen, and R. S. L. Hillman. Influence of pyridoxine, pyridoxal phosphate, deoxypiridoxine, and 2,4-dinitrophenol on methionine absorption. J. Biol. Che. 235: 1372-1375 (1960).

61. K. Ueda, H. Akedo, and M. Suda. Intestinal absorption of amino acids. IV. Participation of pyridoxal phosphate in the active transfer of L-amino acids through the intestinal wall. J. Biol. Chem. 48: 584-592 (1960).

62. M. M. Wintrobe. Clinical Hematology. Lea and Febiger, Philadelphia, 1967, p. 779-782.

63. H. N. Christensen and T. R. Riggs. Structural evidences for chelation and Schiff's base formation in amino acid transfer into cells. J. Biol. Chem. 220: 265-278 (1956).

64. E. R. Stokstad, D. Fordham, and A. DeGrunigen. The inactivation of pteroyglutamic acid (liver Lactobacillus casei factor) by light. J. Biol. Chem. 167: 877-878 (1947).

65. O. H. Lowry, O. A. Bessey, and E. J. Crawford. Photolytic and enzymatic transformations of pteroyglutamic acid. J. Biol. Chem. 180: 389-398 (1949).

66. K. Kuggenheim, S. Halevy, A. Hochman, and M. Benporath. The effect of X-irradiation on the metabolism of folic acid in rat organs. Radiation Res. 12: 567-574 (1960).

67. H. S. Winchell, S. L. Vimokesant, and R. Raley. Relative effect of radiation on de novo DNA base synthesis and thymidine incorporation into DNA. Lawrence Radiation Laboratory Semiannual Report-Biology and Medicine UCRL-Spring 1969, p. 149-154.

68. H. S. Winchell. (Lawrence Radiation Laboratory), personal communication.

69. V. Herbert. Experimental nutritional folate deficiency in man. Trans. Assoc. Am. Physicians 75: 397 (1962).

70. M. B. Fish, (University of California-San Francisco) and M. Pollycove (Lawrence Radiation Laboratory), personal communication.

71. K. F. Nakken and A. Pihl. The X-ray-induced damage to the p-aminobenzoic acid moiety of folic acid and some other p-aminobenzoic acid conjugates irradiated in solution. Radiation Res. 27: 19-31 (1966).

72. J. M. Noronha and N. S. Shad. Effects of X-irradiation on the activation of folic acid by rat organs. Radiation Res. 15: 604-608 (1961).

73. J. Hilgertova, J. Sonka, and Z. Dienstbier. Reduced nicotinamide adenine dinucleotide phosphate in the liver of X-ray-irradiated rats. J. Nucl. Biol. Med. 10: 72 (1966).

74. J. R. Bertino, B. A. Booth, A. L. Bierer, A. Cashmore, and A. C. Sartorelli. Studies on the inhibition of dihydrofolate reductase by the folate antagonists. J. Biol. Chem. 239: 479-485 (1964).

75. W. C. Werkheiser, Specific binding of 4-amino folic acid analogues by folic acid reductase, J. Biol. Chem. 236: 888-893 (1961).

76. D. G. Johns and J. R. Bertino. Folates and megaloblastic anemia: A review, Clin. Pharmacol. Therap. 6: 372-392 (1965).

77. E. M. Greenspan, A. Goldin, and E. B. Schoenback. Studies on the mechanism of action of chemotherapeutic agents in cancer. II. Requirements for the prevention of aminopterin toxicity by folic acid in mice. Cancer 3: 856-863 (1950).

78. E. M. Greenspan, A. Golden, and E. B. Schoenback. Studies on the mechanism of action of chemotherapeutic agents in cancer. V. Influence of the citrovorum factor and folic acid on the toxic manifestations of aminopterin in mice. Cancer 4: 619-625 (1951).

79. J. A. R. Mead, J. M. Venditti, A. M. Schrecker, A. Goldin, and J.C. Keresztesy. The effect of reduced derivative folic acid on toxicity and effect of methotrexate in mice. Biochem. Pharmacol. 12: 371-383 (1963).

80. J. R. Bertino. The mechanism of action of the folate antagonists in man. Cancer Res. 23: 1286-1306 (1963).

81. J. R. Bertino, A. Casmore, M. Fink, P. Calabresi, and E. Lefkowitz. The induction of leucocyte and erythrocyte dihydrofolate reductase by methotrexate in the dog. Clin. Pharmaco. Therap. 6: 763-769 (1965).

82. J. R. Bertino, D. M. Donohue, B. Simons, B. W. Gabrio, R. Silver, and F. M. Huennekens. The induction of dihydrofolic reductase activity in leucocytes and erythrocytes of patients treated with amethopterin. J. Clin. Invest. 42: 466-475 (1963).

83. A. Meister. Biochemistry of Amino Acids. Academic Press, New York., 1965, p. 818-841.

84. D. D. Brown, O. L. Silva, R. C. Gardiner, and M. J. Silverman. Metabolism of formiminoglutamic acid by vitamin B12-and folic acid-deficient rats fed excess methionine. J. Biol. Chem. 235: 2058-2062 (1960).

85. R. L. Blakely and B. M. McRongal. Dihydrofolic reductase from Streptococcus faecalis R. J. Biol. Chem. 236: 1163-1167 (1961).

86. V. Herbert and R. Zalusky. Interrelations of vitamin B12 and folic acid metabolism: folic acid clearance studies. J. Clin. Invest. 41: 1263-1276 (1962).

87. H. Kamin and P. Handler. Effect of infusion of single amino acid upon excretion of other amino acid. Am. J. Physiol. 169: 305-308 (1959).

88. G. Wissman. Preferential transference of amino acids from amino acid mixtures by sacs of everted small intestine of the golden hamster. J. Physiol. 127: 414-422 (1955).

89. E. L. Jervis and D. H. Smyth. Competition between enantiomorphs of amino acids during intestinal absorption. J. Physiol. 145: 57-65 (1959).

90. F. J. R. Hird and G. S. Sidhu. The absorption of amino acids by twin loops of rat intestine. Biochem. Biophys. Acta 23: 388-393 (1957).

91. E. L. Jervis and D. H. Smyth. Competition between enantiomorphs of methionine and histidine during intestinal absorption. J. Physiol. 142: 51P-52P (1958).

92. E. L. Jervis and D. L. Smyth. The effect of concentrations of amino acids on their rate of absorption from the intestine. J. Physiol. 149: 433-441 (1959).

93. D. M. Matthews and D. M. Smyth. The intestinal absorption of amino acids enantiomorphs. J. Physiol. 126: 96-100 (1954).

94. H. Kamin and P. Handler. Effect of presence of other amino acids upon intestinal absorption of single amino acids in the rat. Am. J. Physiol. 164: 654-661 (1959).

95. R. Nakamura. The transport of histidine and methionine in rat brain slices. J. Biochem. 53: 314-322 (1962).

96. M. Lin and H. S. Winchell (Lawrence Radiation Laboratory), personal communication.

97. H. Stahelin and H. S. Winchell (Lawrence Radiation Laboratory),personal communication.

98. M. E. Morton, I. L. Chaikoff, and S. Rosenfell. Inhibiting effect of inorganic iodide on the formation in vitro of thyroxine and diiodotyrosine by surviving thyroid tissue. J. Biol. Chem. 154: 381-387 (1944).

99. J. Wolf and J. L. Chaikoff. Plasma iodide as a homeostatic regulator of thyroid-function. J. Biol. Chem. 174: 555-567 (1948).

100. V. A. Galton and R. Pitt-River. The effect of excessive iodine on the thyroid of the rat. Endocrinol. 64: 835-839 (1964).

101. S. I. Shimoda, K. Inoue, and M. A. Greer. Inhibition of iodoamino acid synthesis in isolated thyroid epithelial cells by high concentrations of inorganic iodide. Endocrinol. 78: 1171-1176 (1966).

102. J. Wolf. Transport of iodide and other aminos in the thyroid gland. Rev. Physiol. 94: 45-90 (1964).

103. J. Wolf and J. L. Chaikoff. The inhibitory action of iodine upon organic binding of iodine by the normal thyroid gland. J. Biol. Chem. 172: 855-856 (1948).

104. M. Barnes. M. Fish, M. Pollycove, and H. S. Winchell. Abnormalities of in vivo tyrosine kinetics in human thyroid disease. Clin. Research. 14: 130 (1966).

TECHNICAL INFORMATION DIVISION
LAWRENCE RADIATION LABORATORY
UNIVERSITY OF CALIFORNIA
BERKELEY, CALIFORNIA 94720